TOPOISOMERASE I INHIBITORY COMPOUNDS FROM THE ROOTS OF *PAPHIOPEDILUM CALLOSUM*

Miss San Yoon Nwe

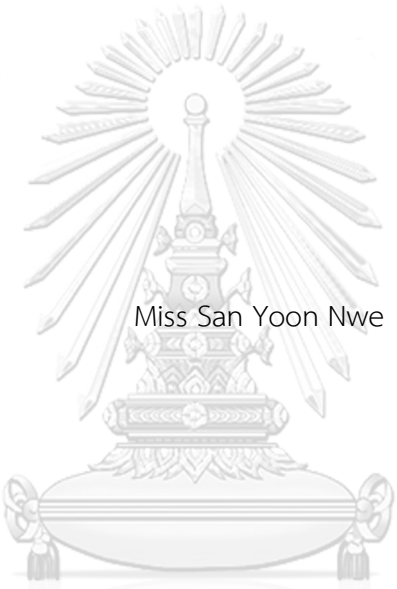

A Thesis Submitted in Partial Fulfillment of the Requirements
for the Degree of Master of Science in Pharmacy in Pharmacognosy
Department of Pharmacognosy and Pharmaceutical Botany
Faculty of Pharmaceutical Sciences
Chulalongkorn University
Academic Year 2018

สารที่มีฤทธิ์ยับยั้งเอนไซม์โทโพไอโซเมอเรสวันจากรากของรองเท้านารีคางกบ

น.ส.ซัน ยูน เนว์

วิทยานิพนธ์นี้เป็นส่วนหนึ่งของการศึกษาตามหลักสูตรปริญญาเภสัชศาสตรมหาบัณฑิต
สาขาวิชาเภสัชเวท ภาควิชาเภสัชเวทและเภสัชพฤกษศาสตร์
คณะเภสัชศาสตร์ จุฬาลงกรณ์มหาวิทยาลัย
ปีการศึกษา 2561

Thesis Title	TOPOISOMERASE I INHIBITORY COMPOUNDS FROM THE ROOTS OF *PAPHIOPEDILUM CALLOSUM*
By	Miss San Yoon Nwe
Field of Study	Pharmacognosy
Thesis Advisor	Associate Professor SUCHADA SUKRONG, Ph.D.
Thesis Co Advisor	Assistant Professor WITCHUDA THANAKIJCHAROENPATH, Ph.D.

Accepted by the Faculty of Pharmaceutical Sciences, Chulalongkorn University in Partial Fulfillment of the Requirement for the Master of Science in Pharmacy

..... Dean of the Faculty of Pharmaceutical Sciences

(Assistant Professor RUNGPETCH SAKULBUMRUNGSIL, Ph.D.)

THESIS COMMITTEE

..... Chairman

(Associate Professor RUTT SUTTISRI, Ph.D.)

..... Thesis Advisor

(Associate Professor SUCHADA SUKRONG, Ph.D.)

..... Thesis Co-Advisor

(Assistant Professor WITCHUDA THANAKIJCHAROENPATH, Ph.D.)

..... Examiner

(Associate Professor BOONCHU SRITULARUK, Ph.D.)

..... External Examiner

(Assistant Professor Somnuk Bunsupa, Ph.D.)

ชัน ยูน เนว์ : สารที่มีฤทธิ์ยับยั้งเอนไซม์โทโพไอโซเมอเรสวันจากรากของรองเท้านารีคางกบ. (TOPOISOMERASE I INHIBITORY COMPOUNDS FROM THE ROOTS OF *PAPHIOPEDILUM CALLOSUM*) อ.ที่ปรึกษาหลัก : รศ. ภญ. ดร.สุชาดา สุขหร่อง, อ.ที่ปรึกษาร่วม : ผศ. ภญ. ดร.วิชชุดา ธนกิจเจริญพัฒน์

รองเท้านารีคางกบ (*Paphiopedilum callosum* (Rchb.f.) Stein) เป็นพืชในวงศ์ Orchidaceae ซึ่งยังไม่มีรายงานการศึกษาด้านพฤกษเคมีและฤทธิ์ทางชีวภาพมาก่อน ในการศึกษาครั้งนี้ได้แยกสารจากสารสกัดชั้นเมทานอลของรากรองเท้านารีคางกบด้วยวิธีทางโครมาโทกราฟี โดยใช้การวิเคราะห์ความเป็นพิษต่อเอนไซม์โทโพไอโซเมอเรสวันด้วยการใช้เซลล์ยีสต์ในการชี้นำการแยกส่วน สารที่แยกได้ประกอบด้วยสารใหม่หนึ่งชนิด คือ 3′-hydroxy-2,6,5′-trimethoxystilbene (PC1) และสารที่เคยมีการรายงานมาแล้วจำนวนห้าชนิด ได้แก่ 3′-hydroxy-2,5′-dimethoxystilbene (PC2), 3-methyethergalangin (PC3), galangin (PC4), 2,3′-dihydroxy-5,5′-dimethoxystilbene (PC5) และ 2,3′-dihydroxy-5′-methoxystilbene (PC6) การพิสูจน์โครงสร้างทางเคมีของสารที่แยกได้อาศัยการวิเคราะห์ข้อมูลทางสเปคโทรสโคปีร่วมกับการเปรียบเทียบข้อมูลที่เคยรายงานมาแล้ว จากการวิเคราะห์ความเป็นพิษของสารที่แยกได้ต่อเอนไซม์โทโพไอโซเมอเรสวันด้วยการใช้เซลล์ยีสต์ พบความเป็นพิษต่อเอนไซม์โทโพไอโซเมอเรสวันโดยเกิดการยับยั้งการเจริญเติบโตของเซลล์ยีสต์ นอกจากนี้ยังได้ทำการยืนยันฤทธิ์ทางชีวภาพโดยศึกษาฤทธิ์ความเป็นพิษต่อเซลล์มะเร็งเต้านมของมนุษย์ชนิด MCF-7 และเซลล์มะเร็งปอดชนิด NCI-H187 พบว่าสารที่แยกได้แสดงฤทธิ์ต่อเซลล์มะเร็งทั้งสองชนิดที่ไม่เท่ากัน เมื่อทดสอบการเกิดดีเอ็นเอคลีเวจของซูเปอร์คอยล์ดีเอ็นเอ พบว่าเกิดคลีเวจคอมเพลกซ์ของสารที่แยกได้ดีเอ็นเอ และเอนไซม์โทโพไอโซเมอเรสวัน ซึ่งสังเกตได้จากเกิดแถบของรอยขาดของดีเอ็นเอที่มากขึ้น การศึกษาสารบริสุทธิ์ที่แยกได้ในรายละเอียดด้านต่างๆ ต่อไป อาจให้ข้อมูลที่เป็นประโยชน์ในการพัฒนายาต้านมะเร็ง

สาขาวิชา เภสัชเวท ลายมือชื่อนิสิต .....

ปีการศึกษา 2561 ลายมือชื่อ อ.ที่ปรึกษาหลัก .....

ลายมือชื่อ อ.ที่ปรึกษาร่วม .....

6076102633 : MAJOR PHARMACOGNOSY

KEYWORD: Paphiopedilum callosum; Orchidaceae; yeast cell-based assay; topoisomerase I poison; stilbene

San Yoon Nwe : TOPOISOMERASE I INHIBITORY COMPOUNDS FROM THE ROOTS OF *PAPHIOPEDILUM CALLOSUM*. Advisor: Assoc. Prof. SUCHADA SUKRONG, Ph.D. Co-advisor: Asst. Prof. WITCHUDA THANAKIJCHAROENPATH, Ph.D.

Paphiopedilum callosum (Rchb.f.) Stein belongs to the Orchidaceae family. The phytochemistry and bioactivity of this plant have not been previously reported. In this study, the chromatographic separation of methanolic extract of *P. callosum* roots was bioassay-guided by a yeast cell-based assay. One new compound, 3′-hydroxy-2,6,5′-trimethoxystilbene (PC1) and five known compounds including 3′-hydroxy-2,5′-dimethoxystilbene (PC2), 3-methylethergalangin (PC3), galangin (PC4), 2,3′-dihydroxy-5,5′-dimethoxystilbene (PC5) and 2,3′-dihydroxy-5′-methoxystilbene (PC6) were isolated. The chemical structures of these isolated compounds were elucidated and identified on the basis of analysis spectroscopic (ESI-MS, NMR and IR), as well as comparison with those reported in the literature. Their topoisomerase I poison activity was examined by a yeast cell-based assay. The results indicated that all the compounds exerted inhibitory effect on the growth of yeast cells, suggesting their TopI poison activities. The cytotoxic activities on human cancer cell lines (MCF-7 and NCI-H187), were also evaluated. The compounds exhibited varying degrees of cytotoxicity on the representative cell lines. Topoisomerase I poison activity of compounds was confirmed by DNA-cleavage assay, using supercoiled DNA. The results suggested that compounds caused the DNA-TopI cleavage complex, characteristics of TopI poison, by forming the nicked DNA. Further detailed studies on the isolated compounds might be provided useful information for cancer drug development.

Field of Study:	Pharmacognosy	Student's Signature .....
Academic Year:	2018	Advisor's Signature .....
		Co-advisor's Signature .....

ACKNOWLEDGEMENTS

First of all, I would like to express my deepest appreciate to my thesis advisor, associate professor Dr. Suchada Sukrong, for giving me a valuable opportunity for research experience. I am most grateful for her valuable advice, support, enthusiastic energy, and encouragement throughout the course of this study.

I wish to express my truthful thanks to my thesis co-advisor, assistant professor Witchuda Thanakijcharoenpath, for her valuable instruction in extraction, isolation, structural elucidation and identification of natural compounds, as well as for her kindness, patience, and her encouragement.

I would like to express my appreciation and grateful thanks to associate professor Dr. Rutt Suttisri, the chairman of my thesis committee, and other committee for their constructive suggestions and critical review of this thesis. I'm also special thanks to associate professor Dr. Boonchoo Sritularak for valuable advices and kindness during research, to associate professor Areerat Laorpaksa for her guidance and support on yeast cell-based assay.

I am grateful to Mr. Nonthalert Lertnitikul for his help to obtain NMR and UV spectrum and for his support, patience and kindness during the time of research, to Mr. Chayapol Tungphatthong for his help and for providing encouragement which helped relieve me from stress, and to Mr. Polapoom Yin Wongsaengpiboon for guidance and assisting me in DNA-cleavage assay.

I am especially grateful to Professor Kazuki Saito, Professor Mami Yamazaki, and associate professor Supaart Sirikantaramas for contributing the yeast strain.

I would like to acknowledge Scholarship Program for ASEAN Countries by Chulalongkorn University for giving me opportunity to study and perform my research at Chulalongkorn University, and also thanks to financially supported by a grant from International Research Integration: Research Pyramid from the the Ratchadaphiseksomphot Endowment Fund.

Special thanks are extended to all teachers, graduate students and staff members of the Department of Pharmacognosy and Pharmaceutical Botany, Faculty of

Pharmaceutical Sciences, Chulalongkorn University for their help and support, for memorable friendship, beneficial advice and kindness.

Finally, I would like to express deepest gratitude to rector of University of Pharmacy (Yangon), family and friends for their long-lasting love, understanding, support, and encouragement.

San Yoon Nwe

TABLE OF CONTENTS

Page

LIST OF TABLES

Page

LIST OF FIGURES

Page

LIST OF ABBREVIATIONS AND SYMBOLS

Acetone d_6	=	Deuterated acetone
α	=	Alpha
β	=	Beta
br s	=	Broad singlet (For NMR spectra)
C	=	Concentration
°C	=	Degree celsius
CC	=	Column chromatography
$CDCl_3$	=	Deuterated chloroform
CD_3OD	=	Deuterated methanol
CH_2Cl_2	=	Dichloromethane
cm	=	Centimeter
cm^{-1}	=	Reciprocal centimeter (unit of wave number)
^{13}C NMR	=	Carbon-13 nuclear magnetic resonance
CPT	=	Camptothecin
d	=	Doublet (for NMR spectra)
dd	=	Doublet of doublets (for NMR spectra)
DMSO	=	Dimethylsulfoxide
DMSO-d_6	=	Deuterated dimethylsulfoxide
DNA	=	Deoxyribonucleic acid
δ	=	Chemical shift
ε	=	molar absorptivity
ESI-MS	=	Electrospray Ionization Mass Spectrometry
EtOAc	=	Ethyl acetate
et al.	=	and others
g	=	Gram
Gal	=	Galactose
Glc	=	Glucose
hr	=	Hour
^{1}H-NMR	=	Proton nuclear magnetic resonance

HMBC	=	Heteronuclear multiple bond correlation
HR-ESI-MS	=	High resolution electrospray ionization mass spectrometry
HSQC	=	Heteronuclear single quantum coherence
Hz	=	Hertz
IC_{50}	=	Median inhibitory concentration
IR	=	Infrared
J	=	Coupling constant
Kg	=	Kilogram
L	=	Liter
λ_{max}	=	Wavelength at maximal absorption
µL	=	Microliter
µM	=	Micromolar
$[M-H]^-$	=	Pseudomolecular ion
m	=	Multiplet (for NMR Spectra)
MeOH	=	Methanol
mg	=	Milligram
MHz	=	Megahertz
Ml	=	Milliter
mM	=	Millimolar
min	=	Minute
mm	=	Millimeter
MS	=	Mass spectrum
MW	=	Molecular weight
m/z	=	Mass to charge ratio
nm	=	Nanometer
NMR	=	Nuclear magnetic resonance
OD	=	Optical density
ppm	=	Part per million
s	=	Singlet (for NMR spectra)
S.C. ura^-	=	Synthetic complete media lacking uracil
t	=	Triplet (for NMR spectra)

TLC	=	Thin layer chromatography
Top	=	Topoisomerase
UV	=	Ultraviolet
YPD	=	Yeast peptone dextrose

CHAPTER I
INTRODUCTION

Cancer is the major cause of mortality in the world due to its abnormal uncontrolled growth and spread of cells. Therefore, it is the major life-threatening disease nowadays. On a global scale according to GLOBOCAN series of the International Agency for Research on Cancer, cancers are the cause of 8.2 million deaths in 2012 (Ferlay et al., 2015) and, as estimated, of 9.6 million deaths in 2018 (Bray et al., 2018). The incidence of cancer is related to environmental, food, lifestyle, chemicals, some microbial infection, radiation, hormones, and genetic factors. Lung cancer, breast cancer and colorectal cancer were the most commonly diagnosed types. Lung cancer, colorectal, liver cancer and stomach cancer were the deadliest cancers (Ferlay et al., 2015). There are many types of cancer treatments including surgery, chemotherapy, radiotherapy, immunotherapy and targeted therapies (Iqbal et al., 2017). The most of currently used chemotherapeutic agents involve DNA topoisomerase inhibitors, alkylating agents, microtubules acting agents etc. DNA topoisomerase are ubiquitous enzymes for DNA replication and transcription. There are two main types of DNA topoisomerases, topoisomerase I (TopI) and topoisomerase II (TopII). TopI is the enzyme that responsible for the relaxation of supercoiled DNA by transiently breaking and resealing the single stranded DNA. TopII breaks and re-ligates to two strands of DNA (Pommier and Osheroff, 2012).

Topoisomerase inhibitors can be divided into two classes depending on their mechanisms: topoisomerase poisons and catalytic inhibitors (Kim et al., 2013). Topoisomerase poisons can stabilize the cleavable covalent complex between enzyme and DNA and prevent the re-ligation step of the reactions (Hsiang et al., 1985). Catalytic inhibitors act on other steps in the catalytic cycle (Larsen et al., 2003). To explore the action of TopI targeting compounds, the budding yeast *Saccharomyces cerevisiae* became a choice (Nitiss and Wang, 1988). TopI mutant yeast strain of *S. cerevisiae* was modified by inserting the TopI gene from *Arabidopsis thaliana*, the plant of the family Brassicaceae, under the control of GAL1 promoter

(Kieber et al., 1992). TopI gene from *A. thaliana* is sensitive to camptothecin, novel TopI poison according to previous investigation (Sirikantaramas et al., 2008).

Many chemotherapeutic agents for cancer treatment are derived from natural sources (plants, marine organisms and micro-organisms) (Mohd Sayeed Akhtar and Swamy, 2017). Natural compounds provide the skeleton for therapeutically effective anticancer drugs. Over 60% of anticancer agents that are currently used come from natural sources. Chemotherapeutic agents that were derived from plants include Vinca alkaloids (vinblastine and vincristine) from *Catharanthus roseus*, podophyllotoxin from *Podophyllum* species (*P. peltatum, P. emodii*), camptothecin from *Camptotheca acuminata*, paclitaxel (taxol) from *Taxus brevifolia* and homoharringtonine from *Cephalotaxus harringtonia* (Cragg and Newman, 2005). The discovery of these anticancer agents support that plants are potential sources of new lead compounds in cancer chemotherapy development.

Orchidaceae is a very large and wide spread family of angiosperms. In addition to high ornamental value, medicinal value of plants in this family has been recognized. Orchids have been used as herbal remedies in China since 2800 BC. The medicinal properties of some species of orchids were described in 'Materia Medica' by a famous Chinese herbalist, Shen Nung. In India and several countries, orchids have been used as folk medicines (Hossain, 2011). A number of secondary metabolites such as alkaloids, bibenzyl derivatives, flavonoids, and phenanthrenes have been reported from orchids. These phytochemicals exert antimicrobial, antitumor, anti-inflammatory, antiviral activities, etc. (Singh et al., 2012). Therefore, orchids are considered as promising sources of compounds with interesting bioactivities.

Paphiopedilum is the largest genus among the five genera of subfamily Cypripedioideae (Iqbal et al., 2017). Plants of this genus are known as Venus slipper orchids (Cribb, 1987). Phytochemical studies of *Paphiopedilum* plants are relatively rare while many phylogenetic studies have been done. Up to the present time, only two species *Paphiopedilum godefroyae* and *Paphiopedilum exul* have been reported for phytochemical compounds (Lertnitikul et al., 2016).

The objective of this study is to isolate topoisomerase I inhibitory compounds from the roots of *Paphiopedilum callosum*. This study may provide useful information for chemotaxonomic study of the genus *Paphiopedilum* and for further study in the development of cancer chemotherapy.

CHAPTER II
HISTORICAL

1. The family Orchidaceae

Orchidaceae, the orchid family, is one of the most species-rich family of Angiosperms (Christenhusz and Byng, 2016). It belongs to the order Asparagales and comprises about 28,000 species under 736 genera (Chase et al., 2015, Hossain, 2011). The family is divided into five subfamilies including Apostasioideae, Cypripedioideae, Epidendroideae, Orchidoideae, and Vanilloideae (Tsai et al., 2013). Orchidaceae is a diverse and widespread flowering plant family with unique characteristics features. Orchids are long-lived, deciduous herbs which grow according to one of two patterns, monopodial and sympodial growths. In the monopodial growth, the stem emerges from the single bud and leaves add to the apex. Sympodial orchids develop a series of adjacent shoots that continue to grow laterally. Orchid plants can be terrestrial, epiphytic, lithophytic or saprophytic. Terrestrial orchids' roots are ground-dwelling, thick and fleshy, whereas epiphytic orchids have modified aerial roots. Leaves of orchids are generally simple with parallel veins except some species of subfamily Vanilloideae which show reticulate venation (Zhang et al., 2018). Flowers of orchids are usually zygomorphic and can be either solitary or in inflorescence. They have two whorls of trimerous perianth: three sepals and three petals. One of three petals is usually differentiated into a labellum (or lip). The androecium and gynoecium are fused together to form a structure called the column or gynostemium. The column contains one, or rarely, two or three anthers and three stigmatic lobes, which are fused to form a stigmatic region. Subfamilies Orchidoideae, Vanilloideae, and Epidendroideae have a single fertile anther while two lateral fertile stamens are found in subfamilies Apostasioideae and Cypripedioideae. The ovary is inferior, comprising three carpels with parietal placentation (or axile in the subfamily Apostasioideae). The fruits are capsules (Pansarin and Pansarin, 2011). The ovary contains thousands of ovules; therefore, an orchid fruit contains thousands of seeds which are very light and usually dispersed by wind.

Members of Orchidaceae have long been used as herbal medicines in several parts of the world including China, India, Europe, America, Australia and Africa (Hossain, 2011). *Dendrobium* species, *Bletilla striata*, and *Gastrodia elata* are well known orchids in Chinese medicine (Hossain, 2011). Orchids have been found to exert a variety of biological activities due to its secondary metabolites such as alkaloids, bibenzyl derivatives, flavonoids, and phenanthrenes (Singh et al., 2012).

2. The subfamily Cypripedioideae

Cypripedioideae is one of the subfamilies of Orchidaceae. Plants in this subfamily are commonly known as lady's slipper orchids or slipper orchids. It comprises five genera including *Cypripedium, Mexipedium, Paphiopedilum, Phragmipedium,* and *Selenipedium*. The subfamily has a wide range of geographical distribution and diverse habitats (Cox et al., 1997). Slipper orchids have a unique morphological characteristic which is a slipper-shaped, pouch-like labellum. Their flowers have two fertile stamens, a shield-like staminode and fused lateral sepals (Lindley, 1840).

Some members of subfamily Cypripedioideae have been reported of their uses in folk medicines. *Cypripedium calceolus*, also known as nerve root, was used as a nerve tonic. *Cypripedium pubescens* was used as a sedative and antispasmodic. It was also use in the treatment of nervous headache, tremors and epilepsy. *C. elegans* and other species were used in madness, rheumatism, and epilepsy. The roots in the form of 'Dry powdered Cypripedium' or 'Fluid extracts Cypripedium', officially described in United States Pharmacopeia (U.S.P) and used in many ailments (Duggal, 1971). Root powder of yellow lady's slipper or *C. parviflorum* was used in the treatment of insomnia, headache, neuralgia, anxiety, fever, and many other diseases (Sievers, 1930). *Selenipedium chica*, belonging to Cypripedioideae is used like vanilla (Duggal, 1971).

3. The genus *Paphiopedilum*

Paphiopedilum is the largest genus among the five genera of subfamily Cypripedioideae (Chochai et al., 2012). Plants of this genus are known as Venus

slipper orchids due to the characteristic shape of the pouch-like labellum of the flower (Cribb, 1987). These orchids grow in sympodial pattern and lack pseudobulbs to store moisture. Therefore, they need permanently moist places for growing. The majority of *Paphiopedilum* species often grow in shading places of the forest floor. Most species are terrestrial but some are epiphytic or lithophytic. These plants have conduplicate leaves, imbricate sepals aestivation and a unilocular ovary with parietal placentation (Chochai et al., 2012).

Paphiopedilum plants found growing in Thailand include 19 taxa as follows (Smitinand, 2014).

(There are two more taxa according to updated information)

1. *Paphiopedilum appletonianum* (Gower) Rolfe
2. *Paphiopedilum bellatulum* (Rcb.f.) Stein
3. *Paphiopedilum callosum* (Rcb. f.) Stein var. *callosum*
4. *Paphiopedilum callosum* (Rcb. f.) Stein var. *potentianum* (O. Gruss & Roeth) P. J .Cribb
5. *Paphipedilum callosum* (Rchb. f.) Stein var. *sublaeve* (Rchb. f.) P. J. Cribb.
6. *Paphiopedilum charlesworthii (Rolfe)* Pfitzer
7. *Paphiopedilum concolor* (Lindl. ex Bateman) Pfitzer
8. *Paphiopedilum esquirolei* Schltr. Or *Paphiopedilum hirsutissimum* (Lindl. ex Hook.) Stein var. *esquirolei* (Schltr.) K. Karas. & K. Saito
9. *Paphiopedilum exul* (Ridl.) Rolfe
10. *Paphiopedilum godefroyae* (God.-Leb.) Stein
11. *Paphiopedilum godefroyae* (God.-Leb.) Stein var. *ang-thong* (Fowlie) Braem
12. *Paphiopedilum godefroyae* (God.-Leb.) Stein var. *leucochilum* (Rolfe) Hallier
13. *Paphiopedilum hirsutissimum* (Lindl. ex Hook.) Stein var. *esquirolei* (Schltr.) K. Karas. & K. Saito
14. *Paphiopedilum niveum* (Rchb. f.) Stein
15. *Paphiopedilum parishii* (Rchb. f.) Stein

16. *Paphiopedilum sukhakulii* Schoser & Senghas
17. *Paphiopedilum thaianum* Iamwir
18. *Paphiopedilum vejvarutianum* O. Gruss & Roellke
19. *Paphiopedilum villosum* (Lindl.) Stein

4. *Paphiopedilum callosum*

Paphiopedilum callosum, commonly called Callus Paphiopedilum, is widely distributed in South East Asia especially in Thailand, Cambodia, Laos, Myanmar and Vietnam. The plant is known in a Thai vernacular name as "Rongthao Nari Khang Kop" (Smitinand, 2014). It is a terrestrial herb. Its leaves are up to 30 cm long and 5 cm wide, elliptic, oblong-elliptic or obovate. Leaf colour is dark green mottled with bright green. The Inflorescence carries one or two 8-10 cm wide flowers with purple peduncle, 20-40 cm tall. The flower is large and the dorsal sepal and petals are white with purple and green stripes. The synsepalum is concave, elliptic or lanceolate, 2.7-3.2 cm long, 1.6-2.5 cm wide. The two upper petals curl downward and have hairy, black, raised spots along the top edge, 4.6-6.8 cm long, 1.2-1.8 cm wide. The labellum is reddish purple. The main flowering season is generally mid-spring (Plants & flowers, 2017). The pictures of *Paphiopedilum callosum* are shown in Figure 1.

Figure 1. *Paphiopedilum callosum* (Rchb.f.) Stein
https://www.plantsrescue.com/paphiopedilum-callosum/

5. Chemical constituents of the subfamily Cypripedioideae

According to previous studies, chemical constituents reported in plants of subfamily Cypripedioideae are classed into stilbenoids, flavonoids, and miscellaneous (**Table 1** and **Figure 2**).

5.1. Stilbenoids

Stilbenoids are plant phenolics of which the structures contain two aromatic rings joined by a C_2 unit. According to (Shen et al., 2013). These compounds are classified into five groups: stilbenes, oligostilbenes, bibenzyls, bisbibenzyls and phenanthrenes. Stilbenoids isolated so far from plants of the subfamily Cypripedioideae belong to the first and the last groups.

Stilbenes are characterized by the basic skeleton, 1,2-diphenylethylene. There are two possible isomers including those with *trans*- and *cis*- configurations. Naturally occurring stilbenes are usually *trans*- stilbenes but *cis*- stilbenes are also observed (Shen et al., 2013). The structures of stilbenes can be modified to form a benzofuran ring, yielding the subgroup of 2-aryl benzofurans. Stlibenes are biosynthesized through the shikimate and acetate-malonate pathways; they are derived from a cinnamoyl-CoA unit and three units of malonyl-CoA (Dewick and Demirci, 2009, Shen et al., 2013). Phenanthrenes, another group of stilbenoids, are formed by oxidative coupling of the aromatic rings of stilbene precursors (Shen et al., 2013).

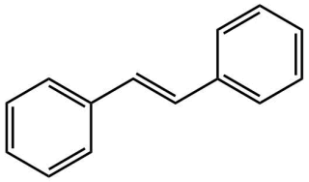

1,2-diphenylethylene (stilbene skeleton)

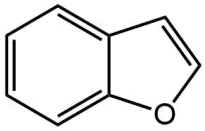

2-aryl benzofuran skeleton

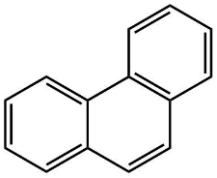

phenanthrene skeleton

According to the literatures reported from 1995 to 2008, about 125 new stilbenes, excluding oligomeric stilbenes, were discovered (Shen et al., 2013). Stilbenes can be found in various families of the plant kingdom, including those of angiosperms (monocots: Cyperaceae, Iridaceae, Liliaceae, Orchidaceae, Stemonaceae, Zingibraceae; dicots: Aceraceae, Asteraceae, Burseraceae, Combretaceae, Dipterocarpaceae, Euphorbiaceae, Leguminosae, Meliaceae, Moraceae, Polygonaceae, Rosaceae, Vitaceae), gymnosperms (Gnetaceae), ferns (Ophioglossaceae) and liverworts (Lejeuneaceae). Phenanthrenes are found in higher plants, mainly in Orchidaceae. A variety of biological activities exhibited by stilbenoids have been reported, for example, antitumor, antioxidant, antimicrobial and antiplatelet activities (Shen et al., 2013).

A number of stilbenoids have been found in the family Orchidaceae. Twenty-seven of them, including twenty-four compounds of the stilbene group and three compounds of the phenanthrene group, were isolated from plants of the subfamily Cypripedioideae. Seventeen stilbenes were isolated from *Phragmipedium longifolium*, *P. calurum* (a hybrid of *P. longifolium* and *P. schlimii*) and *P.* hybrid (a hybrid of *P. longifolium* and *P. lindleyanum*) (Garo et al., 2007). Two new and five known stilbenes have been isolated from *P. calurum* (Starks et al., 2012). These stilbenes exhibited antiproliferative activities on several cancer cell lines (Starks et al., 2012). Two new stilbenes of nine stilbenes were isolated from *Paphiopedilum godefroyae*. These stilbenes from *P. godefroyae* exhibited cytotoxicity against human small cell lung cancer (NCI-H187) cell line (Lertnitikul et al., 2016). A phenanthrene with antifungal activity, lusianthrin was found in *Cypripedium macranthos* var. *rebunense* (Shimura et al., 2007). Orchinol, a dihydrophenanthrene and cypripedin, a

phenanthrenequinone, have been isolated from the leaves of *C. calceolus* (Schmalle and Hausen, 1979).

5.2. Flavonoids

Flavonoids are a large group of plant secondary metabolites, widely found in the plant kingdom. They are biosynthesized through the shikimate and acetate-malonate pathways (Dewick and Demirci, 2009). The structure of flavonoids consists of two benzene rings (A and B) joined by a heterocyclic pyran ring (C) Flavonoids are divided into subclasses according to their basic skeletons, for example, flavones (e.g. luteolin and apigenin), flavonols (e.g. kaempferol, quercetin, and myricetin), flavanones (e.g. hesperetin and naringenin) (Kumar and Pandey, 2013). Flavonoids found so far in plants of the subfamily Cypripedioideae are members of these three groups.

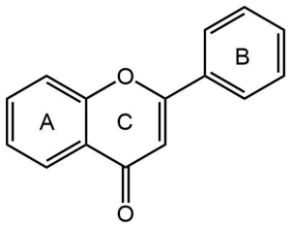

Flavone skeleton

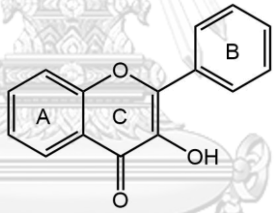

flavonol skeleton

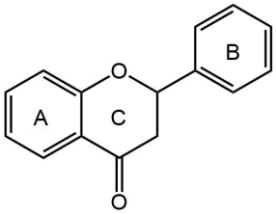

flavanone skeleton

Flavonoids possess various biological effects such as antioxidant, antimutagenic, anticarcinogenic and anti-inflammatory effects. (Panche et al., 2016). Antifungal activity of chrysin from *Cypripedium macranthos* var. *rebunense* (Shimura et al., 2007), and cytotoxicity of pinocembrin from the roots of *Paphiopedilum godefroyae* have been reported (Lertnitikul et al., 2016).

In addition to stilbenoids and flavonoids, an alkyl resorcinol, 5-(2-acetoxynonyl) resorcinol, has been isolated from *Phragmipedium calurum* (Starks et al., 2012). The distribution of compounds found in plants of the subfamily Cypripedioideae, together with their biological activities, and the chemical structures of these compounds are shown in **Table 1** and **Figure 2**, respectively.

Table 1. Distribution of compounds in the subfamily Cypripedioideae

Compounds	Sources	Activity	References
A. Stilbenoids			
(*E*)-3′-hydroxy -5′-methoxystilbene [(*E*)-3-methoxy -5-hydroxystilbene] (1)	*Phragmipedium calurum* *P. longifolium* *Paphiopedilum exul*	-	(Garo et al., 2007, Starks et al., 2012, P et al., 2016)
(*E*)-2,3′-dihydroxy -5′-methoxystilbene [(*E*)-3-methoxy -5,2′-dihydroxystilbene] (2)	*Phragmipedium calurum* *P. longifolium* a hybrid of *Phragmipedium longifolium* and *P. lindleyanum* *Paphiopedilum godefroyae* *P. exul*	Cytotoxic	(Starks et al., 2012, Garo et al., 2007, Lertnitikul et al., 2016)
(*E*)-3,3′-dihydroxy -5′-methoxystilbene (thunalben) (3)	*Phragmipedium longifolium* *Paphiopedilum exul*	-	(Garo et al., 2007, P et al., 2016)
(*E*)-3′,4-dihydroxy -5′-methoxystilbene (4)	*Paphiopedilum godefroyae*	Cytotoxic	(Lertnitikul et al., 2016)
(*E*)-3′-hydroxy -2,5′-dimethoxystilbene (5)	*Paphiopedilum godefroyae*	Cytotoxic	(Lertnitikul et al., 2016)

Table 1. Continued

Compounds	Sources	Activity	References
(*E*)-2,3′-dihydroxy -5,5′-dimethoxystilbene (6)	a hybrid of *Phragmipedium longifolium* and *P. lindleyanum* *Paphiopedilum godefroyae*	Cytotoxic	(Garo et al., 2007, Lertnitikul et al., 2016)
(*E*)-2-hydroxy -3′,5′-dimethoxystilbene (7)	*Phragmipedium calurum* *Paphiopedilum godefroyae*	Cytotoxic	(Starks et al., 2012, Lertnitikul et al., 2016)
(*E*)-2,3-dihydroxy -3′,5′-dimethoxystilbene (8)	*Phragmipedium calurum* *Paphiopedilum godefroyae*	Cytotoxic	(Starks et al., 2012, Lertnitikul et al., 2016)
(*E*)-3′,4′-dihydroxy -5′-methoxystilbene (9)	*Phragmipedium calurum*	-	(Garo et al., 2007)
(*E*)-3-hydroxy -6′-(4-hydroxybenzyl) -5′-methoxystilbene (10)	*Phragmipedium calurum* *P. longifolium* a hybrid of *Phragmipedium longifolium* and *P. lindleyanum*	-	(Garo et al., 2007)

Table 1. Continued

Compounds	Sources	Activity	References
(*E*)-2,3′-dihydroxy -6′-(4-hydroxybenzyl) -5′-methoxystilbene [(*E*)-3-methoxy-2-(4-hydroxybenzyl)-5,2′-dihydroxystilbene)] (11)	*Phragmipedium calurum* *P. longifolium* a hybrid of *Phragmipedium longifolium* and *P. lindleyanum* *Paphiopedilum exul*	-	(Garo et al., 2007, P et al., 2016)
(*E*)-2,5′-dihydroxy -6′-(4-hydroxybenzyl) -5,3′-dimethoxystilbene (12)	a hybrid of *Phragmipedium longifolium* and *P. lindleyanum*	-	(Garo et al., 2007)
(*E*)-5′-hydroxy -6′-(4-hydroxybenzyl) -3′-methoxystilbene (13)	*Phragmipedium calurum* *P. longifolium*	Cytotoxic	(Garo et al., 2007, Starks et al., 2012)
(*E*)-2,5′-dihydroxy -6′-(4-hydroxybenzyl) -3′-methoxystilbene (14)	*Phragmipedium calurum* *P. longifolium*	-	(Garo et al., 2007)
(*E*)-2-hydroxy -6′-(4-hydroxybenzyl) -3′,5′-methoxystilbene (15)	*Phragmipedium calurum*	Cytotoxic	(Starks et al., 2012)

Table 1. Continued

Compounds	Sources	Activity	References
(*E*)-2,3-dihydroxy -6′-(4-hydroxybenzyl) -3′,5′-dimethoxystilbene (16)	a hybrid of *Phragmipedium longifolium* and *P. lindleyanum*	-	(Garo et al., 2007)
(*E*)-3′-hydroxy -2′,6′-bis(4-hydroxybenzyl) -5′-methoxystilbene (17)	*Phragmipedium calurum* *P. longifolium*	-	(Garo et al., 2007)
(*E*)-2,3′-dihydroxy -2′,6′-bis(4-hydroxybenzyl) -5′-methoxystilbene (18)	*Phragmipedium calurum* *P. longifolium*	-	(Garo et al., 2007)
(*E*)-5′-hydroxy -4′-(4-hydroxybenzyl) -3′-methoxystilbene (19)	*Phragmipedium calurum*	Cytotoxic	(Starks et al., 2012)
Phragmidimer A (20)	a hybrid of *Phragmipedium longifolium* and *P. lindleyanum*	-	(Garo et al., 2007)
Phragmidimer B (21)	*Phragmipedium longifolium* a hybrid of *Phragmipedium longifolium* and *P. lindleyanum*	-	(Garo et al., 2007)

Table 1. Continued

Compounds	Sources	Activity	References
2-(5′-hydroxy -3′-methoxyphenyl) -6-hydroxy -5-methoxybenzofuran (22)	*Paphiopedilum godefroyae*	Cytotoxic	(Lertnitikul et al., 2016)
2-(5′-hydroxy-3′-methoxyphenyl)-5,6-dimethoxybenzofuran (23)	*Paphiopedilum godefroyae*	Cytotoxic	(Lertnitikul et al., 2016)
2-(3′,5′-dimethoxyphenyl) -6-hydroxy -5-methoxybenzofuran (24)	*Paphiopedilum godefroyae*	Cytotoxic	(Lertnitikul et al., 2016)
Lusianthrin (25)	*Cypripedium macranthos var. rebunense*	Antifungal	(Shimura et al., 2007)
Orchinol (26)	*C. calceolus*	-	(Schmalle and Hausen, 1979)
Cypripedin (27)	*C. calceolus*	Skin sensitizing	(Schmalle and Hausen, 1979)

Table 1. Continued

Compounds	Sources	Activity	References
B. Flavonoids Chrysin (28)	*Cypripedium macranthos var. rebunense*	Antifungal	(Shimura et al., 2007)
Galangin (29)	*Paphiopedilum godefroyae* *P. exul*	Anticancer Antiinflammatory Antimicrobial	(Lertnitikul et al., 2016, P et al., 2016)
Pinocembrin(30)	*Paphiopedilum exul*	-	(P et al., 2016)
Alpinetin (31)	*Paphiopedilum exul*	Cytotoxic	(P et al., 2016)
C. miscellaneous 5-(2-acetoxynonyl) resorcinol (32)	*Phragmipedium calurum*	-	(Starks et al., 2012)

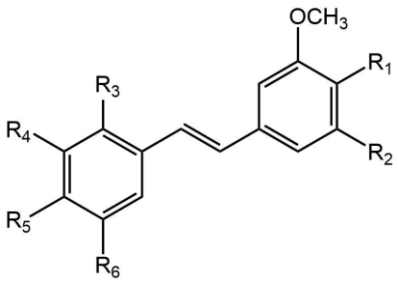

	R_1	R_2	R_3	R_4	R_5	R_6
1	H	OH	H	H	H	H
2	H	OH	OH	H	H	H
3	H	OH	H	OH	H	H
4	H	OH	H	H	OH	H
5	H	OH	OCH_3	H	H	H
6	H	OH	OH	H	H	OCH_3
7	H	OCH_3	OH	H	H	H
8	H	OCH_3	OH	OH	H	H
9	OH	OH	H	H	H	H

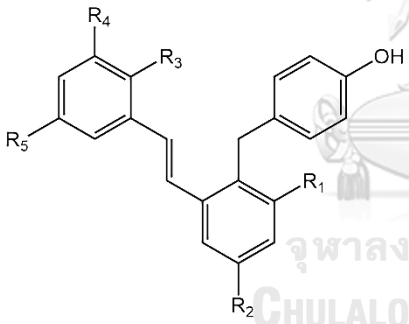

	R_1	R_2	R_3	R_4	R_5
10	OCH_3	H	H	OH	H
11	OCH_3	OH	OH	H	H
12	OH	OCH_3	OH	H	OCH_3
13	OH	OCH_3	H	H	H
14	OH	OCH_3	OH	H	H
15	OCH_3	OCH_3	OH	H	H
16	OCH_3	OCH_3	OH	OH	H

Figure 2. Structures of the compounds distributed in the subfamily Cypripedioideae

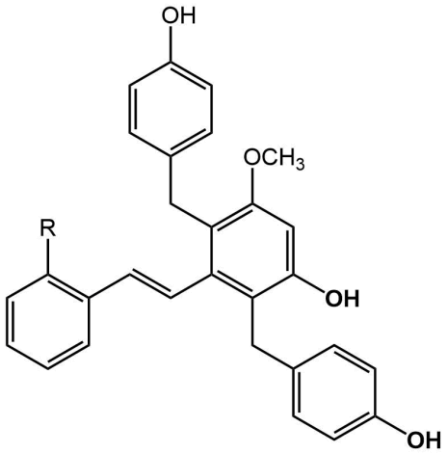

17 R = H

18 R = OH

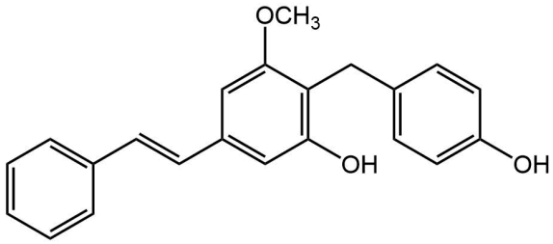

19

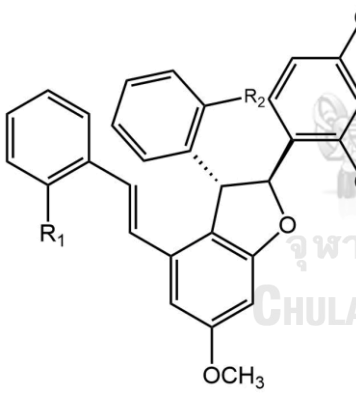

	R_1	R_2
20	H	OH
21	OH	H

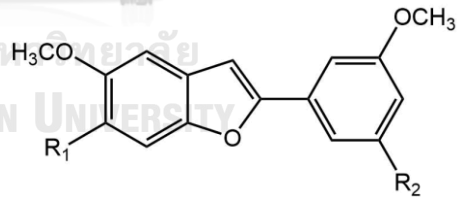

	R_1	R_2
22	OH	OH
23	OCH_3	OH
24	OH	OCH_3

Figure 2. Structures of the compounds distributed in the subfamily Cypripedioideae (Continued)

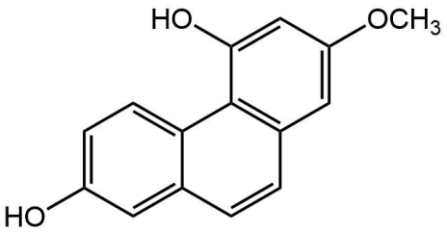

25

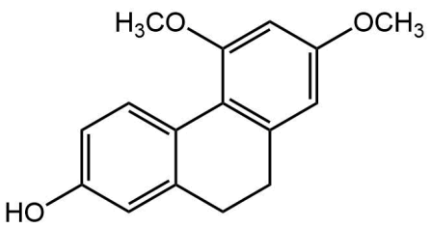

26

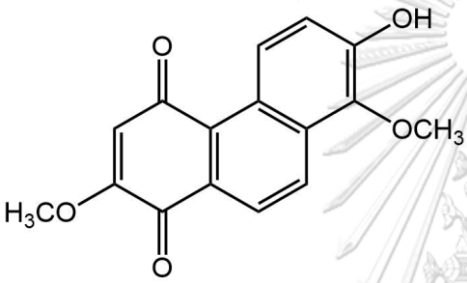

27

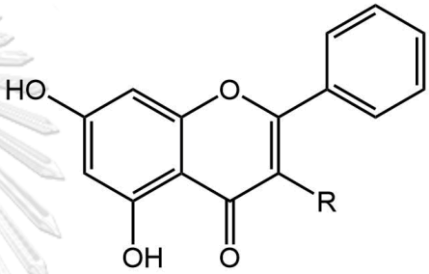

28 R = H

29 R = OH

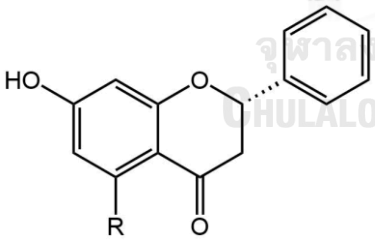

30 R = OH

31 R = OCH_3

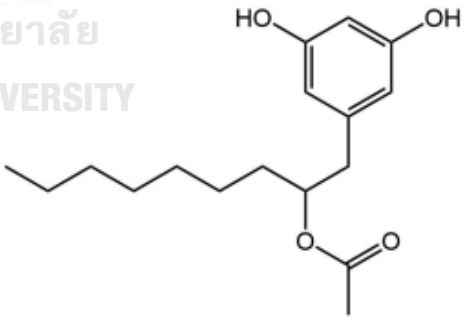

32

Figure 2. Structures of the compounds distributed in the subfamily Cypripedioideae (Continued)

6. Topoisomerase targeting drugs development

Cancer is one of the leading causes of mortality and morbidity around the world. The uncontrolled growth of abnormal cells produces genetic alteration and instability within the cell and then, leads to transformation of normal cells into malignant cells (Iqbal et al., 2017). The interruption of cell proliferation and promotion of apoptosis are the major mechanisms of action of chemotherapy (Freres et al., 2017). Chemotherapeutic agents include topoisomerase I inhibitors (camptothecin, irinotecan, doxorubicin etc.), alkylating agents (cyclophosphamide, cisplatin, oxaliplatin etc.), microtubules acting agents (vincristine, vinblastine, paclitaxel, docetaxel etc.). They are highly effective on many types of cancer. Plants are one of the alternative sources of anticancer agents and many anticancer drugs used in clinical are derived from plant metabolites. The new promising agents flavopiridol and combretastin A4 phosphate are in clinical development based on selective activity against cancer-related molecular targets. The basic novel flavonoid structure of flavopiridol derived from rohitukine, isolated from *Dysoxylum binectariferum* Hook. f. (Meliaceae). Combretastin A4 phosphate is a water-soluble analog of combretastatin, isolated from *Combretum caffrum* (Eckl. & Zeyh.) Kuntze (Combretaceae), South African “bush willow” (Cragg and Newman, 2005).

Research on the underlying mechanisms of anticancer drugs is one of the important steps in drug development. DNA topoisomerase (Top) plays an important role in the control of DNA topology by cleaving and rejoining DNA strand and regulates the physiological function of genome (Kathiravan et al., 2013). Topoisomerase inhibitors interfere the normal function of topoisomerase enzymes I and II in the transcription and replication of DNA and then lead to cell death. There are two types of DNA topoisomerase targeted drug: Top I inhibitors such as irinotecan, and topotecan (camptothecin derivatives) and Top II inhibitors such as etoposide, and teniposide (epipodophyllotoxin) (Freres et al., 2017). Topoisomerase inhibitors can be distinguished into two categories according to the mechanism of inhibition: topoisomerase poisons, and catalytic inhibitors. Topoisomerase poison causes the formation of a ternary protein-DNA-drug complex. This “cleavage complex” prevents the DNA re-ligation and leads to cell death. Catalytic inhibitor

binds to the topoisomerase active site and prevents the binding of the DNA substrate (Hevener et al., 2018). Most of clinically used topoisomerase inhibitors are the topoisomerase poison mechanistic category. Several catalytic inhibitors have been promised as potentially novel anti-cancer agents with significantly reduced toxicity profiles such as evodiamine (quinazoline-carboline alkaloid), dual catalytic inhibitor of topoisomerase I and II (Pan et al., 2012). Furthermore, podophyllotoxin linked β-carboline congeners have reported anticancer activity against human cell lines with suggested topoisomerase II inhibitory mechanism (Sathish et al., 2018).

CHAPTER III
EXPERIMENTAL

1. Source of plant materials

Paphiopedilum callosum plants were purchased from Ao Luek, Krabi, Thailand in September 2017. Plant identification was performed by Associate Professor Thatree Padungcharoen, together with comparison to botanical information in literature (Cribb, 1987). A voucher specimen has been deposited at the Museum of Natural Medicines, Faculty of Pharmaceutical Sciences, Chulalongkorn University, Bangkok, Thailand.

2. General techniques

2.1. Thin layer chromatography

Techniques	:	One dimension, ascending
Adsorbent	:	Silica gel 60 F254 (E. Merck) pre-coated plates
Layer thickness	:	0.2 mm
Distance	:	5 cm
Temperature	:	Laboratory temperature (30-35 °C)
Detection	:	1. Ultraviolet light (254 and 365 nm)
		2. Spraying with anisaldehyde reagents and heating at 105 °C for 10 min
		3. Spraying with Natural product reagent and detection under UV-365 nm

2.2. Column chromatography

2.2.1. Vacuum liquid chromatography (VLC)

Adsorbent : Silica gel 60 (no.7734) particle sizes 0.063-0.200 mm (E.Merck)

Packing method : Dry packing

Sample loading : The sample was dissolved in a small amount of the eluent, mixed with a small quantity of the adsorbent, triturated, dried and then gradually placed on the top of the column.

Detection : Each fraction was examined by TLC as described in 2.1.

2.2.2. Conventional column chromatography

Adsorbent : Silica gel 60 (no.7734) particle size (0.063-0.200 mm) and silica gel 60 (no.9385) particle size 0.040-0.063 mm (E. Merck).

Packing method : Wet packing; the adsorbent was mixed with the eluent into a slurry and then poured into the column and allowed to settle.

Sample loading : The sample was dissolved in the a small amount of the eluent, and then applied gently on the top of the column.

Detection : Each fraction was examined by TLC technique, as described in 2.1.

2.2.3. Size-exclusion column chromatography

Adsorbent : Sephadex LH-20 (Pharmacia Biotech AB)

Packing method : A suitable organic solvent was used as the eluent. Gel filter was suspended in the eluent and allowed to swell for 24 hours and then poured into the column and left to settle.

Sample loading : The sample was dissolved in a small amount of

the eluent, and then applied gently on top of the column.

Detection : Each fraction was examined by TLC as described in 2.1.

2.3. Spectroscopic techniques

2.3.1. Infrared (IR) spectra

The IR spectrum (KBr disc) of PC1 was recorded on a Perkin Elmer FT-IR 1760X Spectrometer (Scientific and Technological Research Equipment Center, Chulalongkorn University).

2.3.2. Mass spectra

Mass spectra were obtained on a microTOF Bruker Daltonics (Department of Chemistry, Faculty of Science, Mahidol University).

2.3.3. Proton and carbon-13 nuclear magnetic resonance (^{1}H and ^{13}C NMR) spectra

^{1}H NMR (300 MHz) and ^{13}C NMR (75 MHz) spectra were recorded on a Bruker DPX-300 FT-NMR spectrometer (Faculty of Pharmaceutical Sciences, Chulalongkorn University).

^{1}H NMR (500 MHz) and ^{13}C NMR (125 MHz) spectra were recorded on an INOVA-500 NMR spectrometer (500 MHz) (Scientific and Technology Research Equipment Center, Chulalongkorn University).

Deuterated acetone (acetone-d_6) was used as the solvent. The chemical shifts in ppm of the solvent signals were recorded as reference for the calibration.

3. Extraction and isolation

3.1. Extraction and fractionation

The roots of *P. callosum* were washed with water, then dried in hot air oven at 50°C. The dried roots (250 g) were powdered and macerated with MeOH at room temperature for three times (3 x 1.5 L). The methanolic extract was filtered and concentrated under reduced pressure at 45°C using the rotatory evaporator. The

resulted methanolic extract (30 g, 12.0% yield of dried weight) was separated by silica gel CC (0.6 kg, 10 x 22 cm), using *n*-hexane-acetone (1:0 to 0:1) and EtOAC - MeOH (20:1 to 1:1) as the mobile phase for gradient elution. Forty-two fractions were collected and the column was washed down with MeOH. Fractions were combined according to TLC profiles into seven fractions including fractions A (1.1 g), B (1.0 g), C (0.2 g), D (0.4 g), E (2 g), F (2.5 g), and G (22.0 g) (**Figure 3**).

3.2. Isolation of compounds from fraction B

Fraction B (1.1 g) was chromatographed on a silica gel column (160 g, 4.5 x 26 cm), eluted with CH_2Cl_2-EtOAc (20:1). Forty-three fractions were obtained and combined according to the similarity of their TLC patterns into thirteen subfractions (BA-BM): BA (20.0 mg), BB (25.0 mg), BC (95.0 mg), BD (70.0 mg), BE (15.0 mg), BF (10.0 mg), BG (30.0 mg), BH (50.0 mg), BI (30.0 mg), BJ (20.0 mg), BK (150.0 mg), BL (250.0 mg), and BM (200.0 mg).

Subfraction BC (95.0 mg) was separated by Sephadex LH-20 CC, using MeOH as the eluent to give fourteen subfractions (BC1-BC14) .Subfraction BC11 was purified on a silica gel column, eluted with *n*-hexane:acetone (8:2) to yield compound PC2 (14.2 mg, 0.005% yield of dried weight) as brown semisolid.

Subfration BJ (20.0 mg) was purified on a Sephadex LH 20 column, eluted with MeOH to yield two (BJ1-BJ2). Compound PC3 (7.0 mg, 0.003% yield of dried weight) was directly obtained from subfraction BJ2 as light-yellow amorphous (**Figure 3**).

3.3. Isolation of compounds from fraction C

Fraction C (0.2 g) was separated on a silica gel column (20 g, 2 x 14 cm), eluted with CH_2Cl_2-MeOH (98:2) to give fifty-eight fractions. Fraction with similar patterns were combined into seven subfractions: CA (20.0 mg), CB (70.0 mg), CC (18.0 mg), CD (20.0 mg), CE (10.0 mg), CF (15.0 mg), and CG (30.0 mg).

Subfraction CB (70.0 mg) was further separated on a Sephadex LH20 column, eluted with MeOH to yield fifteen fractions. They were combined into six subfractions (CB1-CB6). Compound PC1 (38.2 mg, 0.015% yield of dried weight) was directly obtained from subfraction CB4 as yellowish brown semisolid. Subfraction CB6 was

separated on a silica gel column, eluted with *n*-hexane-EtOAc (9:1) to give compound PC4 (17.5 mg, 0.007% yield of dried weight) as yellow needle crystals (**Figure 4**).

3.4. Isolation of compounds from fraction D

Fraction D (0.4 g) was separated on a silica gel column (30 g, 2.5 x 14 cm), eluted with *n*-hexane-EtOAc (3:2) to give fifty fractions which were combined according to TLC patterns into ten subfractions: DA (20.0 mg), DB (6.5 mg), DC (3.0 mg), DD (10.0 mg), DE (40.0 mg), DF (10.0 mg), DG (70.5 mg), DH (90.0 mg), DI (96.0 mg), and DJ (50.0 mg).

Subfraction DD (10.0 mg) was purified on a silica gel column, eluted with CH_2Cl_2-MeOH (98:2) to give compound PC5 (5.0 mg), 0.002% yield of dried weight) as brown semisolid.

Subfraction DE (40.0 mg) was separated on a Sephadex LH20 column to yield six subfractions (DE1-DE6). Purification of DE3 by silica gel CC, using CH_2Cl_2-MeOH (50:1) as the eluent, gave compound PC6 (15.0 mg, 0.006% yield of dried weight) as brown semisolid (**Figure 5**).

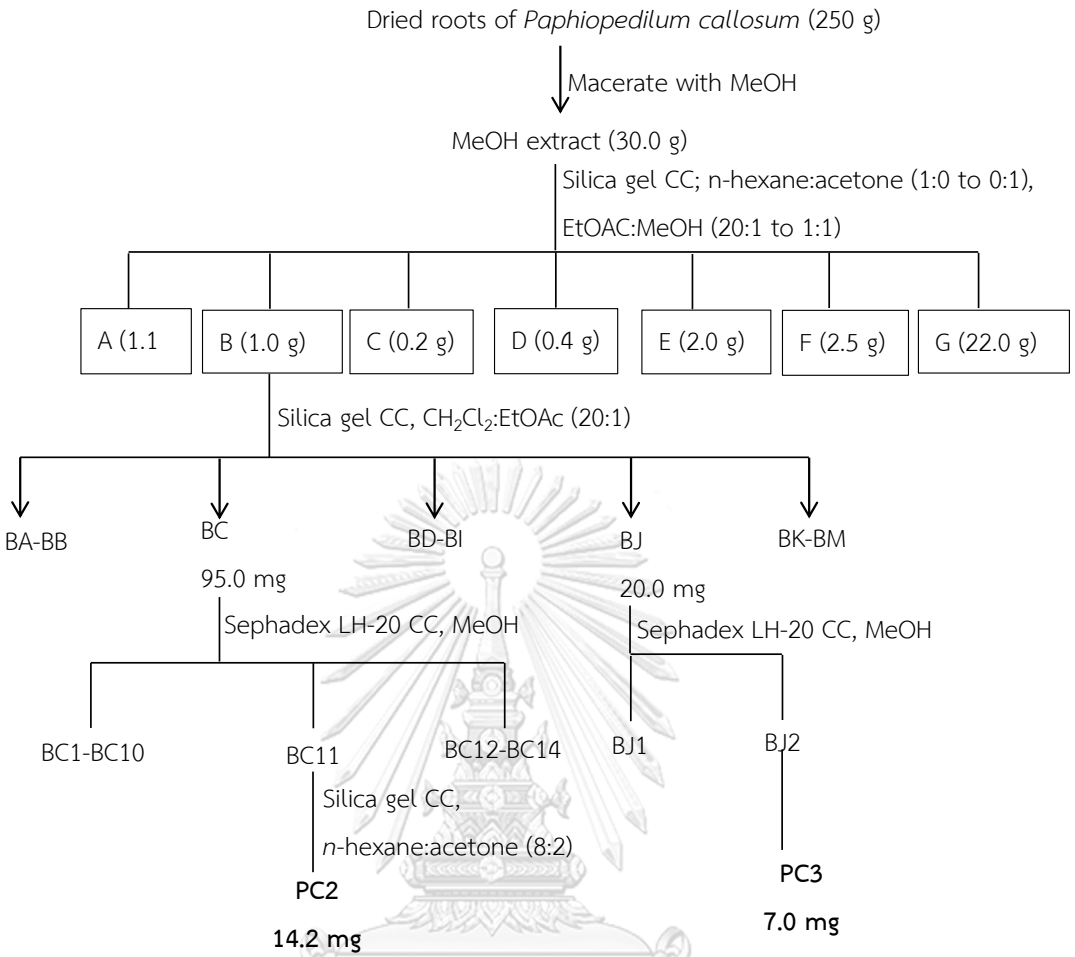

Figure 3. Scheme for the extraction of the methanolic extract of *P. callosum* roots and the isolation of compounds from fraction B

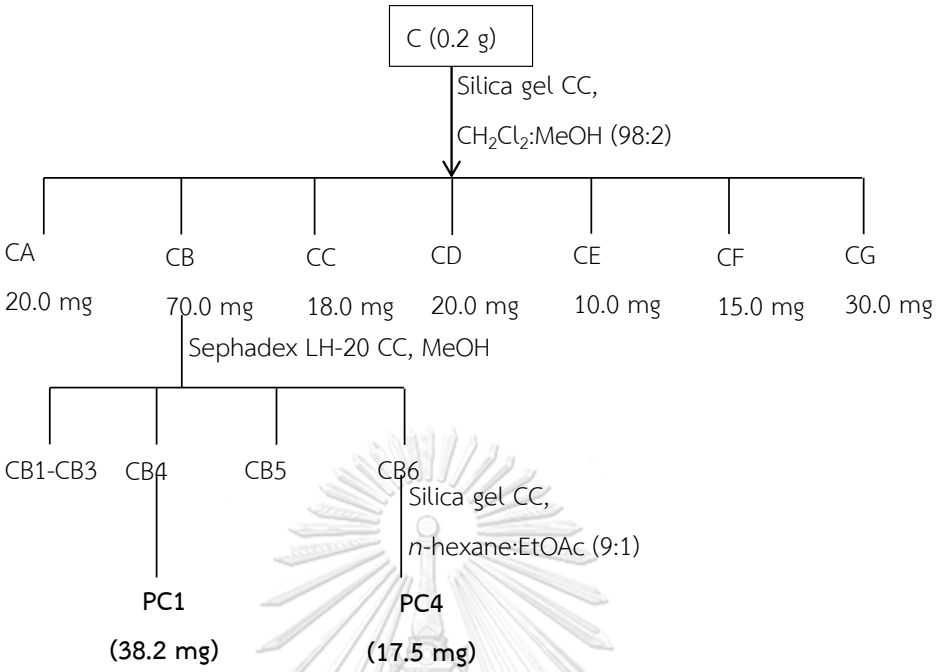

Figure 4. Scheme for the isolation of compounds from fraction C of the methanolic extract of *P. callosum* roots

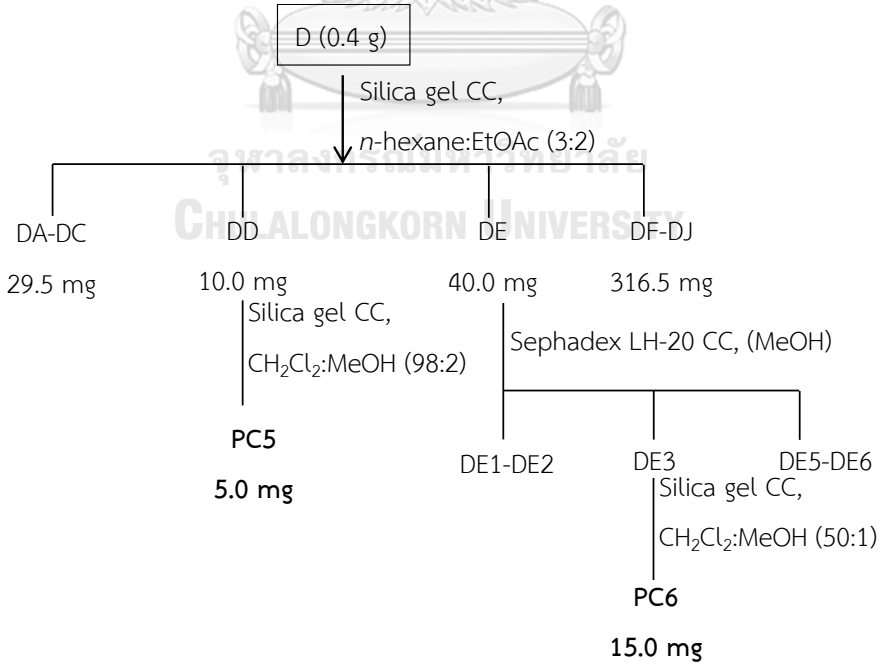

Figure 5. Scheme for the isolation of compounds from fraction D of the methanolic extract of *P. callosum* roots

4. Physical and spectral data of isolated compounds

4.1. Compound PC1

Compound PC1 was obtained as yellowish brown semisolid. The compound was soluble in acetone, dichloromethane and methanol.

IR : V_{max} cm^{-1} (KBr) 3360, 1652, 1590, 1472, 1148, 774; (**Figure 8**)

ESI-MS : *m/z* (% rel. int.) 285.1126 $[M-H]^-$ (calculated for $C_{17}H_{17}O_4$, 285.1127) (**Figure 9**)

^{1}H NMR : **δ** ppm, 500 MHz, in acetone-d_6; 3.77 (1H, *s*), 3.88 (2H, *s*), 6.31 (1H, *t*, *J* = 1.8 Hz), 6.56 (1H, *t*, J = 1.8 Hz), 6.64 (1H, *t*, *J* = 1.8 Hz), 6.67 (2H, *d, J* = 8.4 Hz), 7.18 (1H, *t*, *J* = 8.4 Hz), 7.41 (1H, *d*, *J* = 16.5 Hz), 7.49 (1H, *d*, *J* = 16.5 Hz), 8.30 (1H, *s*); (**Figure 10,11**).

^{13}C NMR : **δ** ppm, 125 MHz, in acetone-d_6; 55.4, 56.1, 101.2, 104.5, 104.9, 106.2, 115.1, 120.8, 129.3, 132.9, 142.4, 159.5, 159.6, 159.6, 162.1; (**Figure 12**).

4.2. Compound PC2

Compound PC2 was obtained as brown semisolid. The compound was soluble in acetone, dichloromethane and methanol.

ESI-MS : *m/z* (% rel. int.) 255.1029 $[M-H]^-$ (calculated for $C_{16}H_{16}O_3$, 255.1021) (**Figure 17**)

^{1}H NMR : **δ** ppm, 300 MHz, in acetone-d_6; 3.79 (1H, *s*), 3.90 (1H, *s*), 6.35 (1H, *t*, *J* = 2.3 Hz), 6.65 (1H, br *s*), 6.69 (1H, br *s*), 6.96 (1H, *t*, *J* = 7.9 Hz), 7.02 (1H, *d*, *J*= 8.1 Hz), 7.12 (1H, *d*, 16.5) 7.27 (1H, *td*, *J* = 7.9, 1.5 Hz), 7.45 (1H, *d*, *J* = 16.5 Hz), 7.65 (1H, *dd*, *J* = 7.9 Hz) 8.38 (1H, *s*) (**Figure 18, 19**)

^{13}C NMR : **δ** ppm, 75 MHz, in acetone-d_6; 54.6, 55.0, 100.8, 103.6, 105.8, 111.1, 120.6, 123.3, 126.0, 126.2, 128.8, 129.0, 140.1, 157.1, 158.7, 161.3; (**Figure 20**).

4.3. Compound PC3

Compound PC3 was obtained as light-yellow amorphous solid. The compound was soluble in acetone and methanol.

ESIMS : *m/z* (% rel. int.) 283.0601 $[M-H]^-$ (calculated for $C_{16}H_{12}O_5$, 283.0606) (**Figure 25**)

^{1}H NMR : **δ** ppm, 500 MHz, in acetone-d_6; **δ** ppm, 500 MHz, in acetone-d_6; 3.88 (1H, *s*), 6.27 (1H, *dd*, *J* = 2.3 Hz), 6.51 (1H, *dd*, *J* = 2.3 Hz), 7.57 (3H, *m*), 8.08 (2H, *m*), 12.68 (1H, *s*); (**Figure 26**).

^{13}C NMR : **δ** ppm, 125 MHz, in acetone-d_6; 60.5, 94.6, 99.5, 106.1, 129.2, 129.5, 131.6, 131.7, 140.1, 156.5, 158.0, 163.3, 165.2, 179.7; (**Figure 27**).

4.4. Compound PC4

Compound PC4 was obtained as yellow needle crystals. The compound was soluble in acetone and methanol.

ESI-MS : *m/z* (% rel. int.) 269.0451 $[M-H]^-$ (calculated for $C_{15}H_{10}O_5$, 269.0450) (**Figure 32**)

^{1}H NMR : **δ** ppm, 300 MHz, in acetone-d_6; 6.29 (1H, *s*), 6.56 (1H, *s*), 7.54 (3H, *m*), 8.25 (2H, *d*, *J* = 7.8 Hz), 12.08 (1H, *s*); (**Figure 33**).

^{13}C NMR : **δ** ppm, 75 MHz, in acetone-d_6; 93.7, 98.4, 103.5, 127.6, 128.5, 130.0, 131.3, 137.0, 145.3, 157.1, 161.6, 164.4, 176.1, (**Figure 34**).

4.5. Compound PC5

Compound PC5 was obtained as brown semisolid. The compound was soluble in acetone, dichloromethane and methanol.

ESI-MS : *m/z* (% rel. int.) 271.0976 $[M-H]^-$ (calculated for $C_{16}H_{16}O_4$, 271.0970) (**Figure 38**).

^{1}H NMR : **δ** ppm, 500 MHz, in acetone-d_6; 3.76 (1H, *s*), 3.77 (1H, *s*), 6.32 (1H, *t*, *J* = 1.9 Hz), 6.63 (1H, *t*, *J* = 1.9 Hz), 6.67 (1H, *t*, *J* = 1.9 Hz), 6.70 (1H, *dd*, *J* = 9.0, 3.0 Hz), 6.82 (1H, *d*, *J* = 9.0 Hz), 7.13 (1H, *d*, *J* = 16.3 Hz), 7.15 (1H, *d*, *J* = 3.0 Hz), 7.44 (1H, *d*, *J* = 16.3 Hz), 8.19 (1H), 8.31 (1H);

(**Figure 39, 40**)

^{13}C NMR : **δ** ppm, 125 MHz, in acetone-d_6; **δ** ppm, 55.5, 55.9, 101.6, 104.4, 106.7, 111.6, 115.6, 117.5, 124.6, 125.7, 129.5, 141.1, 149.9, 154.3, 159.6, 162.2; (**Figure 41**).

4.6. Compound PC6

Compound PC6 was obtained as brown semisolid. The compound was soluble in acetone, dichloromethane and methanol.

ESI-MS : *m/z* (% rel. int.) 241.0869 $[M-H]^-$ (calculated for $C_{15}H_{14}O_3$, 241.0864); (**Figure 44**)

^{1}H NMR : **δ** ppm, 300 MHz, in acetone-d_6; 3.79 (1H, *s*), 6.34 (1H, *t*, *J* = 2.1 Hz), 6.65 (1H, br *s*), 6.69 (1H, br *s*), 6.86 (1H, *t*, *J* = 7.7 Hz), 6.91 (1H, *d*, *J* = 7.7 Hz), 7.11 (1H, *td*, *J* = 7.7 , 1.4 Hz), 7.15 (1H, *d*, *J* = 16.5 Hz), 7.47 (1H, *d*, *J* = 16.5 Hz), 7.59 (1H, *d*, *J* = 7.7, 1.4 Hz), 8.42 (1H, *s*), 8.71 (1H, *s*) (**Figure 45**, **46**).

^{13}C NMR : **δ** ppm, 75 MHz, in acetone-d_6; 54.6, 100.7, 103.4, 105.8, 115.8, 119.8, 123.7, 124.3, 126.5, 128.4, 140.2, 154.9, 158.7, 161.3; (**Figure 47**)

5. Evaluation of cytotoxicity

5.1. Topoisomerase I poison using yeast cell-based assay

5.1.1. Yeast expression

Saccharomyces cerevisiae strain RS 190 (MATa, top 1 **Δ**) was purchased from American Type Culture Collection. The genes of *Arabidopsis thaliana* topoisomerase I were cloned into gateway expression vector pYES-DEST52 by the gateway cloning vector and then the integrity of the constructs was verified by DNA sequencing. The expression vector carries strong inducible promoter (pGAL1) that regulated the expression in *S. cerevisiae*. Moreover, this plasmid has URA3 selectable marker for the selection and integration of construct in auxotrophic yeast strain.

5.1.2. Yeast cell culture media

Growth media (YPD media) (Difco TM) : Two types of media (YPD agar and YPD broth) were used for maintaining and propagation of the yeasts cell in molecular microbiology procedures. The ingredients of culture media are described in (**Table 10**) and (**Table 11**).

Synthetic complete media lacking uracil (S.C. ura$^-$ media) : S.C. ura- media was used for the purpose of selecting and maintaining transgenic yeast. The components of this media are described in (**Table 12**) and (**Table 13**).

5.1.3. Yeast cell-based assay

To evaluate the TopI inhibitory activity of *P. callosum* root extract, yeast cell-based assay was performed using transgenic yeast. Complex media (YPD agar and YPD broth) were used to activate the propagation and growth of yeasts. A yeast colony was taken from the YPD growth media and then suspended in SC ura$^-$ media containing glucose. The suspension of yeast was incubated in a shaking incubator at 30°C (200 rpm) for 18 hours. The yeast suspension was adjusted to 0.3 OD_{600} and diluted as serial ten-fold dilutions (10^0, 10^{-1}, 10^{-2}, and 10^{-3}). Camptothecin (10, 5, and 2.5 µg/mL) was used as a positive control. DMSO (1%) was used as the vehicle control.

The tested samples were dissolved in dimethylsulfoxide (DMSO) and then filtered through a Millipore filter (0.45 µm). They are diluted to different concentrations (500, 250, 125 µg/mL of extract and 100, 50, 25 µM for isolated compounds). The samples were added to selective SC ura$^-$ media containing 2% glucose and galactose. Serially diluted yeast suspensions (5 µL) were spotted on sample-containing media and then spotted plates were incubated at 30°C for 48 hours. The viability of the yeast cells was observed by comparing the viabilities of the colonies on the vehicle control culture (DMSO) and the positive control culture (camptothecin) to those on the two types of media (2% galactose and glucose agar media).

5.2. Cytotoxicity assay against cancer cell lines

The cytotoxicity assay against two human cancer cell lines including NCI-H187 and MCF-7 was done by the Bioassay Laboratory of the National Center for Genetic Engineering and Biotechnology (BIOTEC). The test was performed using resazurin microplate assay (REMA) according to the protocol developed by O'Brien et al. (O'Brien et al., 2000), with camptothecin, tamoxifen, doxorubicin and ellipticin as positive control. The concentration of test compounds (50 µg/mL) was used as final maximum concentration.

In brief, cells at logarithmic growth phase were harvested and diluted to appropriate concentration (9×10^5 cells/mL) for both NCI-H187 and MCF-7 in fresh medium. Test samples (5 µL) and 45 µL of cell suspensions were plated to 384 well-plates and incubated at 37°C under 5% CO_2 overnight. After the incubation period (5 days for NCI-H187 and 3 days for MCF-7), 12.5 µL of 62.5 µg/mL resazurin solution was added to each well, and the cells were further incubated at 37°C for 4 hours. SpectraMax M5 multi-detection microplate reader (Molecular Devices, USA) measured the fluorescence signal at excitation and emission wavelengths of 530 nm and 590 nm, respectively. The percent inhibition of cell growth was calculated as follows.

$$\% \text{ inhibition} = [1-(FUT/FUC)] \times 100$$

FUT and FUC are the mean fluorescent units under treated and untreated conditions, respectively. Dose response curves were plotted for six concentrations of two-fold serially diluted test compounds, and the sample concentration that inhibited cell growth by 50% (IC_{50} value) was derived using SOFTMax pro software (Molecular device, USA).

5.3. DNA-cleavage assay

In the DNA cleavage assay, supercoiled DNA (SC DNA) was used as a substrate. Camptothecin and DMSO were used as positive and vehicle control respectively. The isolated compounds and control were dissolved in DMSO and then diluted to 250 µM and 50 µM respectively. The test compounds added to SC DNA

and TGS buffer and then the reactions started by the addition of 4 units of human topoisomerase I. Deionized water was used to adjust final volume (20 μL). The mixture was incubated at 37ºC for 1 hour. After the incubation period, the reaction was stopped by the addition of SDS buffer (2 μl) followed by the addition of Proteinase K (1 μl) and then incubated again at 37 ºC for 30 min. The reaction was analyzed on a 1.2 % agarose gel by running at 50 V in 0.5 TBE buffer until the dye front is about 70-80% down the gel. Gel was stained with ethidium bromide (EtBr). The area representing supercoiled and relaxed plasmid was determined by Gel Doc machine.

CHAPTER IV
RESULTS AND DISCUSSION

In the present study, the roots of *Paphiopedilum callosum* have been investigated for topoisomerase I (TopI) inhibitory compounds. The investigation was bioassay-guided by a yeast cell-based assay. The methanolic extract of *P. callosum* roots was separated by column chromatography to yield fractions A-G. Fractions B, C, and D showed growth inhibitory activity on modified yeast *Saccharomyces cerevisiae*. They were further separated using chromatographic techniques to yield six compounds. The structure determinations of isolated compounds were based on their spectroscopic data. The isolated compounds were evaluated for the TopI inhibitory activity by a yeast cell-based assay and DNA cleavage assay and for the cytotoxicity against human cancer cell lines including small cell lung carcinoma (NCI-H187) and breast adenocarcinoma (MCF-7).

1. Structure elucidation of compound PC1

Compound PC1 was obtained as yellowish brown semisolid. Its molecular formula of $C_{17}H_{18}O_4$, was established on the basis of the ESI-MS (**Figure 9**) which showed an $[M-H]^-$ ion at *m/z* 285.1126 (calculated for $C_{17}H_{17}O_4$, 285.1127) The IR spectrum (**Figure 8**) displayed the absorption band of hydroxyl at 3360 cm^{-1}.

The ^1H NMR spectrum of PC1 (**Figure 10**) showed one hydroxyl signal at δ_H 8.30 (1H, *s*, 3'-OH), two methoxyl signals at δ_H 3.77 (3H, *s*, 5'-OCH_3) and 3.88 (6H, *s*, 2-OCH_3 , 6-OCH_3), and olefinic signals of a *trans*-double bond at δ_H 7.41 (1H, *d*, *J* = 16.5 Hz, H-**α**) and 7.49 (1H, *d*, *J* = 16.5 Hz, H-**β**). In the aromatic region of δ_H 6.30 - 7.30, two sets of signals representing reciprocally coupled protons were observed. One set was discernible as three triplets, corresponding to three *meta*-coupled protons, at δ_H 6.31 (1H, *t*, *J* = 1.8, H-4′), 6.56 (1H, *t*, *J* = 1.8, H-6′) and 6.64 (1H, *t*, *J* = 1.8, H-2′). The other set, including signals of three *ortho*-coupled protons, appeared as a two-proton doublet at δ_H 6.67 (2H, *d*, *J* = 8.4, H-3, H- 5) and a triplet at δ_H 7.18 (1H, *s*, *J* = 8.4, H-4). The former indicated the presence of a 1,3,5-trisubstituted benzene ring in the structure of PC1 while the latter suggested the presence of a 1,2,3-trisubstituted

benzene ring on which the 1- and 3-substituents were identical. According to the above information, PC1 was proposed as *trans*-stilbene containing two methoxy groups at positions 2 and 6 on one ring, as well as one methoxy and one hydroxy group at positions 3′ and 5′ on the other ring.

The ^{13}C NMR spectrum (**Figure 12**) displayed fourteen carbon signals. The HSQC spectrum (**Figure 13**) revealed that these signals represented seventeen carbons including three methyl, eight methine and six quaternary ones. The presence of three methoxy and one hydroxy groups was evidenced by two methyl signals at δ_C 55.4 (5′-OCH_3) and 56.1 (2-OCH_3/6-OCH_3) together with three methine signals at δ_C 159.5 (C-3′), 159.6 (C2/C6) and 162.1 (C-5′). These information supported the structure proposed for PC1.

The location of the four substituents on the stilbene skeleton was also evidenced by the HMBC spectrum (**Figure 14**, **15, 16**) which exhibited three-bond correlations of C-2/C-6 (δ_C 159.6) with H-4 (δ_H 7.18) and H-**α** (δ_H 7.41), two-bond correlations of C-3′ (δ_C 159.5) with H-2′ (δ_H 6.64) and H-4′ (δ_H 6.31) together with those of C-5′ (δ_C 162.1) with H-4′ (δ_H 6.31) and H-6′ (δ_H 6.56). In addition the HMBC correlations of all oxygenated carbons with their corresponding related methoxyl or hydroxyl protons were clearly observed.

Based on the analysis of all the spectral data, the structure of PC1 was elucidated as 3′-hydroxy-2,6,5′-trimethoxystilbene as shown below. The assignments of its proton and carbon signals, as shown in (**Table 2**) were accomplished on the basis of HSQC and HMBC experiments.

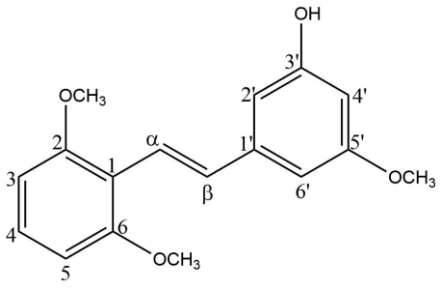

3′-hydroxy-2,6,5′-trimethoxystilbene

Table 2. ^{1}H (500 MHz) and ^{13}C (125 MHz) NMR data of compound PC1 (in acetone-d_6)

Position	δ_H (mult., *J* in Hz)	δ_C	Key HMBC correlation $^{13}C \rightarrow {}^{1}H$
1	-	115.1	H-3, H-5, H-**β**
2	-	159.6	H-4, H-**α**, 2-OCH_3, H-3
3	6.67 (*d*, 8.4)	104.9	H-5
4	7.18 (*t*, 8.4)	129.3	-
5	6.67 (*d*, 8.4)	104.9	H-3
6	-	159.6	H-4, H-**α**, 6-OCH_3, H-5
α	7.41 (*d*, 16.5)	120.8	H-**β**
β	7.49 (*d*, 16.5)	132.9	H-2′, H-6′, H-**α**
1′	-	142.4	H-**α**, H-**β**
2′	6.64 (*t*, 1.8)	106.2	H-4′, H-6′, H-**β**, 3′-OH
3′	-	159.5	H-2′, H-4′, 3′-OH
4′	6.31 (*t*, 1.8)	101.2	H-2′, H-6′, 3'-OH
5′	-	162.1	5′-OCH_3, H-4′, H-6′
6′	6.56 (*t*, 1.8)	104.5	H-2′, H-4′, H-**β**
2-OCH_3	3.88 (*s*)	56.1	-
6-OCH_3	3.88 (*s*)	56.1	-
5′-OCH_3	3.77 (*s*)	55.4	-
3′-OH	8.30 (*s*)	-	-

2. Identification of compound PC2

Compound PC2 was obtained as a brown semisolid. Its molecular formula was determined as $C_{16}H_{16}O_3$ according to its negative $[M-H]^-$ peak at *m/z* 255.1029 (calculated for $C_{16}H_{16}O_3$, 255.1021) in the ESI-MS spectrum (**Figure 17**).

The ^{1}H NMR spectrum of PC2 (**Figure 18**, **19**) was similar to that of PC1 in showing olefinic signals of a *trans*-double bond (δ_H 7.12, 1H, *d*, *J* = 16.5 Hz, H-**β** and δ_H 7.45, 1H, *d*, *J* = 16.5 Hz, H-**α**), three signals corresponding to three *meta*-coupled protons (δ_H 6.35 , 1H, *t*, *J* = 2.3 Hz, H-4′, δ_H 6.65, 1H, br *s,* H-6′ and δ_H 6.69, 1H, br *s*, H-2′), and one hydroxyl signal (δ_H 8.38 , 1H, *s*, 3′-OH). Two methoxyl signals, as shown in the spectrum of PC1, were also observed at δ_H 3.79 (3H, *s*, 5′-OCH_3) and δ_H 3.90 (3H, *s*, 2-OCH_3). However, these signals represented two methoxy groups, differing from those of PC1 which represented three. The rest of signals included four one-proton signals at δ_H 6.96 (*t*, *J* = 7.9 Hz, H-5), 7.02 (*d*, *J* = 7.9 Hz, H-3), 7.27 (*td*, *J* = 7.9 Hz, H-4), 7.65 (*dd*, *J* = 7.9 Hz, H-6). The multiplicity and coupling constants of these four signals implied the presence of a 1,2-disubstitued benzene ring. All of these ^{1}H NMR data indicated that PC2 was an analog of PC1. The only difference was that the methoxy substituent at C-6 of PC1 was missing.

The ^{13}C NMR spectrum (**Figure 20**) exhibited sixteen carbon signals which could be classified, according to the HSQC experiment (**Figure 21**, **22**), into those of two methyl, nine methine and five quaternary carbons. The downfield methine signals at δ_C 157.1(C-2), 158.7 (C-3′) and 161.3 (C-5′) supported the presence of three oxygenated substituents, and the methyl signals at δ_C 54.6 (OCH_3-5′) and 55.0 (OCH_3-2) indicated that two of those substituents were methoxy groups.

In the HMBC spectrum (**Figure 23, 24**), the correlations between the oxygenated carbons and their corresponding hydroxyl or methoxyl protons were observed. The substitution with the hydroxy group at C-3′ was also confirmed by the correlations of C-3′ (δ_C 158.7) with H-4′ (δ_H 6.35) and H-6′ (δ_H 6.65) while the substitution with the methoxy group at C-2 and C-5′ by those of C-2 (δ_C 157.1) with H-4 (δ_H 7.27) , H-6 (δ_H 7.65) and H-**α** (δ_H 7.45), and of C-5′ (δ_C 161.3) with H-6′ (δ_H 6.65), respectively.

On the basis of the above information, as well as the comparison between the ^{1}H and ^{13}C NMR data of PC2 and the reported literature values (Lertnitikul et al., 2016) as shown in (**Table 3**) PC2 was identified as 3′-hydroxy-2,5′-dimethoxystilbene.

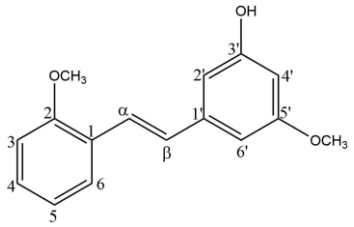

3′-hydroxy-2,5′-dimethoxystilbene

This *trans*-stilbene was first isolated from *Paphiopedilum godefroyae* and found to exhibit cytotoxic activity against human small cell lung cancer (NCI-H187) (Lertnitikul et al., 2016).

Table 3. ^{1}H (300 MHz) and ^{13}C (75 MHz) NMR data of compound PC2 (in acetone-d_6) and the reported data of 3′-hydroxy-2,5′-dimethoxystilbene (in $CDCl_3$)

Position	Compound PC2		3′-hydroxy-2,5′-dimethoxystilbene[a]	
	δ_H (mult., *J* in Hz)	δ_C	δ_H (mult., *J* in Hz)	δ_C
1	-	126.0	-	126.1
2	-	157.1	-	156.8
3	7.02 (*d*, 7.9)	111.1	6.90 (*d*, 8.5)	111.0
4	7.27 (*td*, 7.9, 1.5)	128.8	7.25 (*td*, 8.5, 1.5)	128.7
5	6.96 (*t*, 7.9)	120.6	6.96 (*t*, 7.5)	120.7
6	7.65 (*dd*, 7.9, 1.5)	126.2	7.57 (*dd*, 7.5, 1.5)	126.5
α	7.45 (*d*, 16.5)	123.3	7.45 (*d*, 16.3)	124.2
β	7.12 (*d*, 16.5)	129.0	7.00 (*d*, 16.3)	128.8
1'	-	140.1	-	140.3
2'	6.69 (br *s*)	105.8	6.64 (br *s*)	105.9
3'	-	158.7	-	156.9
4'	6.35 (*t*, 2.3)	100.8	6.33 (*t*, 2.0)	100.7
5'	-	161.3	-	161.0
6'	6.65 (br *s*)	103.6	6.66 (*d*, 2.0)	105.0
2-OCH_3	3.90 (*s*)	55.0	3.89 (*s*)	55.5
5'-OCH_3	3.79 (*s*)	54.6	3.82 (*s*)	55.4
3'-OH	8.38 (*s*)	-	-	-

[a] (Lertnitikul et al., 2016)

3. Identification of compound PC3

Compound PC3 was obtained as light-yellow amorphous. According to the negative $[M-H]^-$ peak at *m/z* 283.0601 (calculated for $C_{16}H_{12}O_5$, 283.0606) in ESI-MS spectrum (**Figure 25**), its molecular formula was determined as $C_{16}H_{12}O_5$.

The ^{13}C NMR (**Figure 27**) showed fourteen carbon signals, revealed by the HSQC experiment (**Figure 28, 29**) as representing sixteen carbons which included one methyl, seven methine and eight quaternary carbons. One methyl signal at δ_C 60.5 (5'-OCH_3) and one downfield signal at δ_C 179.7 (C-4) were observed, suggesting the presence of one methoxy group and the carbonyl functionality, respectively. The established molecular formula, as well as the numbers and types of carbons, as mentioned above was in agreement with the structure of a flavone bearing one methoxy and two hydroxy groups.

In the ^1H NMR spectrum (**Figure 26**), the methyl singlet observed at δ_H 3.89 (3H, 3-OCH_3) represented the methoxy group while the most downfield singlet at δ_H 12.68 (1H, 5-OH) represented the hydroxy group at C-5 on the A ring, forming the H-bond with the carbonyl. The two doublets corresponding to two *meta*-coupled protons appearing at δ_H 6.28 (1H, *J* = 2.0 Hz, H-6) and 6.52 (1H, *J* = 2.0 Hz, H-8) and the two multiplets at δ_H 7.57 (3H, H-3'/H-5', H-4') and 8.09 (2H, H-2'/H-6') suggested that the A ring contained the substituent at C-7 besides the 5-hydroxy group while the B ring contained no substituents. In the HMBC spectrum (**Figure 30, 31**), the correlation between the methyl singlet at δ_H 3.89 (3-OCH_3) and the carbon signal at δ_C 140.1 (C-3), as well as those between the two doublets at δ_H 6.28 (H-6) and 6.52 (H-8) and the carbon signal at δ_C 165.2. (C-7), was observed. These data indicated that the methoxy group was attached at C-3 and the other hydroxy group, rather than that at C-5, was attached at C-7.

Therefore, PC3 was identified as 3-methylethergalangin (5,7-dihydroxy-3-methoxyflavone). The comparison between the ^1H and ^{13}C NMR data of PC3 and the reported literature values (Shin et al., 2003) is shown in (**Table 4**).

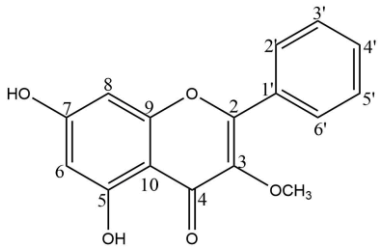

3-methylethergalangin

It was isolated from *Alpinia officinarum*. It exhibited the pancreatic lipase inhibitory activity (Shin et al., 2003), marked inhibitory activity of platelet aggregation (Chen et al., 2007) and antibacterial and antifungal activities (Hernandez Tasco et al., 2018).

Table 4. ^{1}H (500 MHz) and ^{13}C (125 MHz) NMR data of compound PC3 (in acetone-d_6) and the reported data of 3-methylethergalangin (in pyridine-d_5)

Position	Compound PC3		3-methylethergalangin[a]	
	δ_H (mult., *J* in Hz)	δ_C	δ_H (mult., *J* in Hz)	δ_C
1	-	-	-	-
2	-	156.5	-	146.2
3	-	140.1	-	139.2
4	-	179.7	-	177.6
5	-	163.3	-	162.4
6	6.28 (*d*, *J*=2.0 Hz)	99.5	6.82 (*s*)	98.4
7	-	165.2	-	165.6
8	6.52 (*d*, *J*=2.0 Hz)	94.6	6.74 (*s*)	94.4
9	-	158.0	-	157.5
10	-	106.1	-	104.6
1'	-	131.6	-	132.4
2'	8.09 (*m*)	129.2	8.48 (*d*, 7.6)	128.9
3'	7.57 (*m*)	129.5	7.39-7.51 (*m*)	128.7
4'	7.57 (*m*)	131.7	7.39-7.51 (*m*)	130.1
5'	7.57 (*m*)	129.5	7.39-7.51 (*m*)	128.7
6'	8.09 (*m*)	129.2	8.48 (*d*, 7.6)	128.9
3-OCH_3	3.89 (*s*)	60.5	3.71 (*s*)	55.4
5-OH	12.68 (*s*)	-	-	-

[a] (Shin et al., 2003)

4. Identification of compound PC4

Compound PC4 was obtained as yellow needle crystals. Its molecular formula was identified as $C_{15}H_{10}O_5$ based on the $[M-H]^-$ peak at *m/z* 269.0451 (calculated for $C_{15}H_{10}O_5$, 269.0450) in the mass spectrum (**Figure 32**).

The ^{1}H NMR spectrum (**Figure 33**) of PC4 exhibited four signals in the aromatic region, including two singlets at δ_H 6.29 (1H, H-6) and 6.56 (1H, H-8), one multiplet at δ_H 7.54 (3H, H-3'/H-5', H-4') and one doublet 8.25 at δ_H (2H, *J* = 7.8 Hz, H-2'/H-6'). The most downfield signal was observed as a singlet at δ_H 12.08 (1H, 5-OH).

The ^{13}C NMR (**Figure 34**) and HSQC (**Figure 35**) spectra revealed the presence of fifteen carbons, including seven methine and eight quaternary carbons. The carbonyl signal was observed at δ_C 176.1 (C-4). The ^{1}H and ^{13}C NMR spectra of PC4 were found to be similar with those of PC3. The notable difference was the absence of the proton and carbon signals corresponding to the methoxy group. PC4 was thus indicated to be an analog of PC3 of which C-5 was substitued with the hydroxy instead of the methoxy group. In the HMBC spectrum (**Figure 36**, **37**), the correlations between the 5-hydroxyl proton (δ_H 12.08) and the three carbons, C-5 (δ_C 161.6), C-6 (δ_C 98.4) and C-10 (δ_C 103.5), were observed.

Based on the above information, confirmed by the comparison with the reported literature values (Wawer and Zielinska, 2001, de Souza and De Giovani, 2005) as shown in (**Table 5**), PC4 was identified as 3,5,7-trihydroxyflavone (galangin).

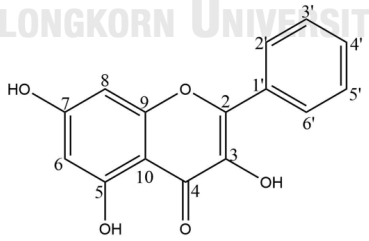

3,5,7-trihydroxyflavone (galangin)

Galangin has been found in several plants like *Helichrysum aureonitens* (Asteraceae) (Meyer et al., 1997), *Alipina officinarum* (Zingiberaceae) (Zhang et al., 2010), and also commonly found in honey bee propolis (Bankova et al., 1983). It

showed various activity including anti-mutagenic, anti- cancers, anti-oxidative, radical scavenging effect, modulatory activity for metabolic enzyme (Patel et al., 2012).

Table 5. ^{1}H (300 MHz) and ^{13}C (75 MHz) NMR data of compound PC4 (in acetone-d_6) and the reported data of galangin (^{1}H NMR in CD_3OD and ^{13}C NMR in DMSO-d_6)

Position	Compound PC4		3,5,7-trihydroxyflavone (galangin)	
	δ_H (mult., *J* in Hz)	δ_C	δ_H (mult., *J* in Hz)[a]	δ_C[b]
1	-	-	-	-
2	-	145.3	-	146.5
3	-	137.0	-	138.0
4	-	176.1	-	177.1
5	-	161.6	-	161.6
6	6.29 (*s*)	98.4	6.23 (*d*)	99.2
7	-	164.4	-	165.1
8	6.56 *(s)*	93.7	6.45 (*d*)	94.4
9	-	157.1	-	157.3
10	-	103.5	-	104.1
1'	-	131.3	-	130.7
2'	8.25 (*d,* 7.8)	127.6	8.32 (*dd*)	128.4
3'	7.54 (*m*)	128.5	7.64 (*dd*)	129.3
4'	7.54 (*m*)	130.0	7.55 (*m*)	131.8
5'	7.54 (*m*)	128.5	7.64 (*dd*)	129.3
6'	8.25 (*d,* 7.8)	127.6	8.32 (*dd*)	128.4
5-OH	12.08 (*s*)	-	-	-

[a](de Souza and De Giovani, 2005)

[b](Wawer and Zielinska, 2001)

5. Identification of compound PC5

Compound PC5 was obtained as a brown semisolid. Based on the $[M-H]^-$ peak at *m/z* 271.0976 (calculated for $C_{16}H_{16}O_4$, 271.0970) in the ESI-MS (**Figure 38**). The molecular formula of PC5 was established as $C_{16}H_{16}O_4$.

The ^{1}H NMR spectrum of PC5 (**Figure 39**, **40**) displayed the signals of a stilbene like those of PC1 and PC2. It revealed the presence of a *trans*-double bond (δ_H 7.13, 1H, *d*, *J* = 16.3 Hz, H-**α** and δ_H 7.44, 1H, *d*, *J* = 16.3 Hz, H-**β**), two hydroxy groups (δ_H 8.19, 1H, *s*, 2-OH. and δ_H 8.31, 1H, *s*, 3'-OH) and two methoxy groups (δ_H 3.76, 3H, *s*, 5-OCH_3 and δ_H 3.77, 3H, *s*, 5'-OCH_3). The aromatic protons on the two benzene rings were represented by two sets of reciprocally coupled signals. One set was observed as three triplets of three *meta*-coupled protons at δ_H 6.32 (1H, *J* = 1.9 Hz, H-4'), 6.63 (1H, *J* = 1.9 Hz, H-6') and 6.67 (1H, *J* = 1.9 Hz, H-2'), indicating the presence of a 1,3,5-trisubstituted benzene ring. The other set included three signals; two of them were the doublets of *ortho*-coupled and *meta*-coupled protons at δ_H 6.82 (1H, *J* = 9.0 Hz, H-3) and 7.15 (1H, *J* = 3.0 Hz, H-6), respectively. The third signal appeared as the double doublet at δ_H 6.70 (1H, *J* = 9.0, 3.0 Hz, H-4), corresponding to the proton coupled with both of the aforementioned ones. These data indicated the presence of a 1,2,5-trisubstituted benzene ring. The above information suggested that PC5 was a *trans*-stilbene bearing the benzene rings with 1,3,5- and 1,2,5- trisubstitution patterns; each of the two rings was substituted with one hydroxy and one methoxy groups. The ring with the former pattern was thus the same as those of PC1 and PC2 bearing the hydroxy and methoxy groups at C-3' and C-5', respectively.

The ^{13}C-NMR spectrum (**Figure 41**) displayed sixteen carbon signals which were classified with the aid of HSQC experiment (**Figure 42**) into those of two methyl, eight methine and six quaternary carbons. Signals of two methoxy groups were observed at δ_C 55.5 (C-5) and 55.9 (C-5'). In the HMBC spectrum (**Figure 43**), the downfield singlet at δ_H 8.31 (3'-OH) exhibited correlations with the carbon signals at δ_C 106.7 (C-2'), 159.6 (C-3') and 101.6 (C-4') while the methyl singlet at δ_H 3.77 (5'-OCH_3) with the carbon signal at δ_C 55.5 (C-5'). This information confirmed the substitutions with the hydroxy and methoxy groups at C-3' and C-5', respectively. The correlation observed between the doublet at δ_H 7.44 (H-**α**), as well as the downfield

singlet at δ_H 8.19 (2-OH), and the carbon signals at δ_C 149.9 (C-2) pointed out that the other hydroxy group was substituted at C-2. The other methoxy group was indicated to be substituted at C-5 by the correlations between the carbon signal at δ_C 154.3 (C-5) and the three proton signals at δ_H 3.76 (5-OCH_3), 6.82 (H-3) and 7.15 (H-6).

Therefore, PC5 was identified as 2,3′-dihydroxy-5,5′-dimethoxystilbene . The comparison between the ^{1}H and ^{13}C NMR data of PC5 and the reported literature values (Garo et al., 2007) is shown in (**Table 6**)

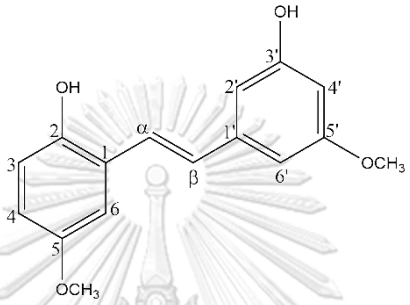

2,3′-dihydroxy-5,5′-dimethoxystilbene

It was noticable that the chemical shifts assigned for C-2′and C-6′ of PC5 and the values reported in the literature were in reverse. However, the chemical shift assignments for H-2′ and H-5′ were in agreement. The assignments for C-2′ (δ_C 106.7) and C-6′ (δ_C 104.4) of PC5 were evidenced from the HSQC correlations of the proton signals at δ_H 6.67 (H-2′) and δ_H 6.63 (H-6′) with the carbon signals at δ_C 106.7 and δ_C 104.4, respectively. In addition, these assignments were also confirmed by the HMBC spectrum where the proton signal at δ_H 8.31 (3′-OH) showed a correlation with the carbon signal at δ_C 106.7 (C-2′), while the correlation of the same proton signal with the carbon signal at δ_C 104.7 (C-6′) could not be observed.

Compound PC5 was found in *Phragmipedium* hybrid of *P. longifolium* and *P. lindleyanum* (Garo et al., 2007). It was isolated from another species of *Paphiopedilum godefroyae* and showed its cytotoxic activity with an IC_{50} value of 64.09 µM on NCI-H187, small cell lung cancer cell line (Lertnitikul et al., 2016).

Table 6. ^{1}H (500 MHz) and ^{13}C (125 MHz) NMR data of compound PC5 (in acetone-d_6) and the reported data of 2,3′-dihydroxy-5,5′-dimethoxystilbene (in CD_3OD)

Position	Compound PC5		2,3′-dihydroxy-5,5′-dimethoxystilbene[a]	
	δ_H (mult., *J* in Hz)	δ_C	δ_H (mult., *J* in Hz)	δ_C
1		125.7	-	126.3
2	-	149.9	-	150.4
3	6.82 (*d*, 9.0)	117.5	6.74 (8.7)	117.6
4	6.70 (*dd*, 9.0, 3.0)	115.6	6.68 (*dd*, 8.7, 2.9)	115.8
5	-	154.3	-	154.7
6	7.15 (*d*, 3.0)	111.6	7.08 (*d*, 2.8)	112.0
α	7.44 (*d*, 16.3)	124.6	7.38 (*d*, 16.4)	125.5
β	7.13 (*d*, 16.3)	129.5	7.02 (*d*, 16.4)	129.8
1'	-	141.1	-	141.6
2'	6.67 (*t*, 1.9)	106.7	6.60 (*brd*, 2.0)	104.7
3'	-	159.6	-	159.8
4'	6.32 (*t*, 1.9)	101.6	6.27 (*t*, 2.0)	101.9
5'	-	162.2	-	162.8
6'	6.63 (*t*, 1.9)	104.4	6.59 (*brd*, 2.20)	107.1
5-OCH_3	3.76 (*s*)	55.9	3.78 (*s*)	56.0
5'-OCH_3	3.77 (s)	55.5	3.77 (*s*)	55.6
2-OH	8.19 (s)	-	-	-
3'-OH	8.31 (s)	-	-	-

[a](Garo et al., 2007)

6. Identification of compound PC6

Compound PC6 was obtained as a brown semisolid. According to its negative ESI-MS (**Figure 44**) $[M-H]^-$ peak at *m/z* 241.0869 (calculated for $C_{15}H_{14}O_3$, 241.0864), the structure of the compound was established as $C_{15}H_{14}O_3$.

The ^1H NMR spectrum of PC6 (**Figure 45**, **46**) was similar to that of PC5, suggesting that PC6 is a stilbene. The differences from the proton signals of PC5 were the absence of one methoxyl signal and the addition of one aromatic proton signal. The two doublets appearing at (δ_H 7.15, 1H, *d*, *J* = 16.5 Hz, H-**β** and δ_H 7.47, 1H, *d*, *J* = 16.5 Hz, H-**α**) represented the olefinic protons of a *trans*-double bond. One methyl singlet at δ_H 3.79 (3H, 5′-OCH_3) and two broad singlets at δ_H 8.42 (1H, 3′-OH) and 8.71 (1H, 2-OH) indicated the presence of one methoxy and two hydroxy groups, respectively. The presence of a 1,3,5-trisubstituted benzene ring could be deduced from three one-proton signals at (δ_H 6.34, *t*, *J* = 2.1Hz, H-4′; δ_H 6.65 , br *s*, H-6′ and δ_H -6.69, br*s*, H-2′). The rest of signals were four one-proton signals at δ_H 6.86 (1H, *t*, *J* = 7.8, H-5), 6.91 (1H, *d*, *J* = 7.8, H-3), δ_H 7.11 (1H, *td*, *J* = 7.8, 1.4 Hz, H-4), and δ_H 7.59 (1H, *dd*, *J* = 7.8, 1.4 Hz, H-6). The multiplicity and coupling constants of these four signals suggested that there were four adjacent protons on the other benzene ring. All of the above data were indicative of a *trans*-stilbene with 2,3′-dihydroxy and 5′-methoxy substituents.

The numbers and types of carbons corresponding to this structure were in agreement with the data obtained from the ^{13}C-NMR (**Figure 47**) and HSQC (**Figure 48**) spectra, where fifteen carbon signals including those of one methyl, nine methine and five quaternary carbons were observed. The only one methoxy group was represented by the signal at δ_C 54.6 (5′-OCH_3).

Based on the above information, confirmed by the comparison with the reported literature values (Garo et al., 2007) as shown in (**Table 7**) , PC6 was identified as 2,3′-dihydroxy-5′-methoxystilbene.

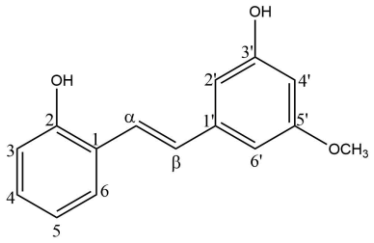

2,3′-dihydroxy-5′-methoxystilbene

It was found that the chemical shifts assigned for C-2′ and C-6′ of PC6 and the values reported in the literature were in reverse. The assignments for C-2′ (δ_C 105.8) and C-6′ (δ_C 103.4) of PC6 were deduced from the HSQC correlations of the proton signals at δ_H 6.69 (H-2′) and δ_H 6.65 (H-6′) with the carbon signals at δ_C 105.8 and δ_C 103.4, respectively. The signal assignments for H-2′ and H-6′ of PC6 followed those of PC1, PC2 and PC5 which were analyzed through their HMBC spectra. The more downfield signal (δ_H 6.69) was thus assigned for H-2′and the less one (δ_H 6.65) for H-6′.

Previously, it was found in *Phragmipedium calurum* (Garo et al., 2007) and *Paphiopedilum godefroyae* (Lertnitikul et al., 2016). Its cytotoxic activity against on small cell lung carcinoma (NCI-H187) with IC_{50} value 168.02 μM has been reported (Lertnitikul et al., 2016).

Table 7. ^{1}H (300 MHz) and ^{13}C (75 MHz) NMR data of compound PC6 (in acetone-d_6) and the reported data of 2,3′-dihydroxy-5′-methoxystilbene (in CD_3OD)

Position	Compound PC6		2,3′-dihydroxy-5′-methoxystilbene[a]	
	δ_H (mult., *J* in Hz)	δ_C	δ_H (mult., *J* in Hz)	δ_C
1	-	124.3	-	-
2	-	154.9	-	155.6
3	6.91 (*d,* 8.1)	115.8	6.81 (*m*)	116.9
4	7.11 (*td*, 8.1, 1.4)	128.5	7.06 (*t*, 6.8)	129.5
5	6.86 (*t,* 7.7)	119.8	6.81 (*m*)	120.7
6	7.59 (*dd*, 7.7, 1.4)	126.5	7.51 (*d*, 7.5)	127.5
α	7.47 (*d*, 16.5)	123.7	7.39 (*d*, 16.4)	125.0
β	7.15 (*d*, 16.5)	128.4	7.03 (*d*, 16.5)	129.2
1'	-	140.2	-	141.2
2'	6.69 (br *s*)	105.8	6.59 (br *s*)	104..4
3'	-	158.7	-	158.0
4'	6.34 (*t,* 2.1)	100.7	6.26 (br *s*)	101.5
5'	-	161.3	-	162.0
6'	6.65 (br *s*)	103.4	6.59 (br *s*)	106.7
5'-OCH_3	3.79 (*s*)	54.6	3.78 (*s*)	55.5
2-OH	8.71 (*s*)	-	-	-
3'-OH	8.42 (*s*)	-	-	-

[a](Garo et al., 2007)

7. Cytotoxicity of isolated compounds

7.1. Yeast cell-based assay

The budding yeast *S. cerevisiae* has been recognized for the study of DNA-topoisomerase targeting antitumor drugs (Nitiss and Wang, 1988). This transgenic yeast strains were used as model system for biological studies because of their rapid growth, flexible for DNA transformation system and the ease of replication and mutation (Sherman, 2002). Yeast cell-based assay was successfully utilized for screening of TopII poisons from plant extracts (Sangmalee et al., 2012).

In the assay, the transformant yeast was used for exploring TopI inhibitory compounds from *P. callosum*. The expression of the *Top*I gene of *Arabidopsis thaliana*, which has homology to the human gene, in *S. cerevisiae* strain RS190, conferred TopI inhibitory sensitivity (Sirikantaramas et al., 2008). To set up a transgenic yeast for screening, TopI gene of *A. thaliana* was cloned in expression vector pYES-DEST52 and the respective constructs were transformed into *S. cerevisiae* strain RS190 (MATa, top1**Δ**) under the control of GAL1 promoter (Sirikantaramas et al., 2008). The mechanism of topoisomerase poison drugs result from the formation of enzyme/DNA cleavage complex (Pommier and Osheroff, 2012). Therefore, two types of media 2% galactose and glucose were used as carbon sources for yeast growth as parallel models. TopI will be expressed and suppressed in yeast growing in galactose and glucose media, respectively. Cleavage complex could not be formed in glucose media due to the lack of TopI enzyme, thus the cell can survive in glucose media even the presence of TopI inhibitory compounds (Sirikantaramas et al., 2008). On the other hand, the expression of TopI in the galactose media caused enzyme/DNA complex with TopI inhibitory compounds and this covalent complex leads to cell death. In the assay, camptothecin was used as a positive control because it is the potent TopI inhibitory which targets TopI by stabilization of cleavable complex through inhibition of the religation steps (Svejstrup et al., 1991). DMSO was used as a vehicle control.

All of the pure compounds obtained from *P. callosum* were proceeded to yeast assay for determining their TopI inhibitory activity by observing the growth in galactose and glucose media. In the assay, the isolated compounds with different

concentrations (100, 50, 25 μM) showed growth inhibitory activity on yeast cells in galactose media. Compounds, PC1, PC2, PC3, PC5 and PC6 caused yeast cell death in galactose media. The lesser extent of cell death was observed when the concentrations were decreased. Yeast was not able to grow in the presence of compound PC4, galangin, at the concentration more than 50 μM. Our result for galangin was in agreement with previous report of its TopI inhibitory activity (Zhao and Zhang, 2015). The TopI inhibitory activity of the tested samples was compared to DMSO and camptothecin as the vehicle and positive control, respectively (Figure 6). The result suggested that all of isolated compounds from
P. callosum showed TopI inhibitory activity on the yeast system that used for screening of TopI inhibitory compounds.

7.2. Cytotoxicity against human cancer cell lines

Cytotoxicity of the isolated compounds against human small cell lung cancer (NCI-H187) and breast adenocarcinoma (MCF-7) cell lines was examined by using the Resazurin assay. The results are described in percent inhibition and IC_{50} values (**Table 8, Table 9**). TopI poison drug, camptothecin, and TopII poison, tamoxifen, doxorubicin, and ellipticine were used as positive controls. The maximum concentration tested for percent inhibition and IC50 was 50 μg/mL. Concentrations of compounds required to inhibit the cell proliferation more than 50 % was considered as cytotoxic. Compound PC1, PC2, PC4, and PC6 showed cytotoxic activity on both cancer cell lines (NCI-H187 and MCF-7). Compound PC4 and PC6 exhibited higher cytotoxicity toward NCI-H187 (IC_{50}=74.1 and 77.94 μM, respectively) than MCF-7 (IC_{50}=182.48 and 142.63 μM, respectively). A new compound, PC1, was more cytotoxic to MCF-7 (IC_{50}=82.45 μM) than NCI-H187 (IC_{50}=170.24) whereas 2 exhibited cytotoxicity against both NCI-H187 and MCF-7 (IC_{50}=62.82 and 74.30 μM, respectively). It showed that the IC_{50} of those compounds against the cancer cells are highly variable depending on types of cell lines. Compounds PC2, PC5 and PC6 had been reported with moderate cytotoxic activity on NCI-H187 in the previous study (Lertnitikul et al., 2016). In this study, compound PC3 and PC5 exhibited no cytotoxicity on representative cell lines. The higher dose may be required for PC3

and PC5 or the cytotoxic activity may be specific to certain types of cancer cells. Overall, taken together, our study provided information that isolated compounds *P. callosum* roots can be developed as a lead candidate to combat cancer with TopI inhibitory mechanism.

7.3. DNA-cleavage assay

Topoisomerase (TopI and TopII) became the target for anticancer drug discovery because they are essential enzymes that regulate the topology of DNA by making strands break. The function of TopI is to catalyze the relaxation of supercoiled DNA by transiently breaking and resealing the single stranded DNA (Pommier and Osheroff, 2012). Topoisomerase poisons drug inhibit the re-ligation step of relaxation process by stabilizing the cleavable complex between enzyme and DNA, thus prevents the re-ligation step of the reactions (Hsiang et al., 1985). TopI inhibitory activity of polyphenolic compounds and flavonoids was evaluated using the DNA assay and they have been shown the TopI inhibitory in the previous study (Webb and Ebeler, 2004).

The isolated compounds were tested by DNA-cleavage assay to evaluate their TopI inhibitory on human DNA. In the interpretation of assay, the topoisomers will be moved towards the directions of supercoiled if the relaxation activity of enzyme is inhibited. Otherwise, the intensity of nicked band will be increased in the presence of topoisomerase poison compounds by forming the cleavage complex (Webb and Ebeler, 2003). In this experiment, camptothecin, reference TopI poison drug, was used as internal standard to evaluate the poisoning activity of compounds. Camptothecin and tested compounds showed nicked open circular DNA at the concentration of 50 and 250 μM, respectively (Figure 7). The results from assay suggested that compounds isolated from *P. callosum* cause the DNA-TopI cleavage complex, characteristic of TopI inhibitory by forming the nicked DNA. In here, the nicked bands of compounds PC1, PC4 and PC3 showed more intensity than the others. The results demonstrated that the compounds isolated from *P. callosum* have been evaluated as potential anticancer drugs that responsible for TopI inhibitory activity.

Table 8. Cytotoxicity of isolated compounds

Compound	% inhibition	
	NCI-H187	MCF7
PC1	99.36	93.83
PC2	99.79	84.37
PC3	-10.26	10.77
PC4	94.31	53.96
PC5	6.87	22.47
PC6	99.44	75.40
Tamoxifen	-	98.50
Doxorubicin	98.50	89.32
Ellipticine	99.98	-
Camptothecin	99.99	99.99

(reported in percent inhibition of cell growth)

Table 9. Cytotoxicity of isolated compounds

Compound	IC_{50} (μM)	
	NCI-H187	MCF-7
PC1	170.24	82.45
PC2	62.82	74.30
PC3	Inactive	Inactive
PC4	74.10	182.48
PC5	Inactive	Inactive
PC6	77.94	142.63
Tamoxifen	-	7.04
Doxorubicin	0.097	10.00
Ellipticine	2.00	-
Camptothecin	0.0112±0.003	0.0170±0.004

(reported in IC_{50} values)

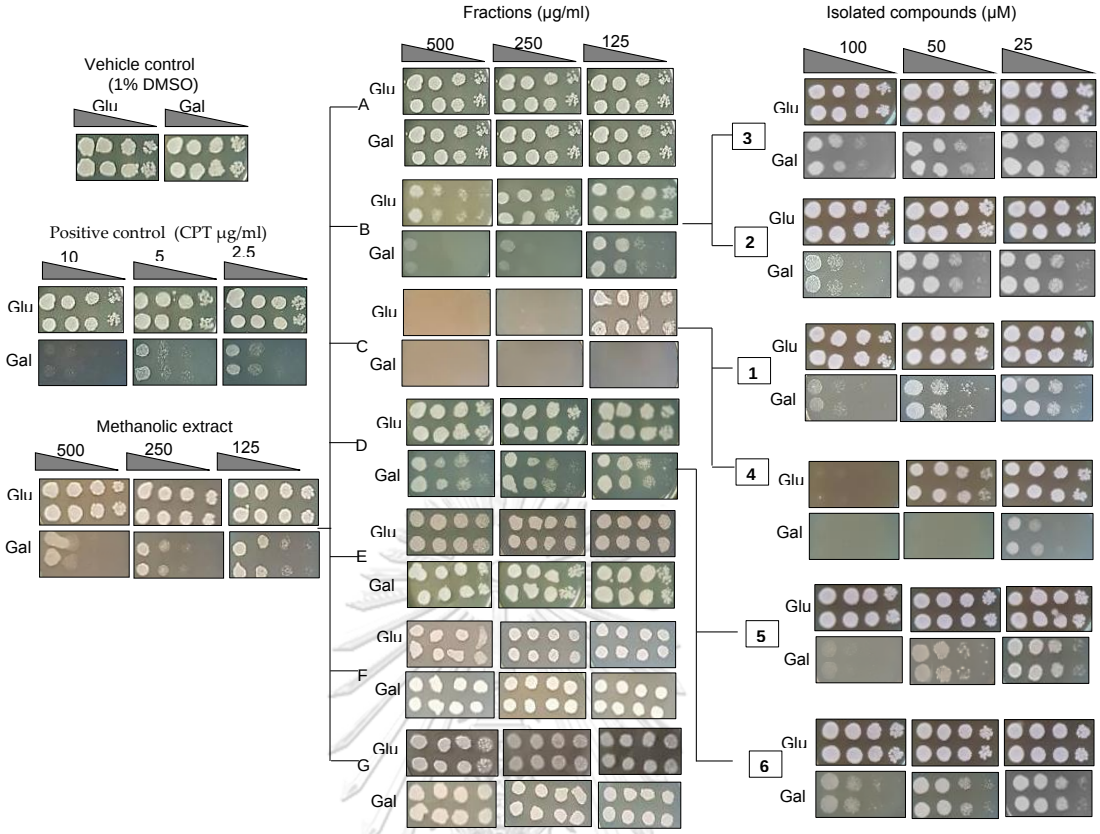

Figure 6. Scheme for bioassay-guided isolation of *P. callosum* by yeast cell-based assay.

Serial diluted tenfold of *S. cerevisiae* were grown in culture media containing various concentrations of extract (500, 250, 125 μg/mL), fractions, A-G (500, 250, 125 μg/mL) and compounds 1-6 (100, 50, 25 μM). Camptothecin (10, 5 and 2.5 μg/mL) and 1% DMSO. The results were observed and photographed.

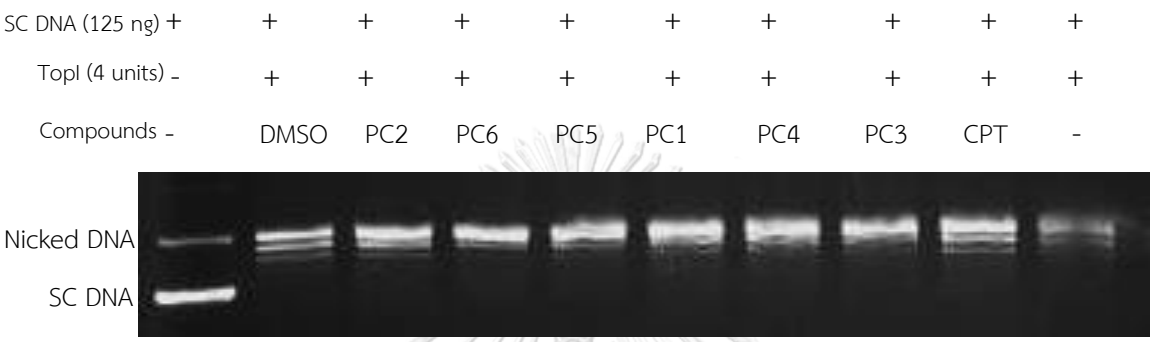

Figure 7. Agarose gel photograph of DNA-cleavage assay in the presence of camptothecin and compounds.

Lane 1, supercoiled DNA (SC DNA) only; Lane 2, supercoiled and TopI in the presence of 3% DMSO; Lane 3-8, supercoiled DNA treated with 250 μM of compounds (PC2, PC6, PC5, PC1, PC4, and PC3, respectively) in the presence of TopI; Lane 9, supercoiled DNA treated with camptothecin (50 μM) in the presence of TopI; lane 10, supercoiled DNA in the presence of TopI.

CHAPTER V
CONCLUSION

In this study, six compounds with topoisomerase I poison activities were isolated from the methanolic extract of *Paphiopedilum callosum* roots. Four of them are stibenoids while the other two are flavonoids. The stilbenoids were shown to be 3′-hydroxy-2,6,5′-trimethoxystilbene, 3′-hydroxy-2,5′-dimethoxystilbene, 2,3′-dihydroxy-5,5′-dimethoxystilbene and 2,3′-dihydroxy-5′-methoxystilbene. The flavonoids were identified as galangin and 3-methylethergalangin. Among them, 3′-hydroxy-2,6,5′-trimethoxystilbene was found to be a new compound. All of the isolated compounds showed growth inhibitory activity on transgenic *S. Cerevisiae*. 3′-Hydroxy-2,6,5′-trimethoxystilbene, 3′-hydroxy-2,5′-dimethoxystilbene, galangin, and 2,3′-dihydroxy-5′-methoxystilbene showed cytotoxic activities against both cancer cell lines (NCI-H187 and MCF-7) with varying cytotoxic activity at 50 µg/mL, while 3-methylethergalangin and 2,3′-dihydroxy-5,5′-dimethoxystilbene exhibited no cytotoxicity on the representative cell lines. The investigation on effects of the isolated compounds on supercoiled DNA was performed by DNA-cleavage assay. The results suggested that all compounds caused nicked DNA, a DNA-TopI cleavage complex which is a characteristic of TopI poison activity.

REFERENCES

Bankova, V. S., Popov, S. S. & Marekov, N. L. 1983. A study on flavonoids of propolis. Journal of Natural Products; 46**:** 471-474.

Bray, F., ferlay, J., Soerjomataram, I., Siegel, R. L., Torre, L. A. & Jemal, A. 2018. Global cancer statistics 2018: GLOBOCAN estimates of incidence and mortality worldwide for 36 cancers in 185 countries. A Cancer Journal for Clinicians.

Chase, M. W., Cameron, K. M., Freudenstein, J. V., Pridgeon, A. M., Salazar, G., Van Den Berg, C. & Schuiteman, A. 2015. An updated classification of Orchidaceae. Botanical Journal of the Linnean Society; 177**:** 151-174.

Chen, J. J., Lee, H. H., Shih, C. D., Liao, C. H., Chen, I. S. & Chou, T. H. 2007. New dihydrochalcones and anti-platelet aggregation constituents from the leaves of *Muntingia calabura*. Planta Medica; 73**:** 572-7.

Chochai, A., Leitch, I., J. Ingrouille, M. & Fay, M. 2012. Molecular phylogenetics of *Paphiopedilum* (Cypripedioideae; Orchidaceae) based on nuclear ribosomal ITS and plastid sequences. Botanical Journal of the Linnean Society; 170:176-96.

Christenhusz, M. J. & Byng, J. W.. 2016. The number of known plants species in the world and its annual increase. Phytotaxa; 261**:** 201-217.

Cox, A. V., Pridgeon, A. M., Albert, V. A. & Chase, M. W. 1997. Phylogenetics of the slipper orchids (Cypripedioideae, Orchidaceae): nuclear rdna ITS sequences. P lant Systematics and Evolution; 208**:** 197-223.

Cragg, G. M. & Newman, D. J. 2005. Plants as a source of anti-cancer agents. Journal of Ethnopharmacology; 100**:** 72-9.

Cribb, P. 1987. The genus Paphiopedilum / Phillip Cribb ; London, Royal Botanic Gardens, Kew in association with Collingridge.

De Souza, R. F. & De Giovani, W. F. 2005. Synthesis, spectral and electrochemical properties of Al(III) and Zn(II) complexes with flavonoids. Spectrochimica Acta Part A: Molecular and Biomolecular Spectroscopy; 61**:** 1985-90.

Dewick, P. M. & Demirci, F. 2009. P.M. Medicinal Natural Products: A Biosynthetic Approach; 3rd edition; John Wiley & Sons; Chichester, UK;. Journal of

Ethnopharmacology, 124**,** 656-656.

DuggaL, S. C. 1971. Orchids in Human Affairs (A Review). Quarterly Journal of Crude Drug Research; 11**:** 1727-1734.

Ferlay, J., Soerjomataram, I., Dikshit, R., Eser, S., Mathers, C., Rebelo, M., Parkin, D. M., Forman, D. & Bray, F. 2015. Cancer incidence and mortality worldwide: sources, methods and major patterns in GLOBOCAN 2012. International Journal of Cancer; 136**:** E359-86.

Freres, P., Jerusalem, G. & Moonen, M. 2017. Anti-cancer treatments and cardiotoxicity. Boston: Academic Press.

Garo, E., Hu, J. F., Goering, M., Hough, G., O'Neil-Johnson, M. & Eldridge, G. 2007. Stilbenes from the Orchid *Phragmipedium* sp. Journal of Natural Product; 70**:** 968-73.

Hernandez Tasco, A. J., Ramirez Rueda, R. Y., Alvarez, C. J., Sartori, F. T., Sacilotto, A., Ito, I. Y., Vichnewski, W. & Salvador, M. J. 2018. Antibacterial and antifungal properties of crude extracts and isolated compounds from *Lychnophora markgravii*. Natural Product Research**;** 1-5.

Hevener, K., Verstak, T. A., Lutat, K. E., Riggsbee, D. L. & Mooney, J. W. 2018. Recent developments in topoisomerase-targeted cancer chemotherapy. Acta pharmaceutica Sinica. B; 8**:** 844-861.

Hossain, M. M. 2011. Therapeutic orchids: traditional uses and recent advances--an overview. Fitoterapia; 82**:** 102-40.

Hsiang, Y. H., Hertzberg, R., Hecht, S. & Liu, L. F. 1985. Camptothecin induces protein-linked DNA breaks via mammalian DNA topoisomerase I. Journal of Biological Chemistry; 260**:** 14873-8.

Iqbal, J., Abbasi, B. A., Mahmood, T., Kanwal, S., Ali, B., Shah, S. A. & Khalil, A. T. 2017. Plant-derived anticancer agents: A green anticancer approach. Asian Pacific Journal of Tropical Biomedicine, 7**,** 1129-1150.

Kathiravan, M. K., Khilare, M. M., Nikoomanesh, K., Chothe, A. S., Jain, K. S. J. J. O. E. I. & Chemistry, M. 2013. Topoisomerase as target for antibacterial and anticancer drug discovery. Journal of enzyme inhibition and medicinal chemistry; 28**:** 419-435.

Kieber, J. J., Tissier, A. F. & Signer, E. R. 1992. Cloning and characterization of an *Arabidopsis thaliana* topoisomerase I gene. Plant Physiology; 99**:** 1493-501.

Kim, S. O., Sakchaisri, K., Thimmegowda, N. R., Soung, N. K., Jang, J. H., Kim, Y. S., Lee, K. S., Kwon, Y. T., Asami, Y., Ahn, J. S., Erikson, R. L. & Kim, B. Y. 2013. STK295900, a dual inhibitor of topoisomerase 1 and 2, induces G(2) arrest in the absence of DNA damage. Plos One; 8**:** e53908.

Kumar, S. & Pandey, A. K. 2013. Chemistry and biological activities of flavonoids: an overview. Scientific World Journal; 2013**:** 162750.

Larsen, A. K., Escargueil, A. E. & Skladanowski, A. 2003. Catalytic topoisomerase II inhibitors in cancer therapy. Pharmacology & Therapeutics; 99**:** 167-181.

Lertnitikul, N., Jittham, P., Khankhampoch, L., Pattamadilok, C., Sukrong, S. & Suttisri, R. 2016. Cytotoxic stilbenes from the roots of *Paphiopedilum godefroyae.* Journal of Asian Natural Product Research; 18**:** 1143-1150.

Lindley, J. 1840. The genera and species of orchidaceous plants, Ridgways, Piccadilly.

Meyer, J. J., Afolayan, A. J., Taylor, M. B. & Erasmus, D. 1997. Antiviral activity of galangin isolated from the aerial parts of *Helichrysum aureonitens*. Journal of Ethnopharmacology; 56**:** 165-9.

Mohd Sayeed Akhtar & Swamy, M. K. 2017. Anticancer Plants: Clinical Trials and Nanotechnology.

Nitiss, J. & Wang, J. C. 1988. DNA topoisomerase-targeting antitumor drugs can be studied in yeast. Proceedings of the National Academy of Sciences of the United States of America; 85**:** 7501-5.

O'brien, J., Wilson, I., Orton, T. & Pognan, F. 2000. Investigation of the Alamar Blue (resazurin) fluorescent dye for the assessment of mammalian cell cytotoxicity. European Journal of Biochemistry; 267**:** 5421-6.

Pooreecharurot, N., Lertnitikul, N., Suttisri, R. & Sukrong, S. 2016. Stilbenes from *Paphiopedilum exul* roots. Thai Journal of Pharmaceutical Sciences; 40**:** 116-119.

Pan, X., Hartley, J. M., Hartley, J. A., White, K. N., Wang, Z. & Bligh, S. W. 2012. Evodiamine, a dual catalytic inhibitor of type I and II topoisomerases, exhibits enhanced inhibition against camptothecin resistant cells. Phytomedicine; 19**:**

618-24.

Panche, A. N., Diwan, A. D. & Chandra, S. R. 2016. Flavonoids: an overview. Journal of Nutral Science; 5**:** e47.

Pansarin, E. R. & Pansarin, L. M. 2011. The Family Orchidaceae. In: Pansarin, E. R. & Pansarin, L. M. (Eds.) The family Orchidaceae in the Serra do Japi, São Paulo State, Brazil. Vienna: Springer Vienna; 6-11.

Patel, D. K., Patel, K., Gadewar, M. & Tahilyani, V. 2012. Pharmacological and bioanalytical aspects of galangin-a concise report. Asian Pacific Journal of Tropical Biomedicine; 2**:** S449-S455.

Plants & flowers. 2017. A comprehensive plants and flowers database [online]. Available from (**http://www.plantsrescue.com/*paphiopedilum-callosum/*)** [accessed November 1 2018].

Pommier, Y. & Osheroff, N. 2012. Topoisomerase-Induced DNA Damage. In: POMMIER, Y. (ed.) DNA Topoisomerases and Cancer. New York, NY: Springer New York.

Sangmalee, S., Laorpaksa, A. & Sukrong, S. 2012. A topoisomerase II poison screen of ethnomedicinal Thai plants using a yeast cell-based assay. Journal of Ethnopharmacology; 142**:** 432-7.

Sathish, M., Kavitha, B., Nayak, V. L., Tangella, Y., Ajitha, A., Nekkanti, S., Alarifi, A., Shankaraiah, N., Nagesh, N. & Kamal, A. 2018. Synthesis of podophyllotoxin linked beta-carboline congeners as potential anticancer agents and DNA topoisomerase II inhibitors. European Journal of Medicinal Chemistry; 144**:** 557-571.

Schmalle, H. & Hausen, B. M. 1979. A new sensitizing quinone from lady slipper (*Cypripedium calceolus*). Naturwissenschaften; 66**:** 527-8.

Shen, T., Xie, C.-F., Wang, X.-N. & Lou, H.-X. 2013. Stilbenoids. In: Ramawat, K. G. & Mérillon, J.-M. (eds.) Natural Products: Phytochemistry, Botany and Metabolism of Alkaloids, Phenolics and Terpenes. Berlin, Heidelberg: Springer Berlin Heidelberg.

Sherman, F. 2002. Getting Started With Yeast. In: Guthrie, C. & Fink, G. R. (Eds.) Methods In enzymology. Academic Press.

Shimura, H., Matsuura, M., Takada, N. & Koda, Y. 2007. An antifungal compound

involved in symbiotic germination of *Cypripedium macranthos var. Rebunense* (Orchidaceae). Phytochemistry; 68**:** 1442-1447.

Shin, J. E., Joo Han, M. & Kim, D. H. 2003. 3-Methylethergalangin isolated from *Alpinia officinarum* inhibits pancreatic lipase. Biological & Pharmaceutical Bulletin; 26**:** 854-7.

Sievers, A. F. 1930. The Herb Hunters Guide.

Singh, S., Singh, A., Kumar, S., Kumar, M., Pandey, P. & Chandra Kumar Singh, M. 2012. Medicinal properties and uses of orchids: a concise review. Elixir Applied Botany; 52:11627-34.

Sirikantaramas, S., Yamazaki, M. & Saito, K. 2008. Mutations in topoisomerase I as a self-resistance mechanism coevolved with the production of the anticancer alkaloid camptothecin in plants. Proceedings of the National Academy of Sciences of the United States of America; 105**:** 6782-6.

Smitinand, T. 2014. Thai plant names, Bangkok, Forest Herbarium, Royal Forest Department

Starks, C. M., Williams, R. B., Norman, V. L., Lawrence, J. A., O'neil-Johnson, M. & Eldridge, G. R. 2012. Phenylpropanoids from *Phragmipedium calurum* and their antiproliferative activity. Phytochemistry; 82**:** 172-5.

Svejstrup, J. Q., Christiansen, K., Gromova, Ii, Andersen, A. H. & Westergaard, O. 1991. New technique for uncoupling the cleavage and religation reactions of eukaryotic topoisomerase I. The mode of action of camptothecin at a specific recognition site. Journal of Molecular Biology; 222**:** 669-78.

Tsai, W. C., Fu, C. H., Hsiao, Y. Y., Huang, Y. M., Chen, L. J., Wang, M., Liu, Z. J. & Chen, H. H. 2013. Orchidbase 2.0: comprehensive collection of Orchidaceae floral transcriptomes. Plant Cell Physiology; 54**:** e7.

Wawer, I. & Zielinska, A. 2001. 13C CP/MAS NMR studies of flavonoids. Magnetic resonance in chemistry; 39**:** 374-380.

Webb, M. R. & Ebeler, S. E. 2003. A gel electrophoresis assay for the simultaneous determination of topoisomerase I inhibition and DNA intercalation. Analalytical Biochemistry; 321**:** 22-30.

Webb, M. R. & Ebeler, S. E. 2004. Comparative analysis of topoisomerase IB inhibition

and DNA intercalation by flavonoids and similar compounds: structural determinates of activity. Biochemical Journal; 384: 527-41.

Zhang, H.-T., Luo, H., Wu, J., Lan, L.-B., Fan, D.-H., Zhu, K.-D., Chen, X.-Y., Wen, M. & Liu, H.-M. 2010. Galangin induces apoptosis of hepatocellular carcinoma cells via the mitochondrial pathway. World journal of gastroenterology; 16: 3377-3384.

Zhang, S., Yang, Y., Li, J., Qin, J., Zhang, W., Huang, W. & Hu, H. 2018. Physiological diversity of orchids. Plant Diversity; 40: 196-208.

Zhao, X. & Zhang, J. 2015. Inhibitory effect of galangin on DNA topoisomerases in lung cancer cells. Zhong Nan Da Xue Xue Bao Yi Xue Ban; 40: 479-85.

APPENDIX

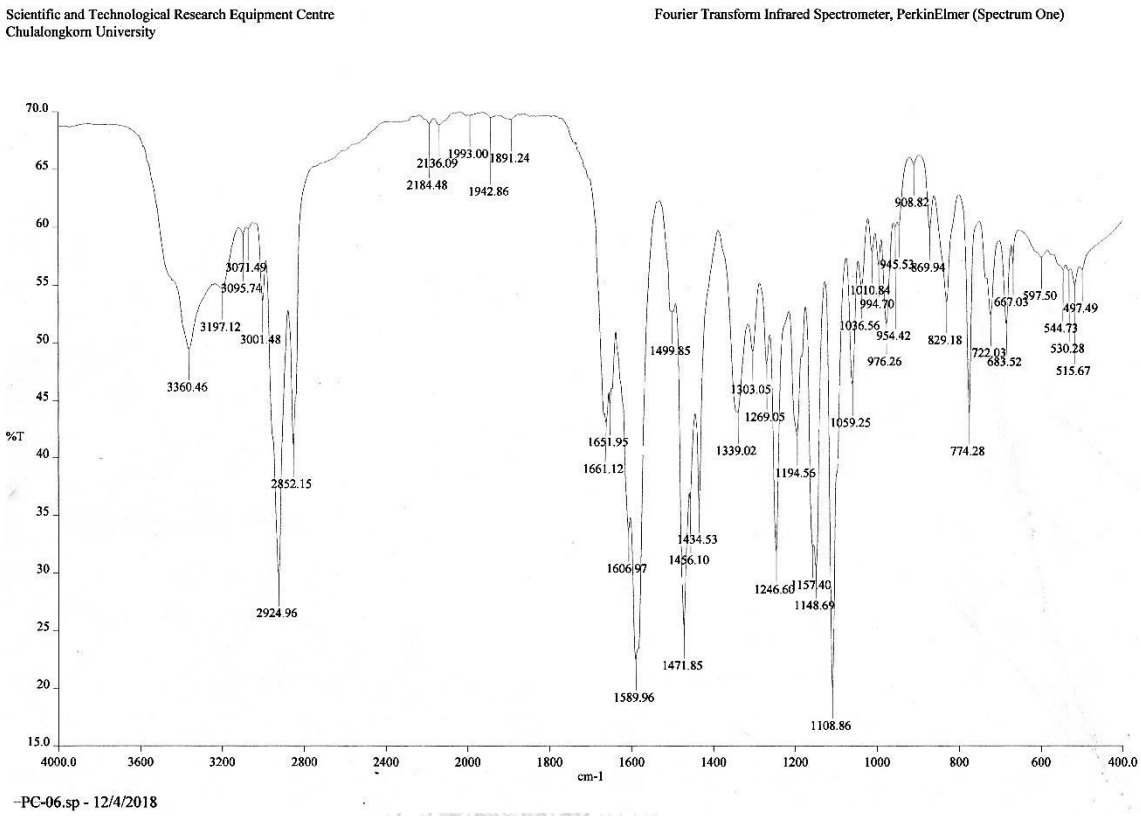

Figure 8. IR spectrum of compound PC1

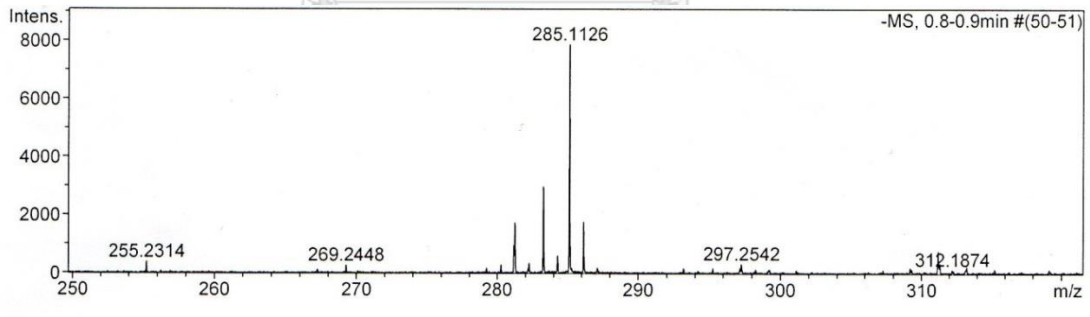

Figure 9. ESI-MS of compound PC1

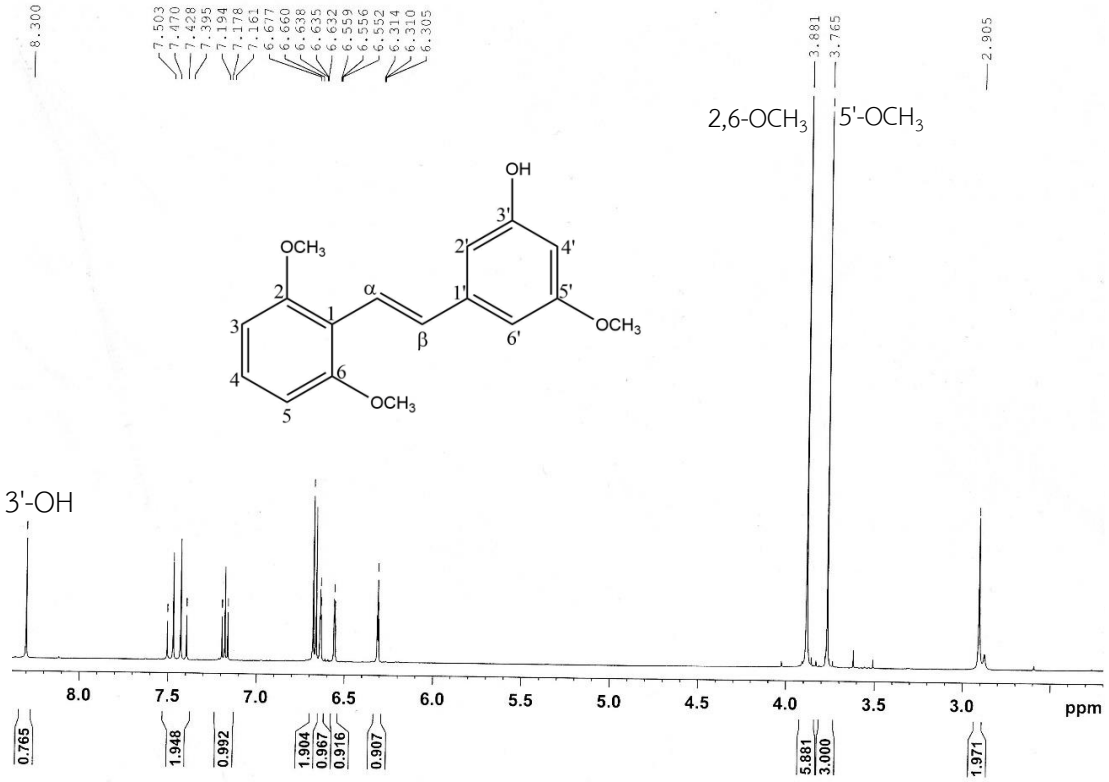

Figure 10. ^{1}H NMR (500 MHz) spectrum of compound PC1 in acetone-d_6

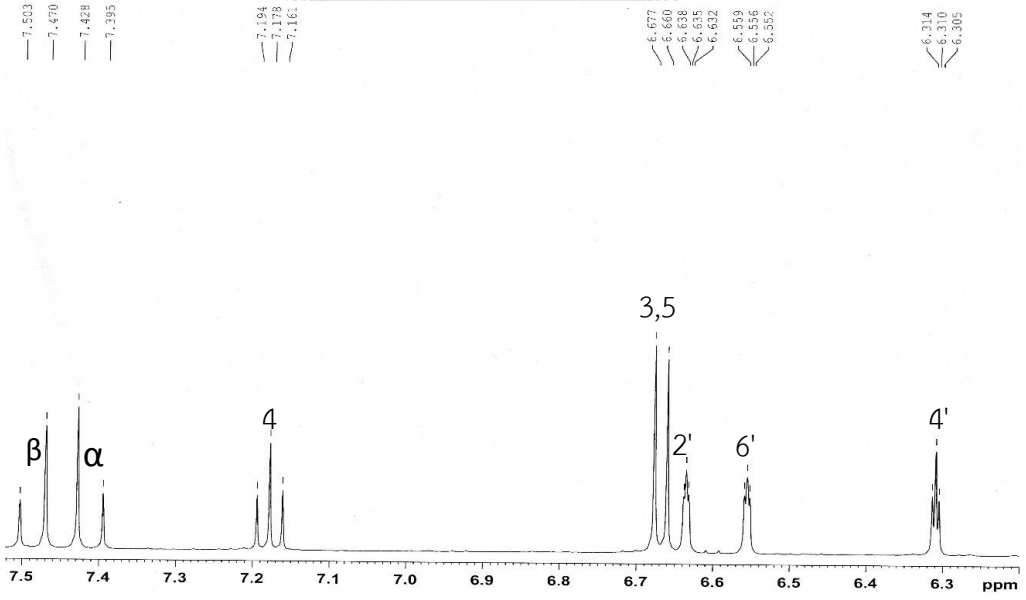

Figure 11. ^{1}H NMR (500 MHz) spectrum of compound PC1 in acetone-d_6 (expanded)

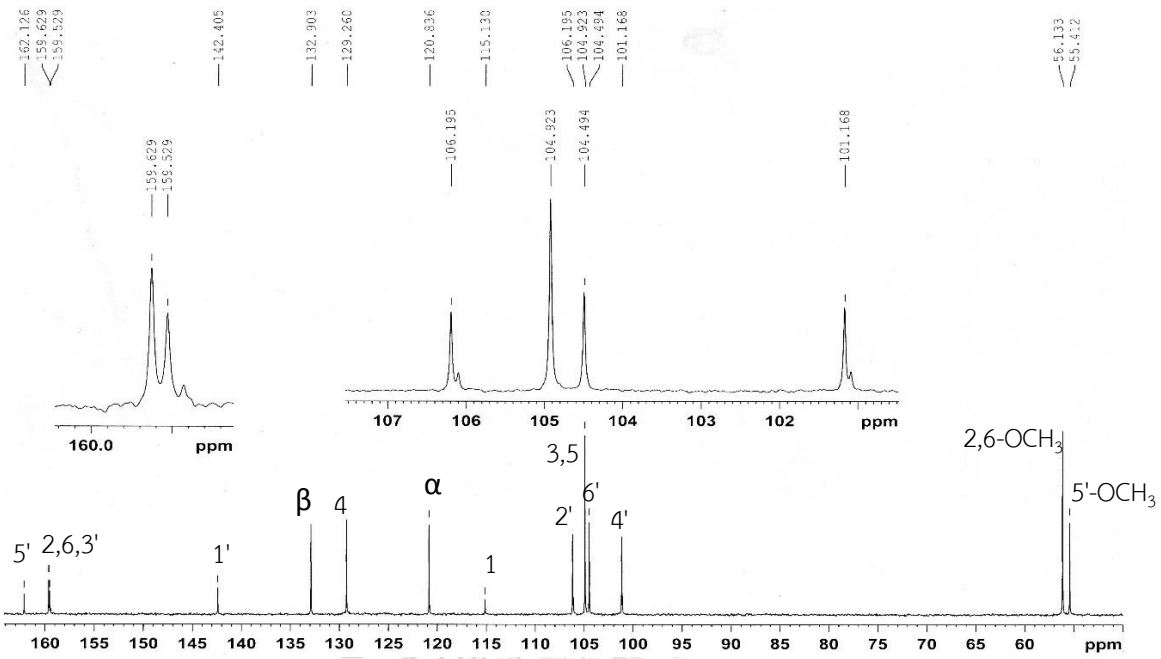

Figure 12. ^{13}C NMR (125 MHz) spectrum of compound PC1 in acetone-d_6

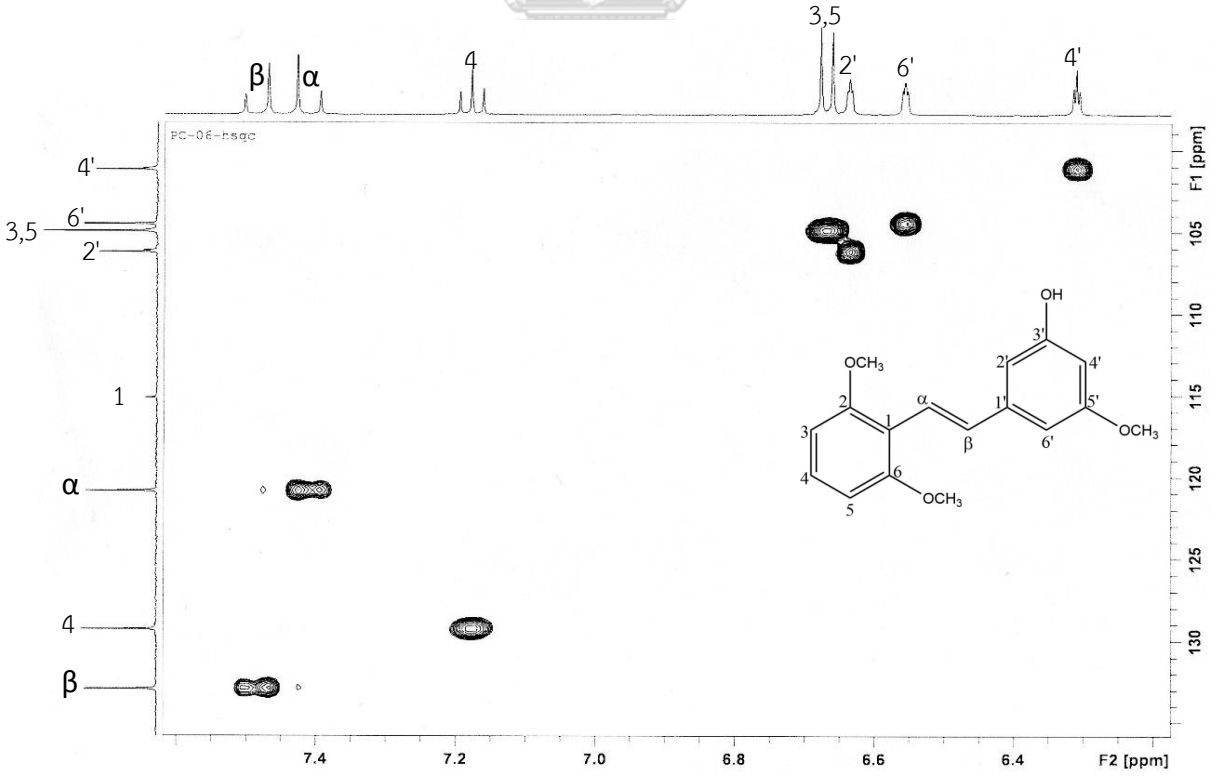

Figure 13. HSQC spectrum of compound PC1 in acetone-d_6

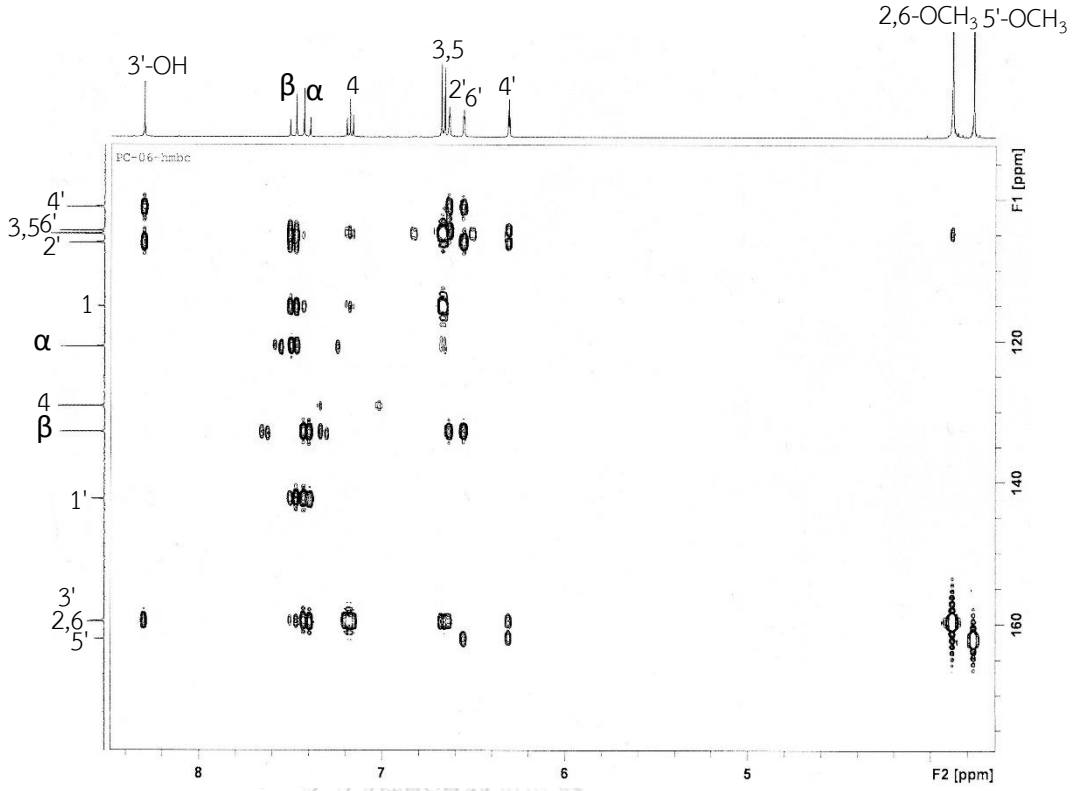

Figure 14. HMBC spectrum of compound PC1 in acetone-d_6

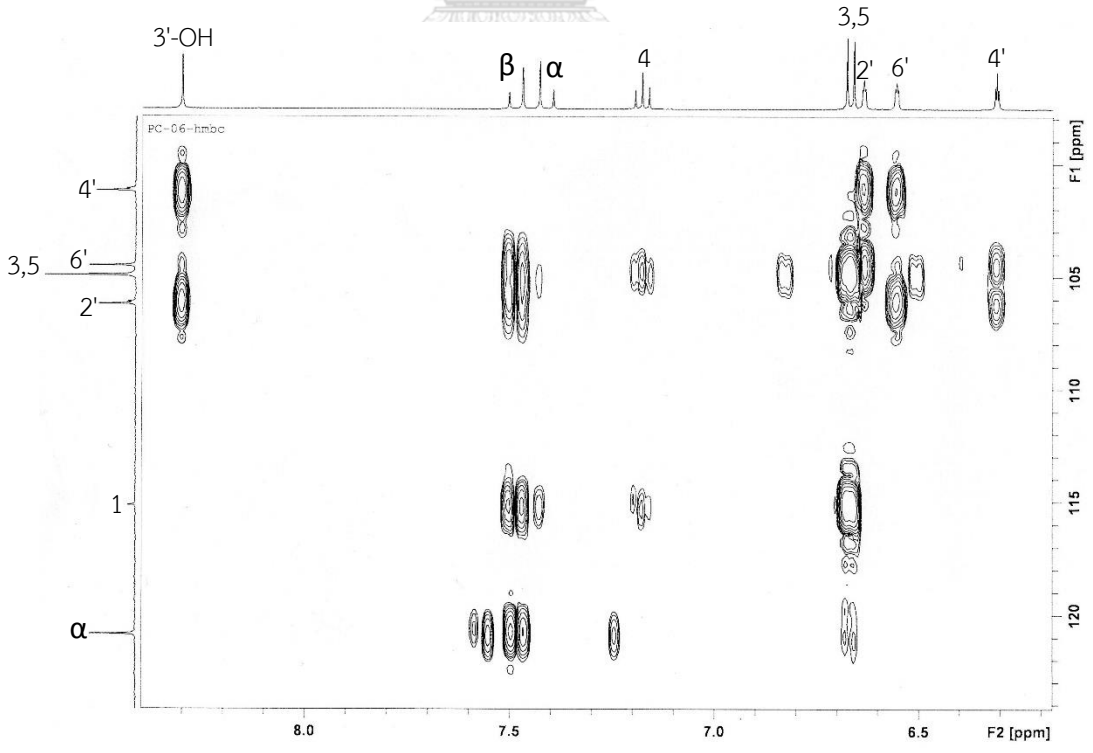

Figure 15. HMBC spectrum of compound PC1 in acetone-d_6 (expanded)

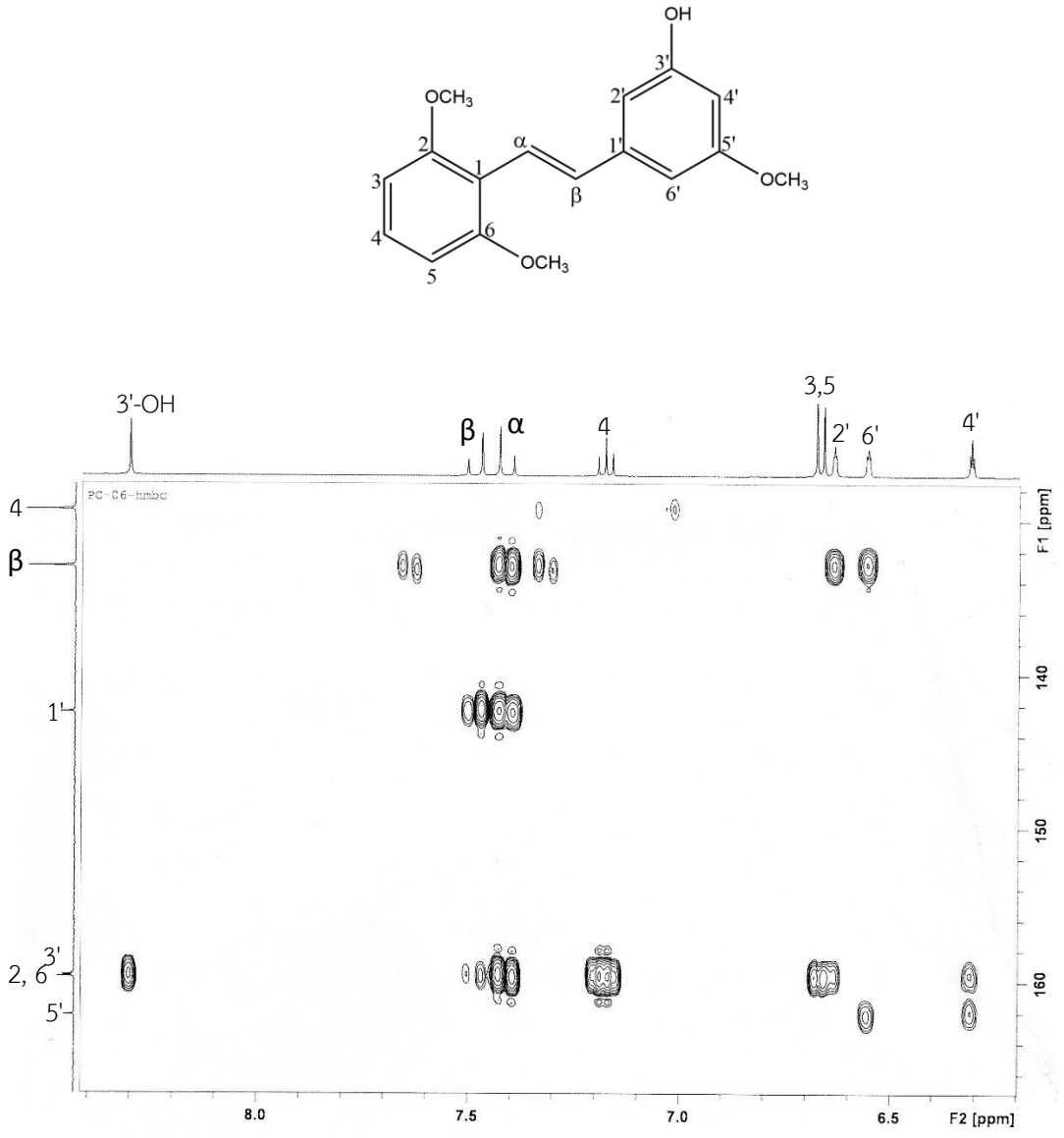

Figure 16. HMBC spectrum of compound PC1 in acetone-d_6 (expanded)

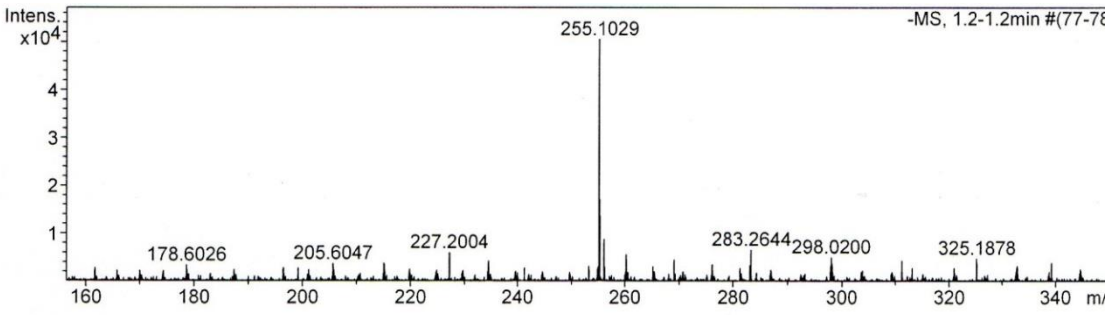

Figure 17. ESI-MS of compound PC2

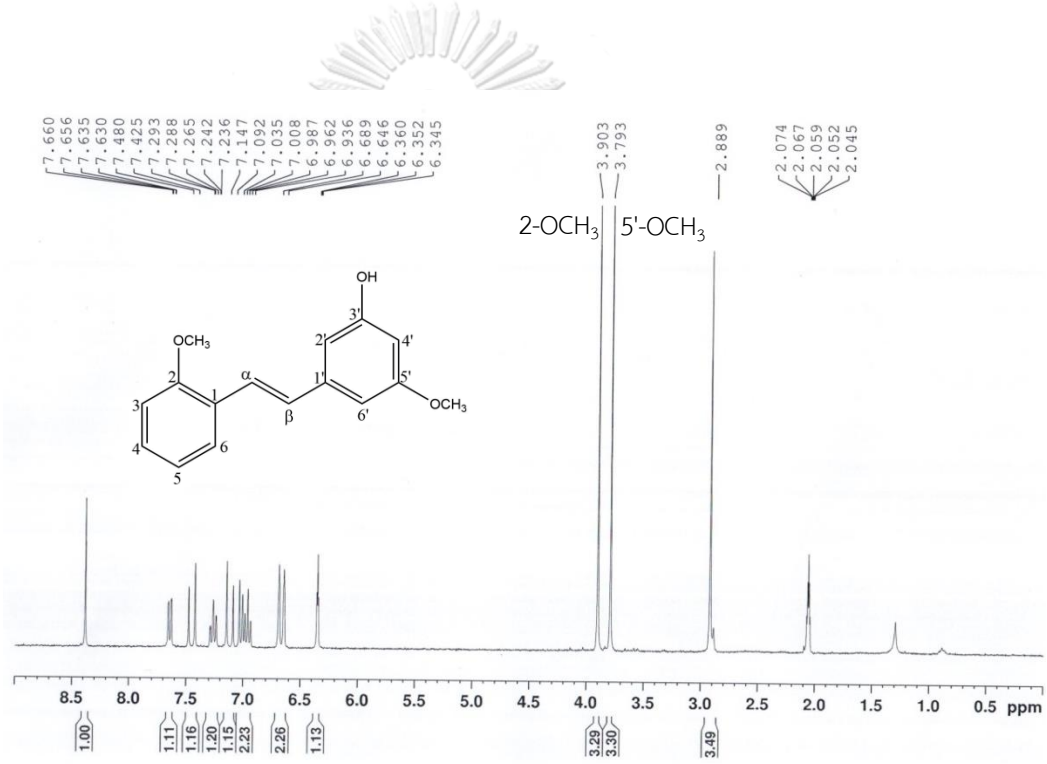

Figure 18. ^{1}H NMR (300 MHz) spectrum of compound PC2 in acetone-d_6

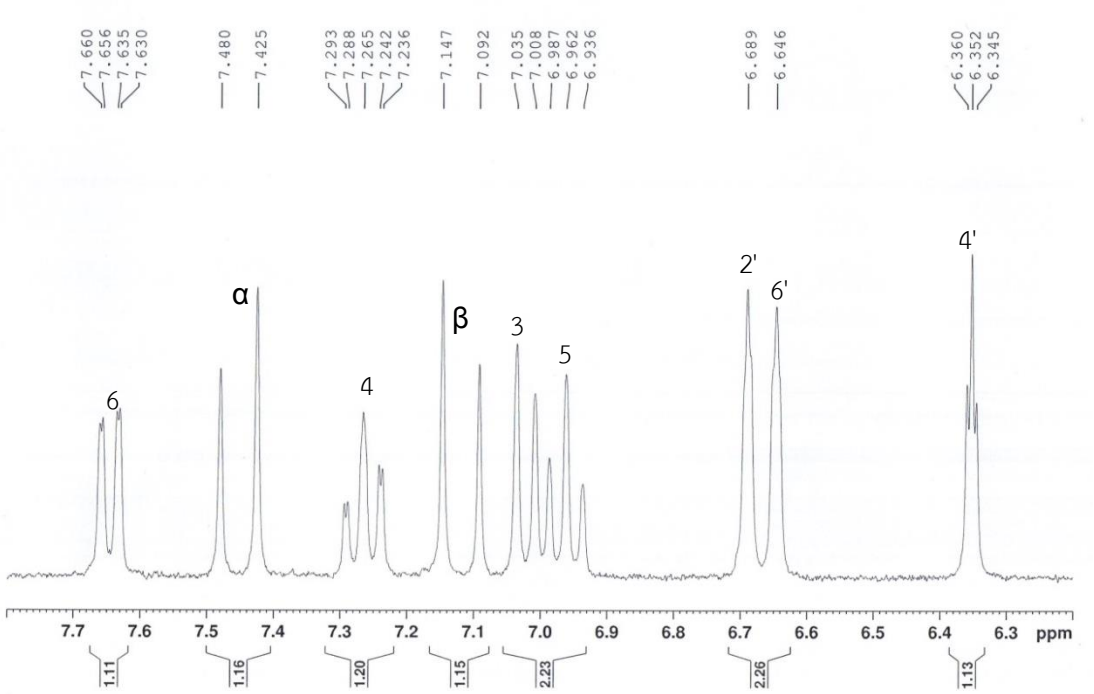

Figure 19. ^{1}H NMR (300 MHz) spectrum of compound PC2 in acetone-d_6 (expanded)

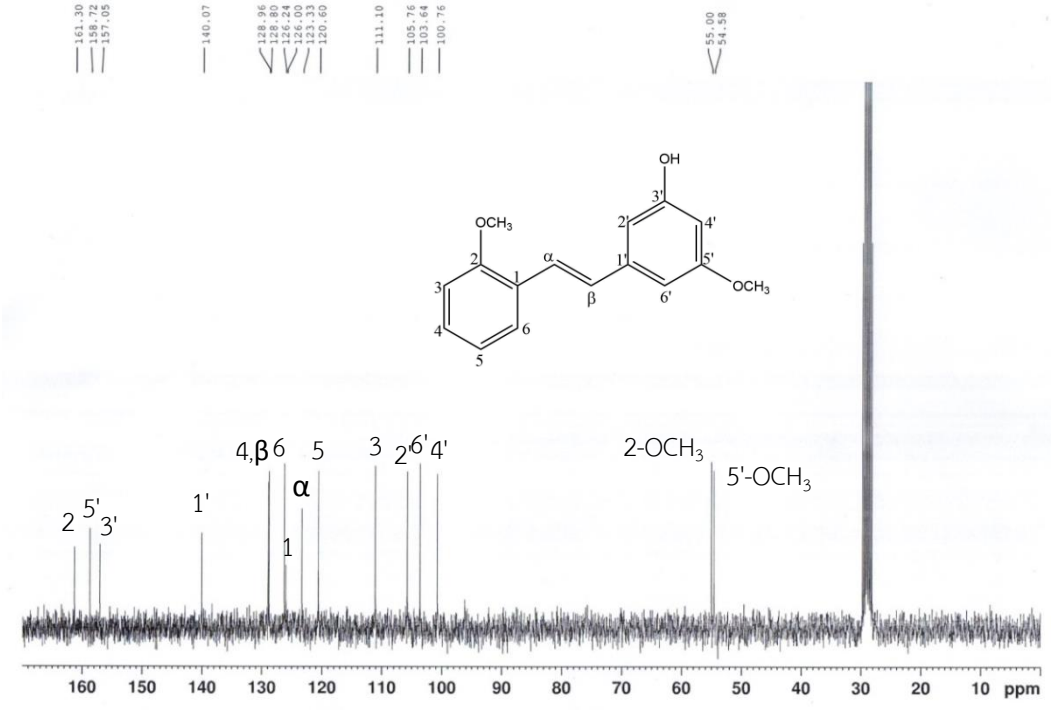

Figure 20. ^{13}C NMR (75 MHz) spectrum of compound PC2 in acetone-d_6

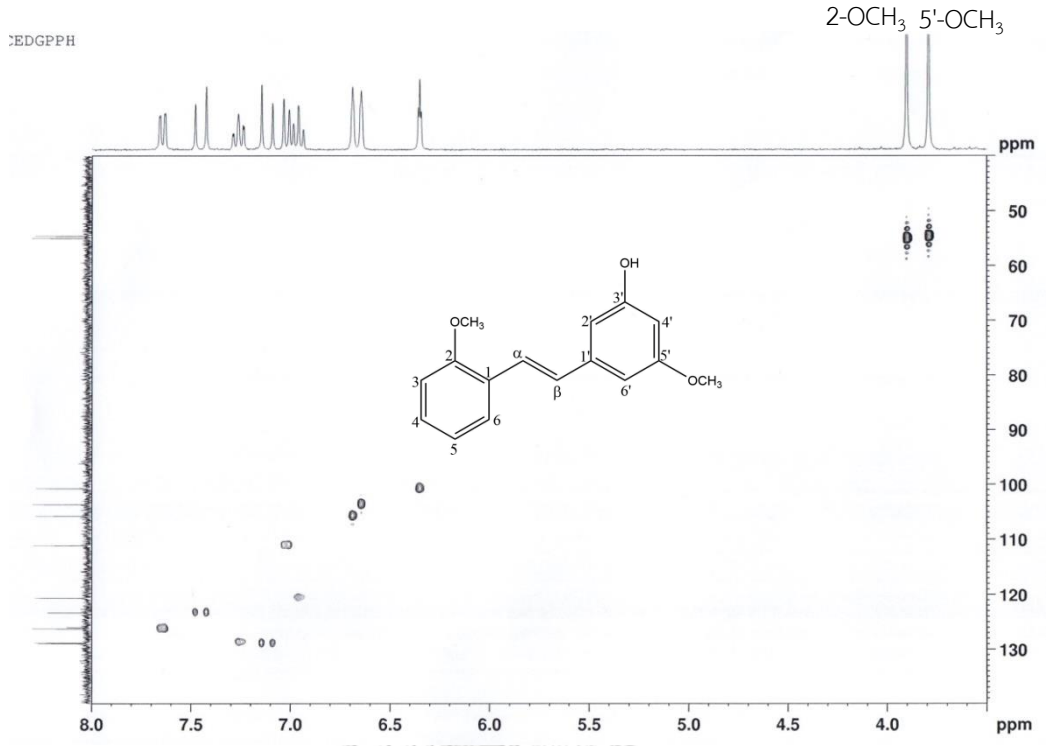

Figure 21. HSQC spectrum of compound PC2 in acetone-d_6

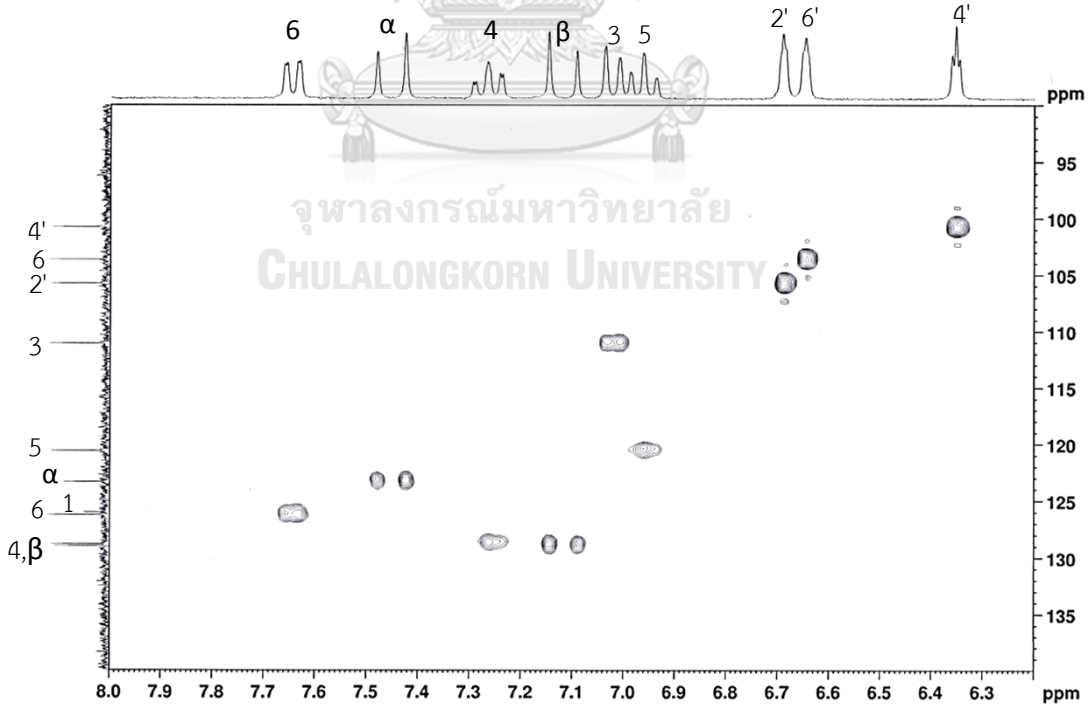

Figure 22. HSQC spectrum of compound PC2 in acetone-d_6 (expanded)

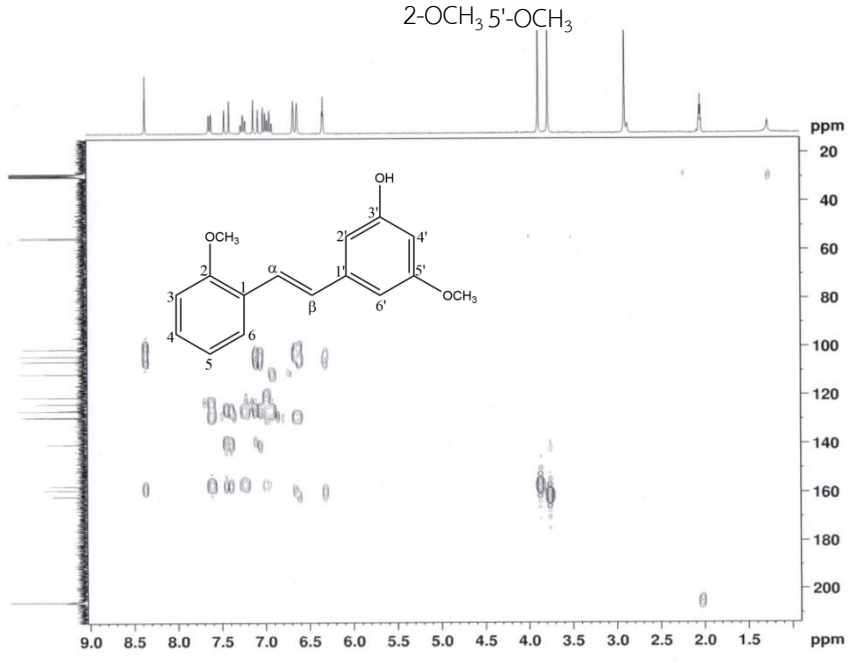

Figure 23. HMBC spectrum of compound PC2 in acetone-d_6

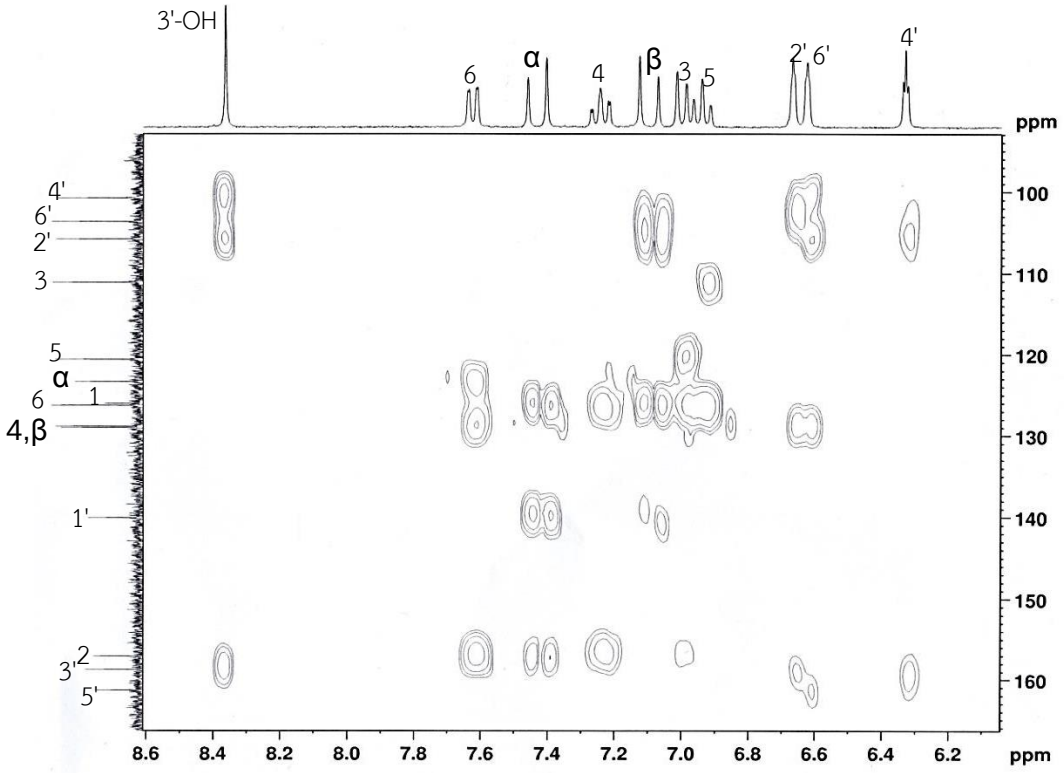

Figure 24. HMBC spectrum of compound PC2 in acetone-d_6 (expanded)

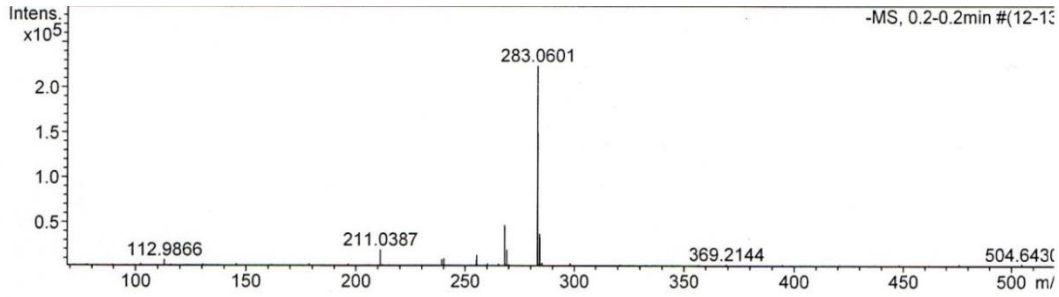

Figure 25. ESI-MS of compound PC3

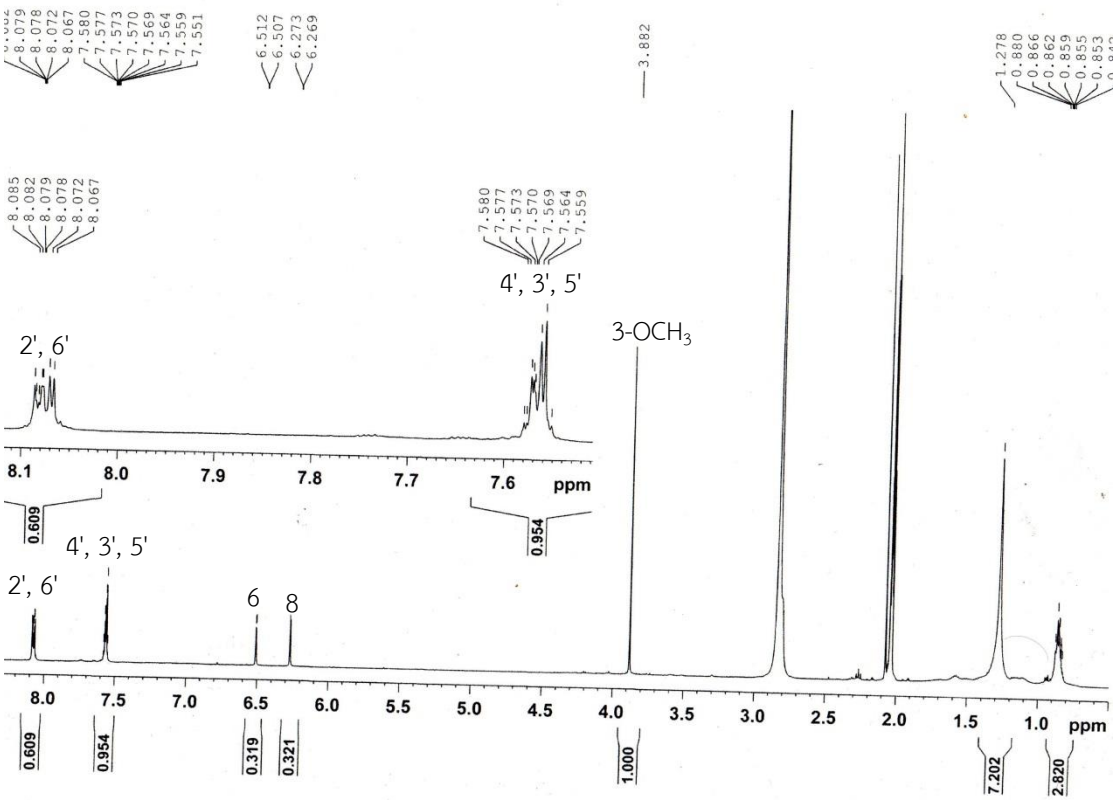

Figure 26. ^{1}H NMR (300 MHz) spectrum of compound PC3 in acetone-d_6

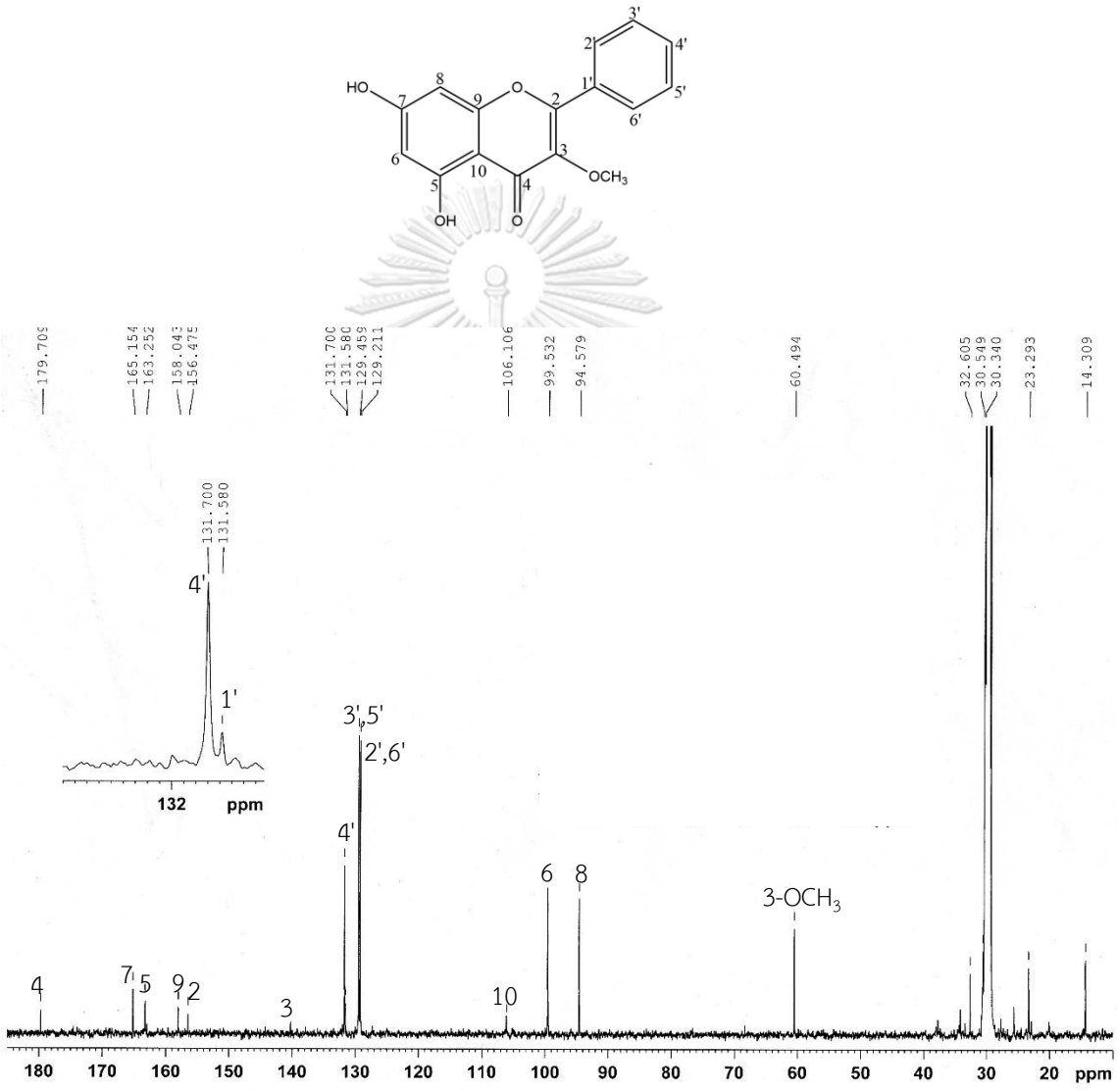

Figure 27. ^{13}CNMR (125 MHz) spectrum of compound PC3 in acetone-d_6

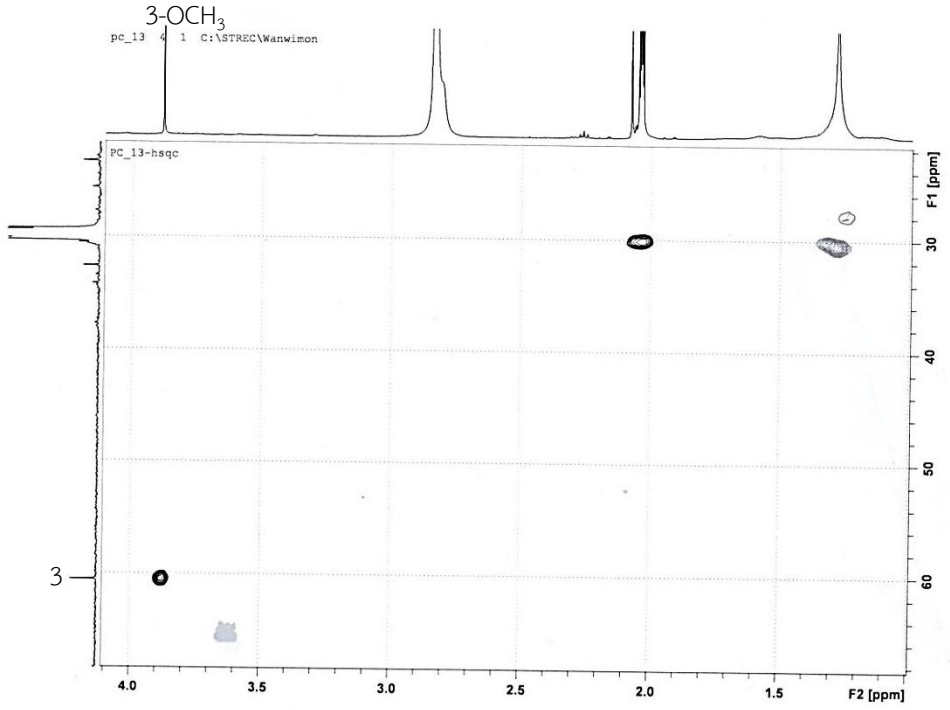

Figure 28. HSQC spectrum of compound PC3 in acetone-d_6

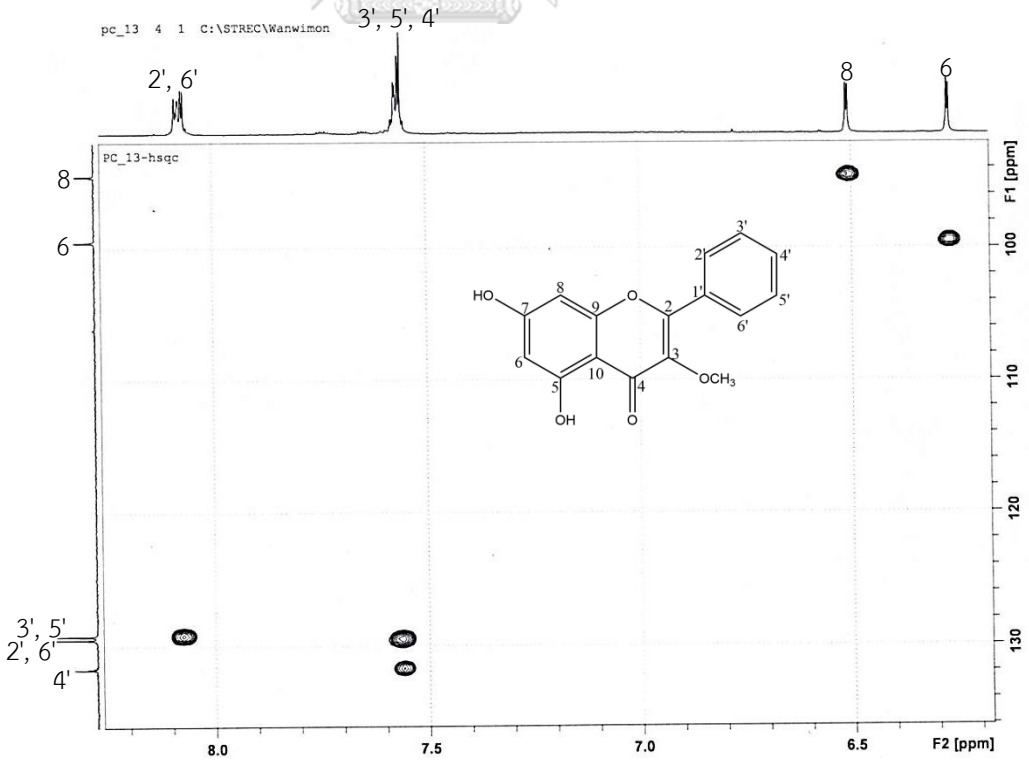

Figure 29. HSQC spectrum of compound PC3 in acetone-d_6 (expanded)

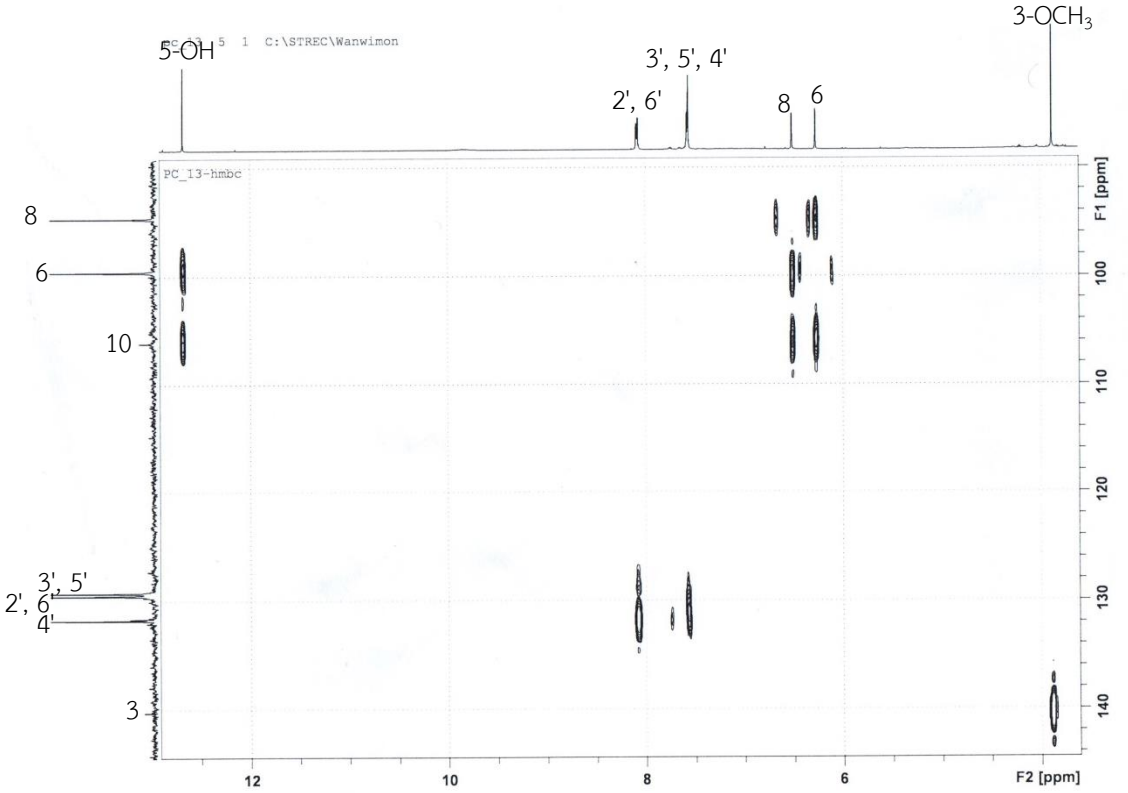

Figure 30. HMBC spectrum of compound PC3 in acetone-d_6

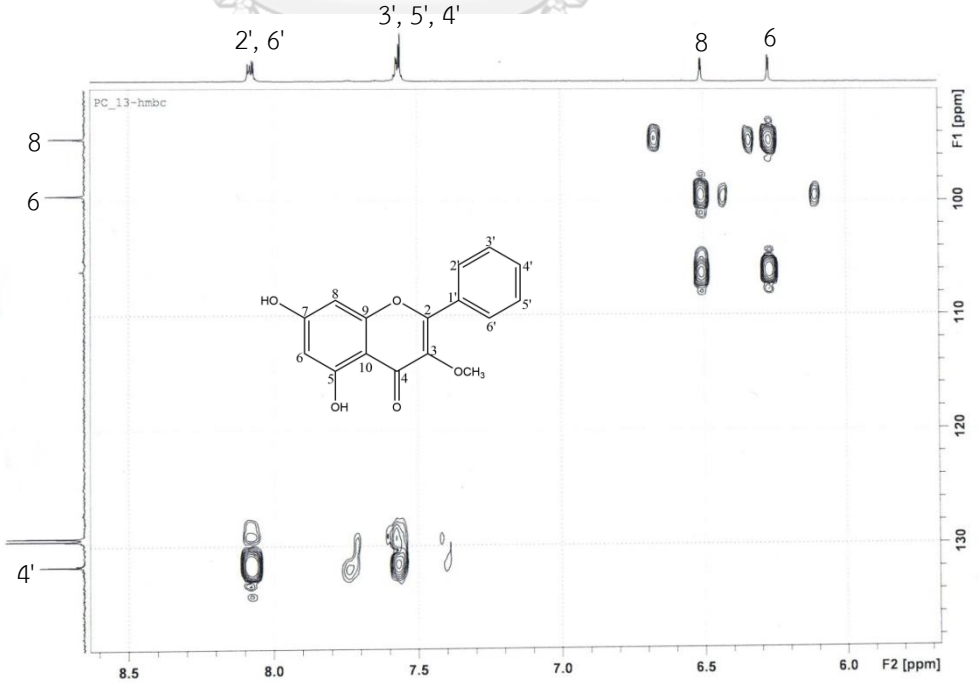

Figure 31. HMBC spectrum of compound PC3 in acetone-d_6

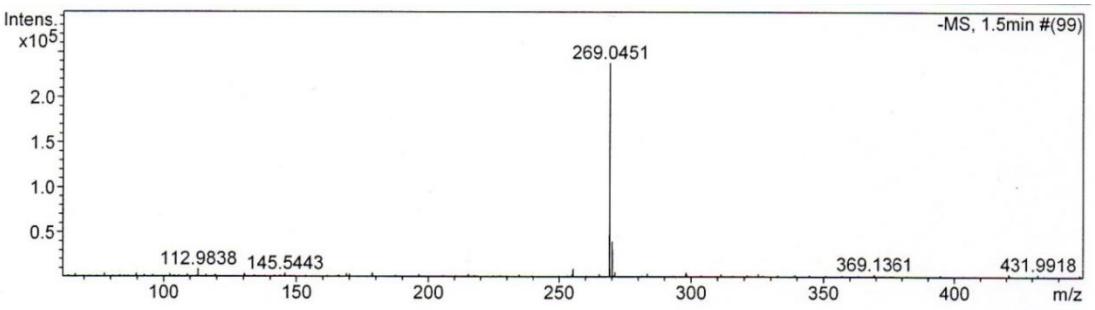

Figure 32. ESI-MS of compound PC4

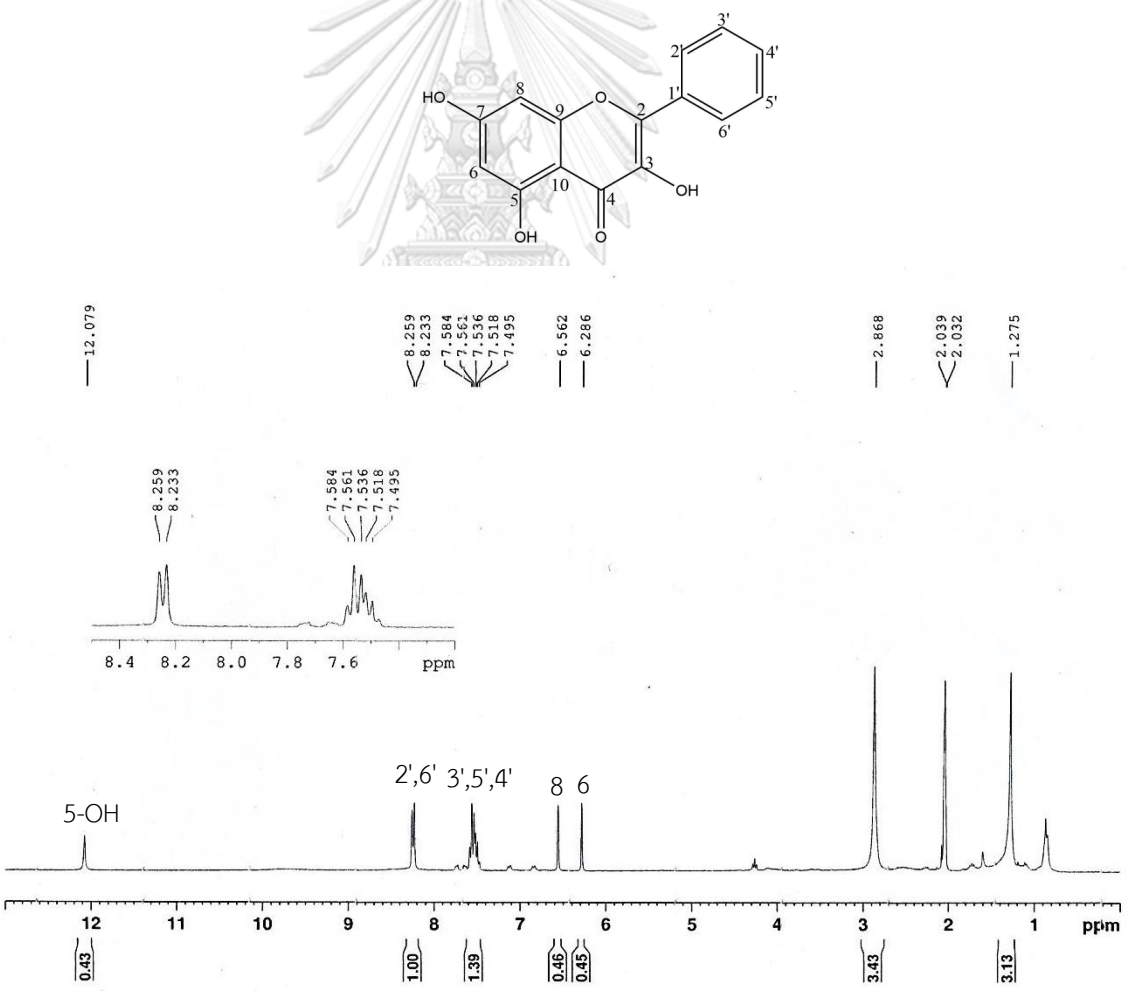

Figure 33. ^{1}H NMR (300 MHz) spectrum of compound PC4 in acetone-d_6

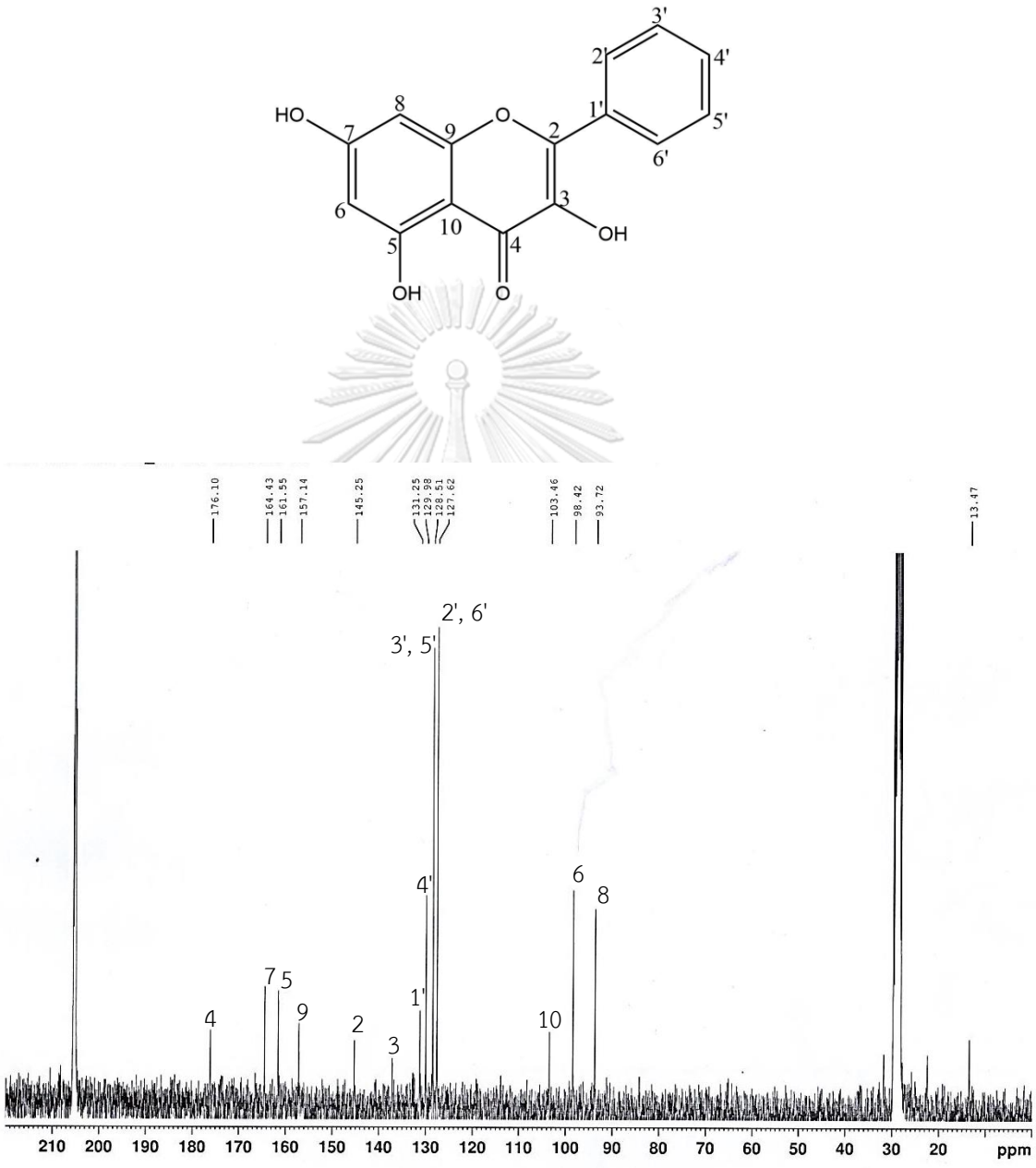

Figure 34. ^{13}C NMR (75 MHz) spectrum of compound PC4 in acetone-d_6

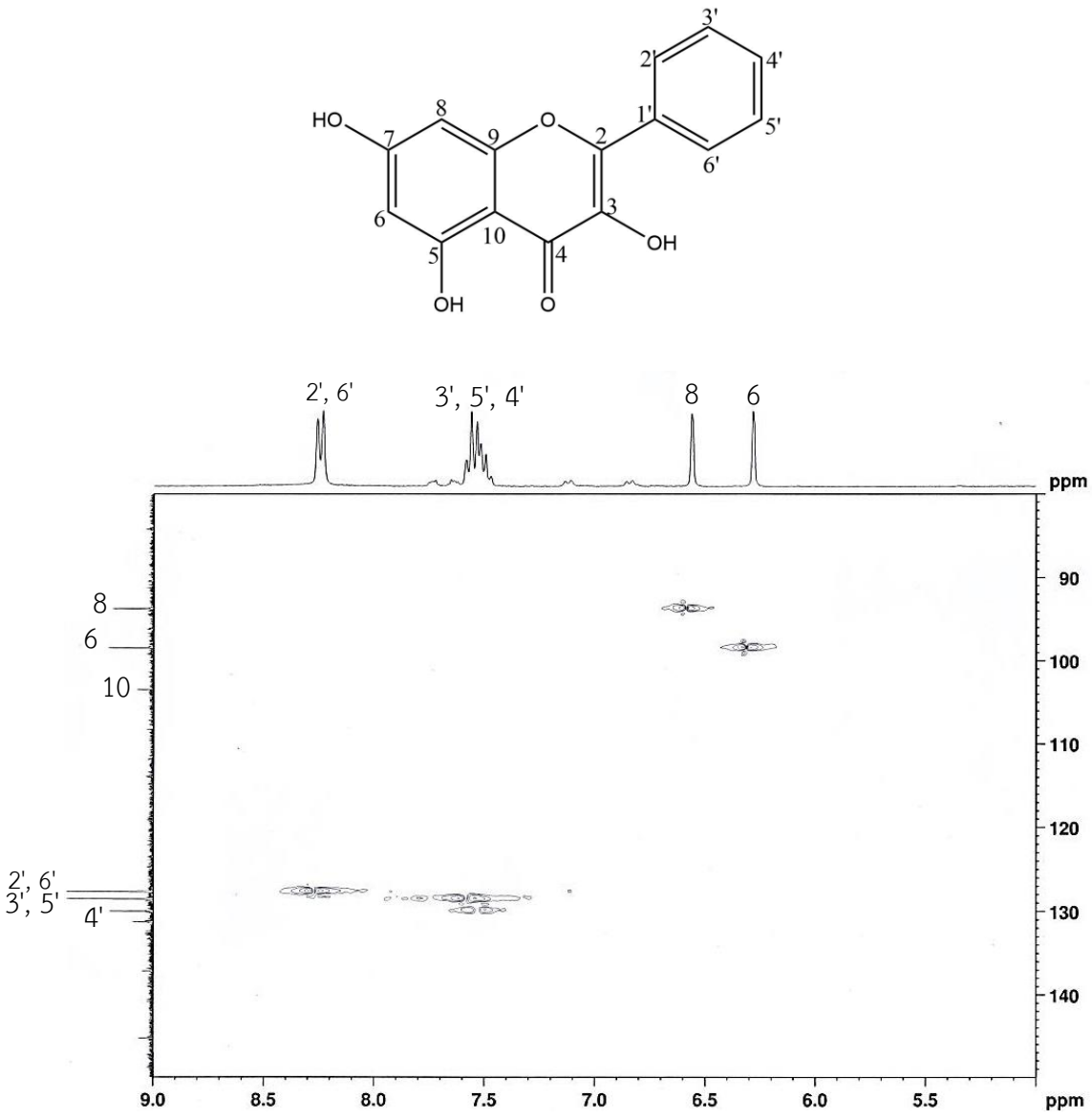

Figure 35. HSQC spectrum of compound PC4 in acetone-d_6

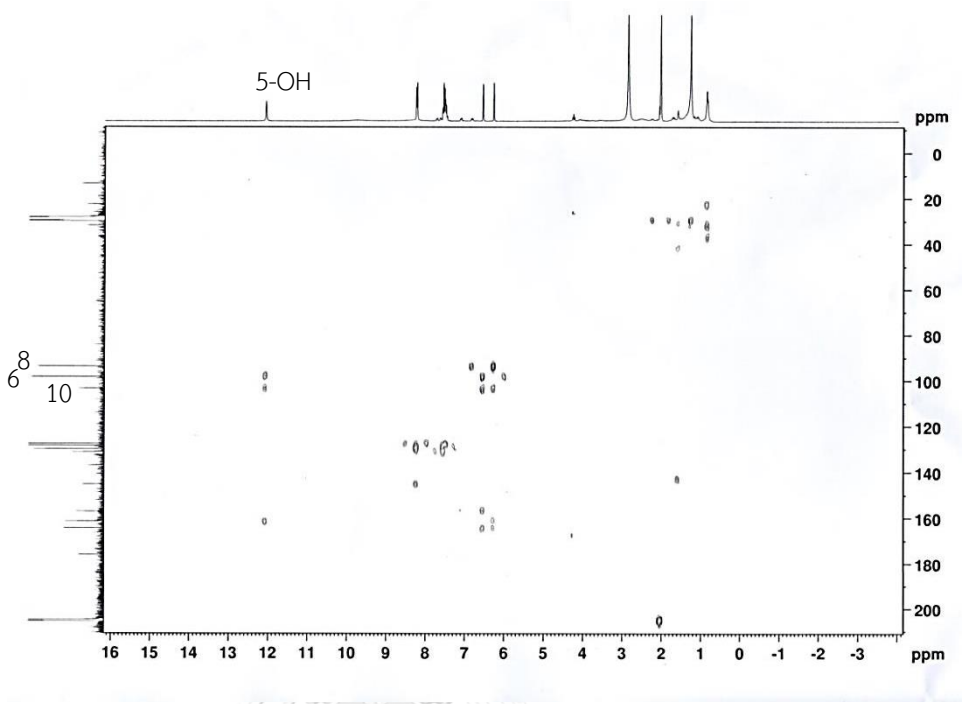

Figure 36. HMBC spectrum of compound PC4 in acetone-d_6

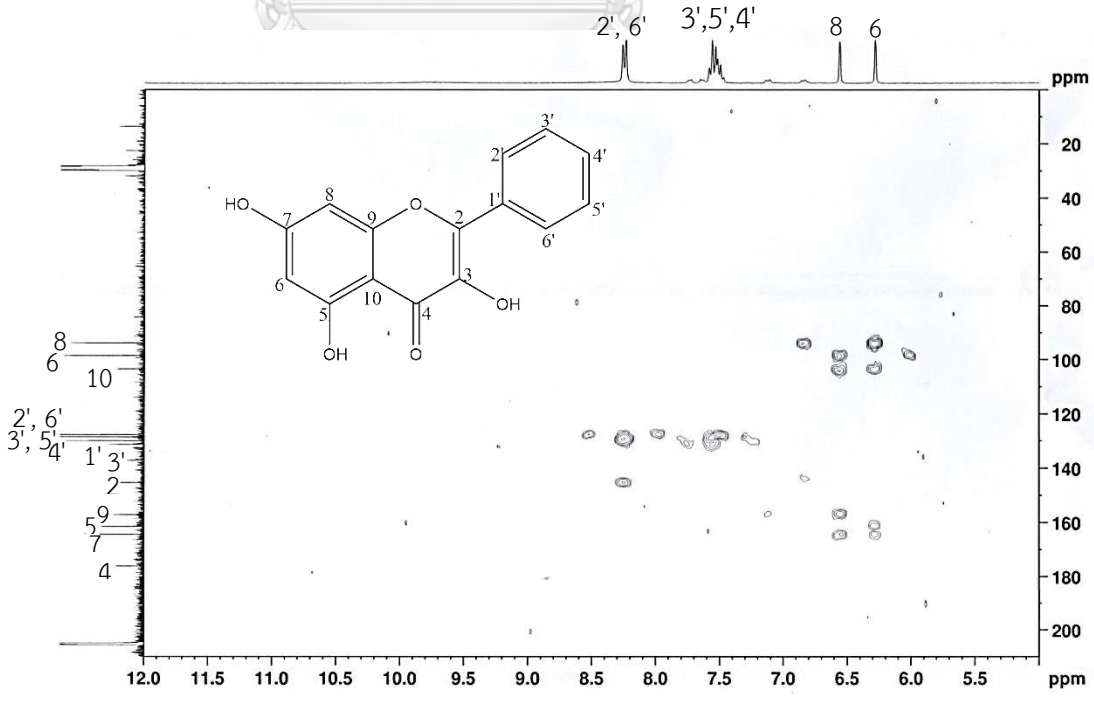

Figure 37. HMBC spectrum of compound PC4 in acetone-d_6

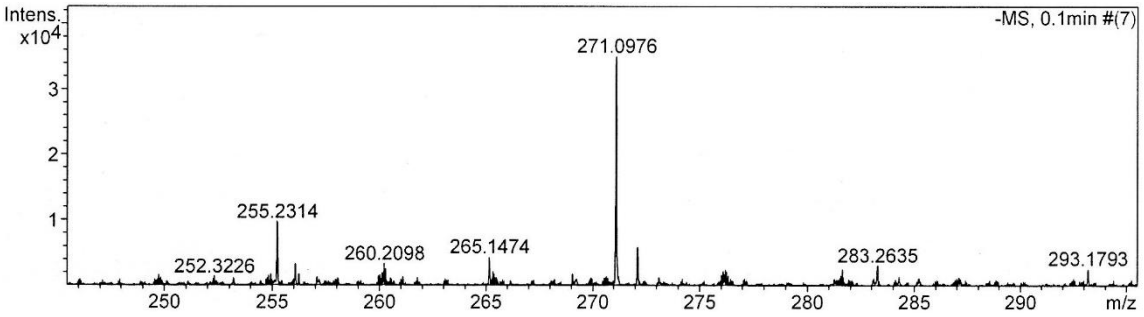

Figure 38. ESI-MS of compound PC5

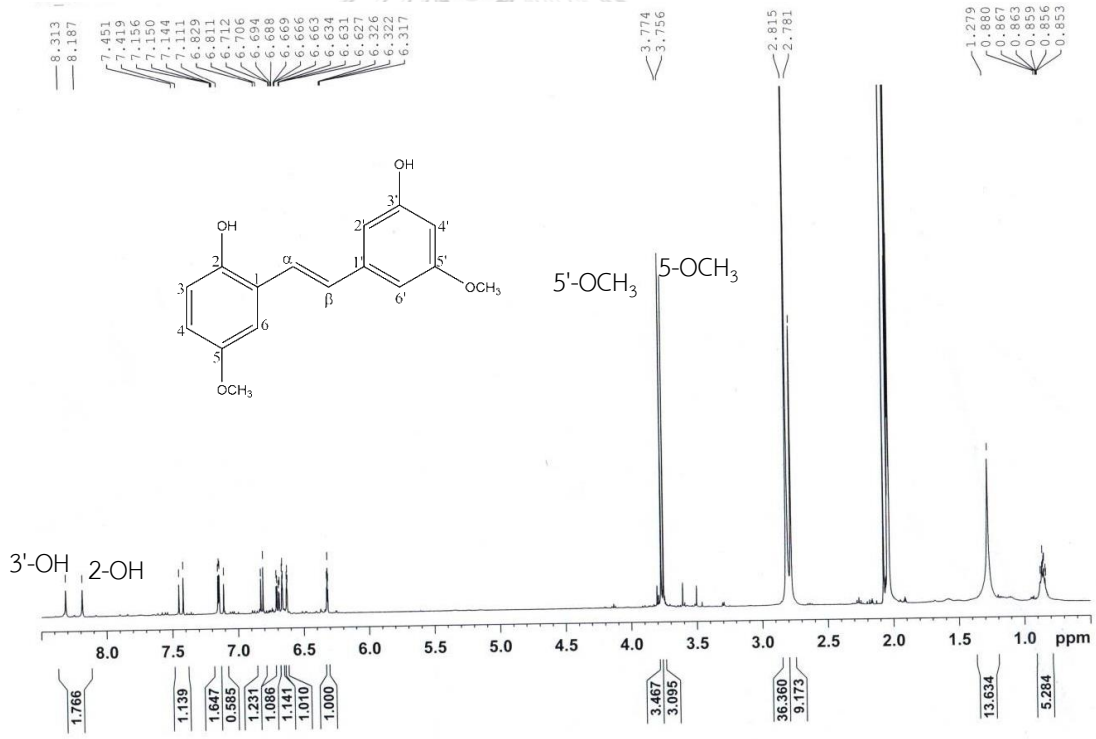

Figure 39. ^{1}H NMR (500 MHz) spectrum of compound PC5 in acetone-d_6

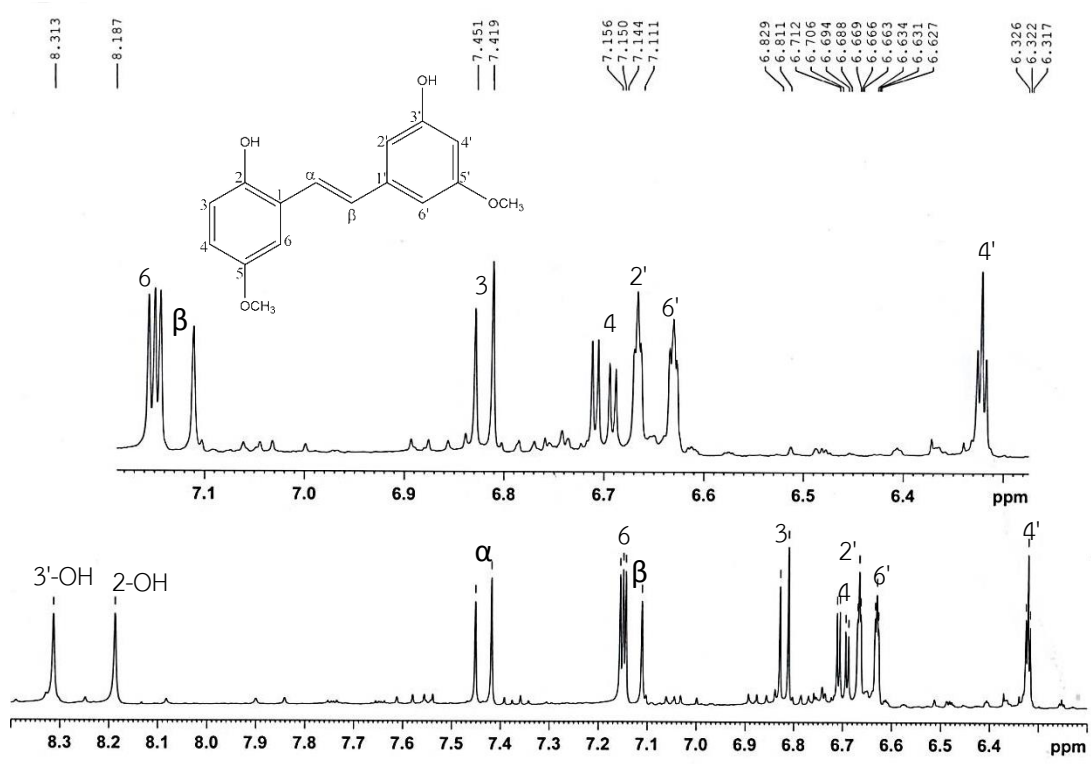

Figure 40. ^{1}H NMR (500 MHz) spectrum of compound PC5 in acetone-d_6 (expanded)

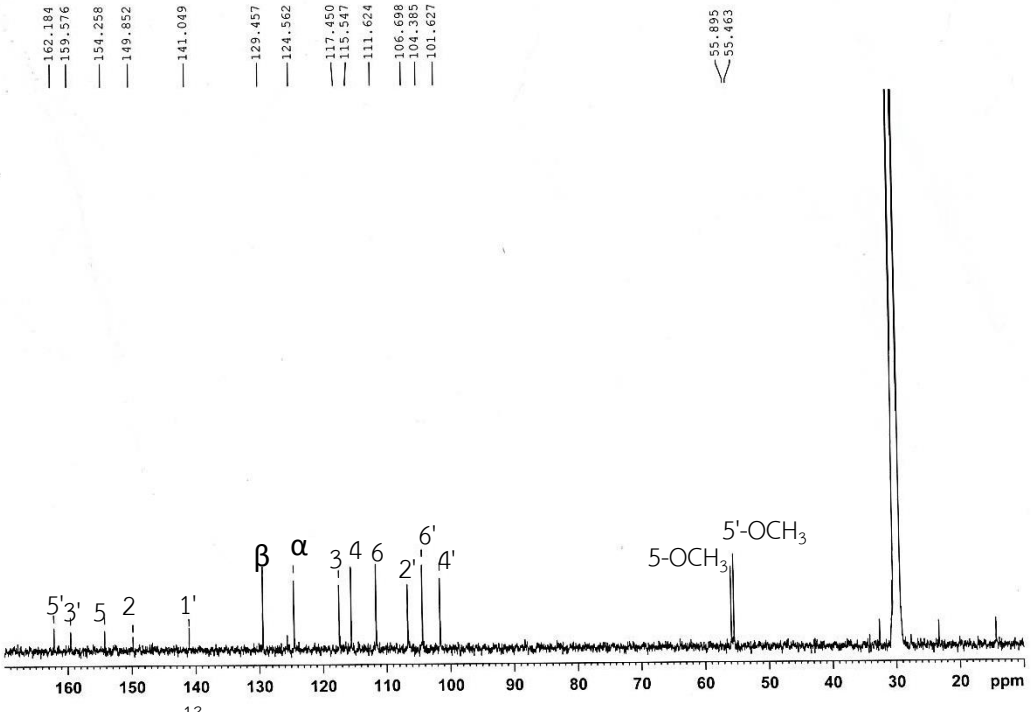

Figure 41. ^{13}C NMR (125 MHz) spectrum of compound PC5 in acetone-d_6

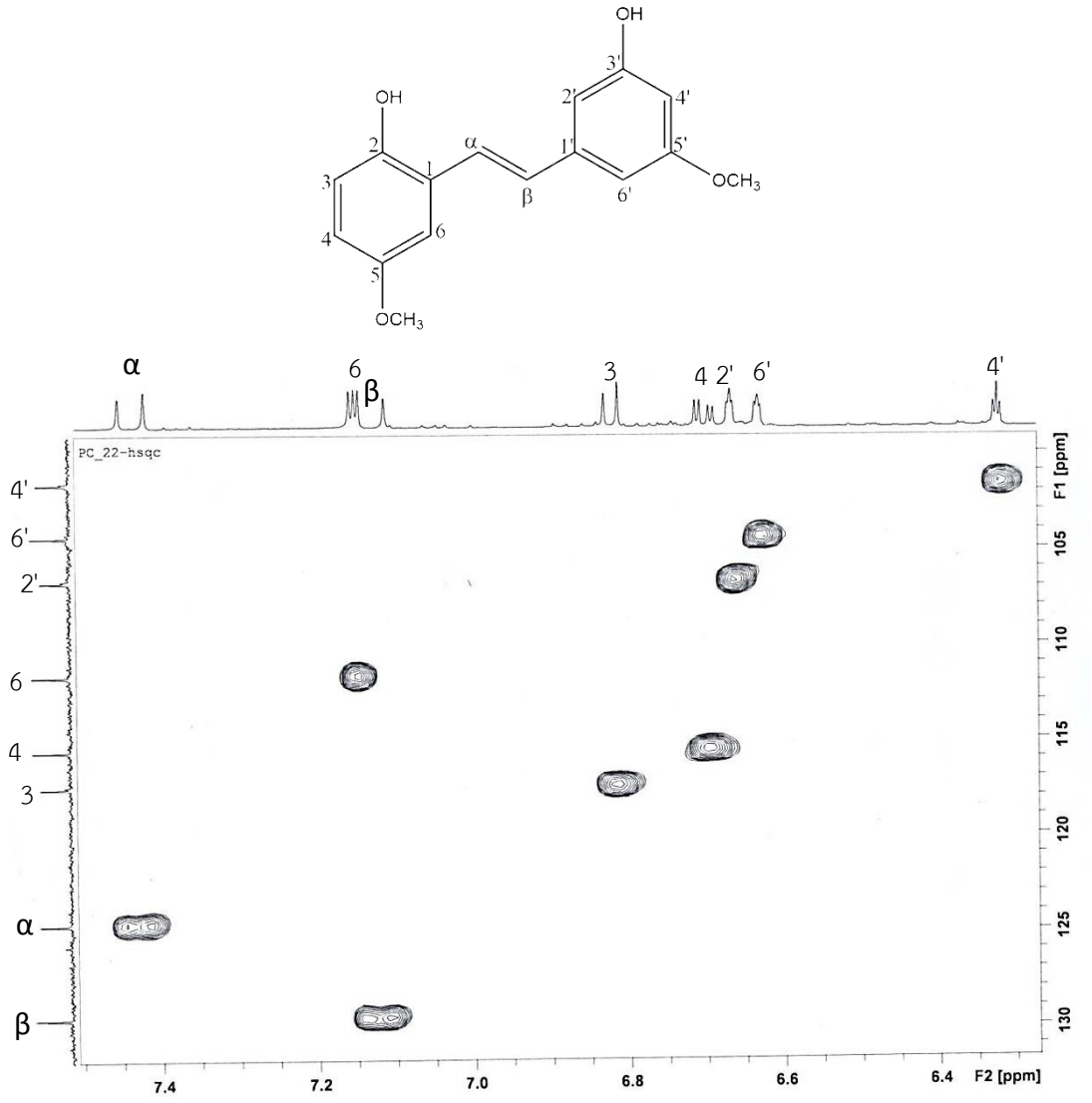

Figure 42. HSQC spectrum of compound PC5 in acetone-d_6

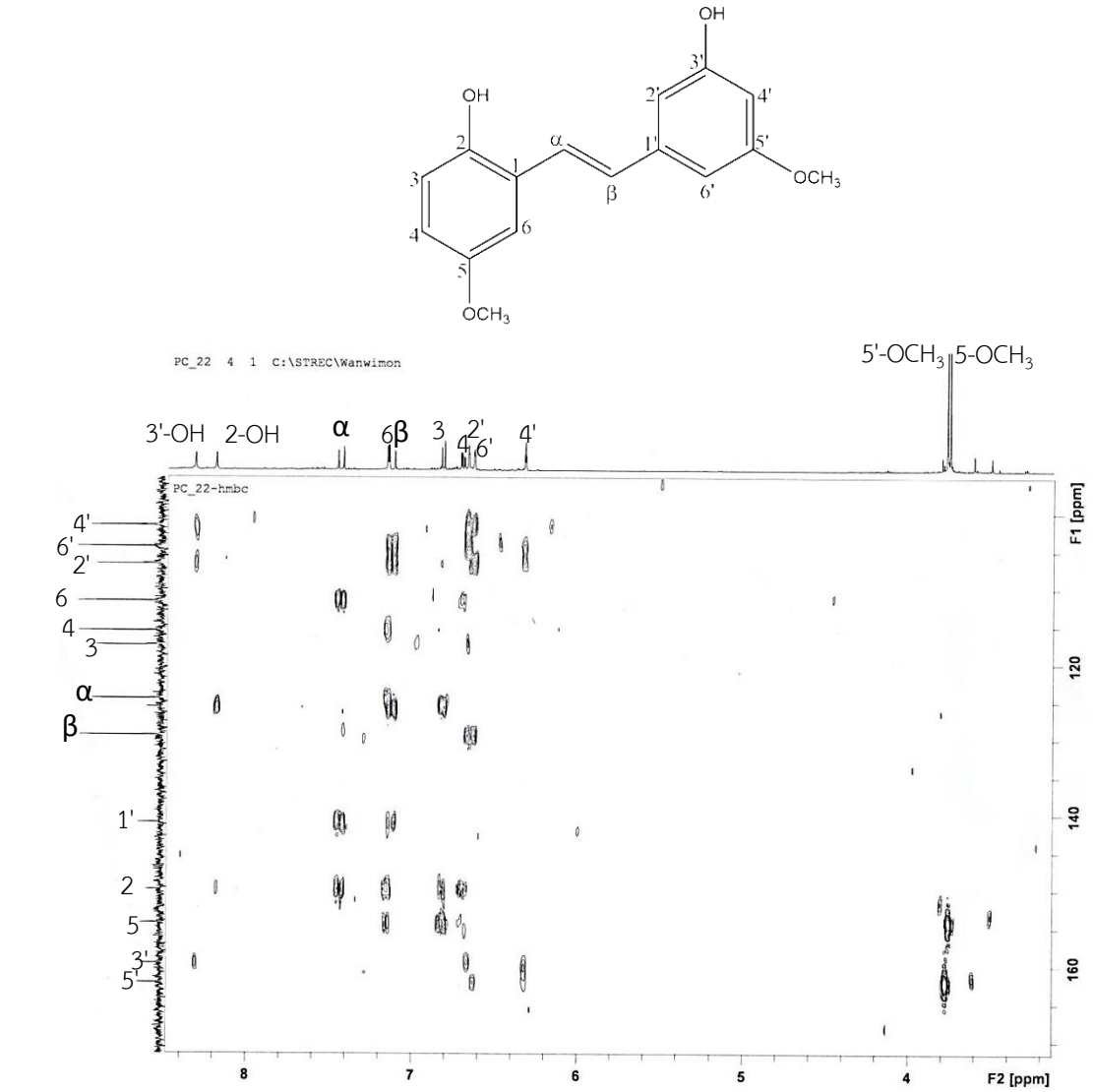

Figure 43. HMBC spectrum of compound PC5 in acetone-d_6

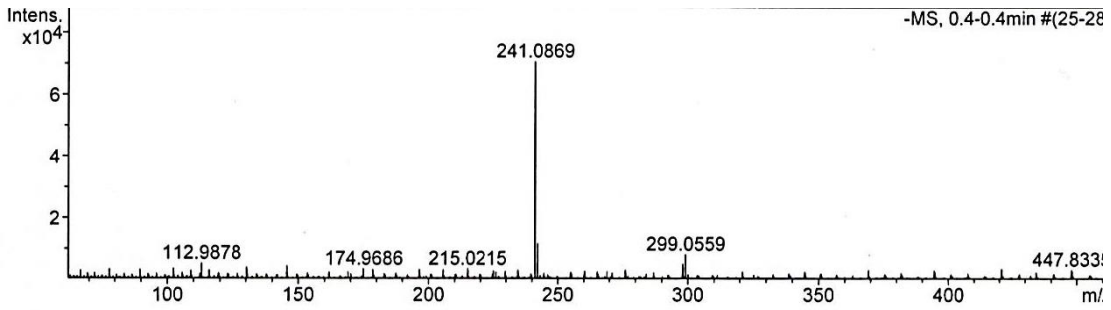

Figure 44. ESI-MS of compound PC6

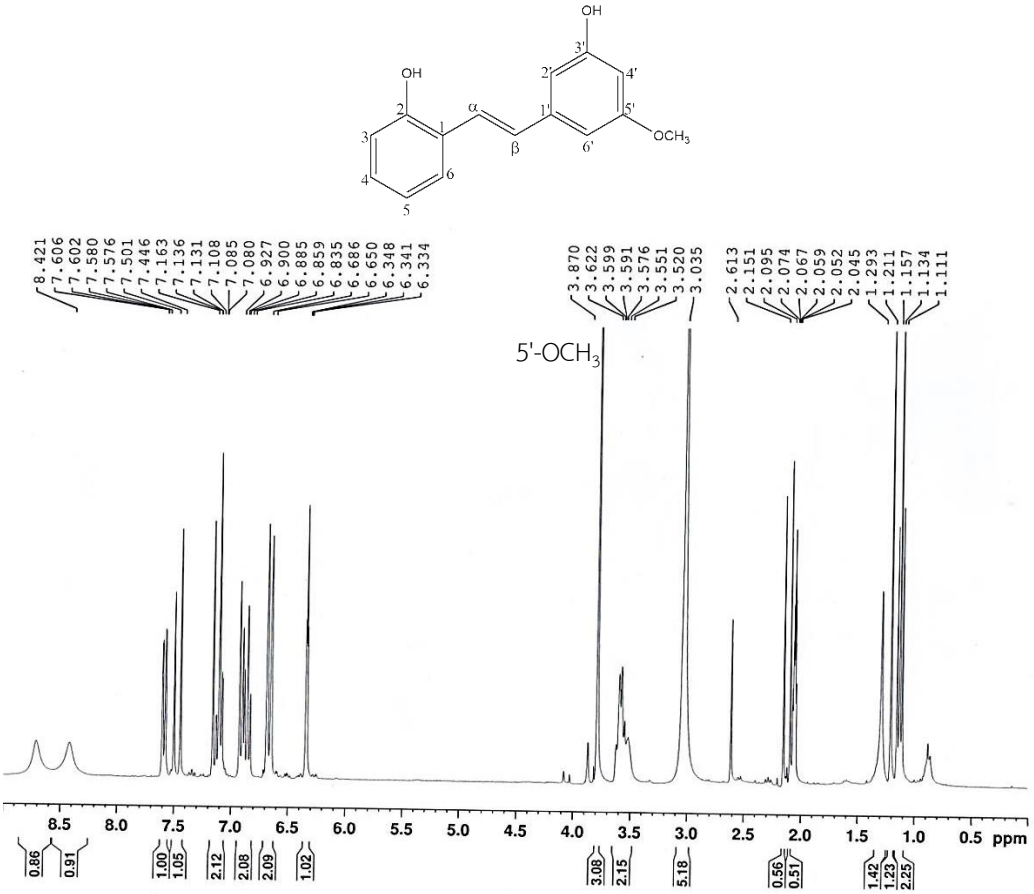

Figure 45. ^{1}H NMR (300 MHz) spectrum of compound PC6 in acetone-d_6

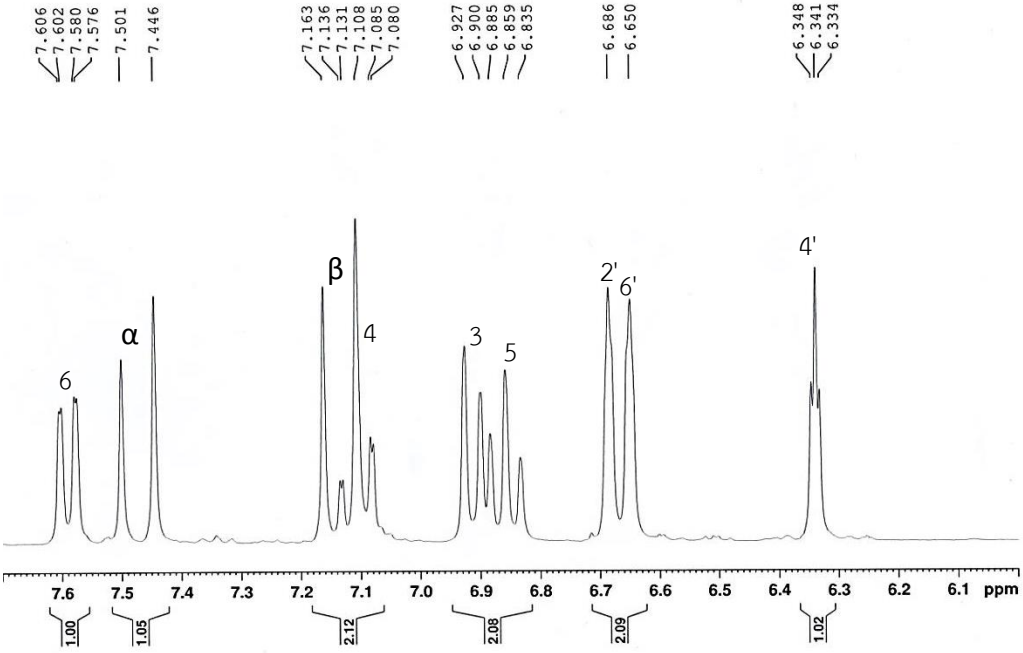

Figure 46. ^{1}H NMR (300 MHz) spectrum of compound PC6 in acetone-d_6 (expanded)

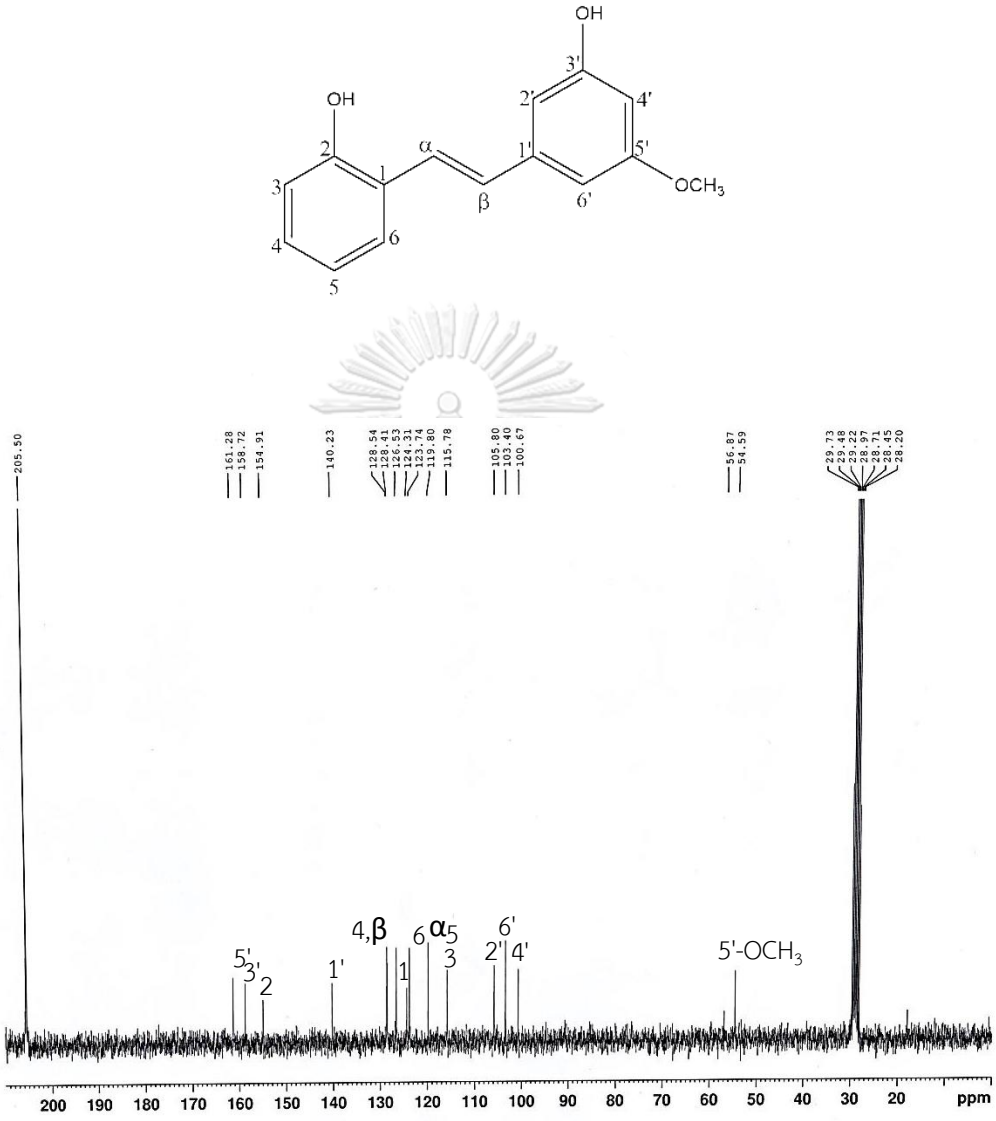

Figure 47. ^{13}C NMR (75 MHz) spectrum of compound PC6 in acetone-d_6

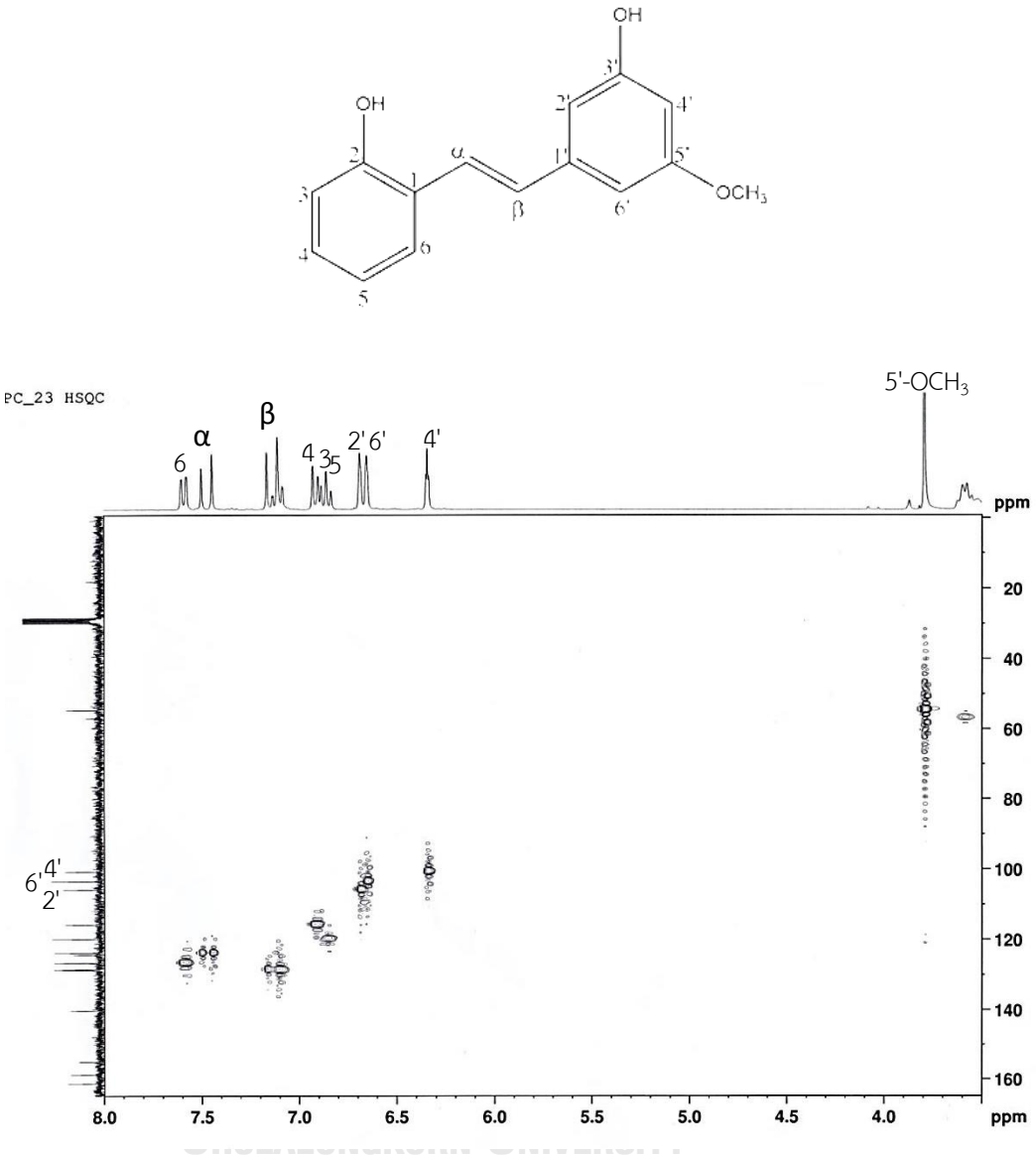

Figure 48. HSQC spectrum of compound PC6 in acetone-d_6

Table 10. Growth media (YPD broth)

Ingredient	1L
Yeast extract	10 g
Peptone	20 g
Dextrose	20 g

Table 11. Growth media (YPD agar)

Ingredient	1L
Yeast extract	10 g
Peptone	20 g
Dextrose	20 g
Agar	15 g

Table 12. Agar formula for S.C. ura- media (repressed system)

Ingredient	1L
Yeast nitrogen base W/O amino acid (Difco)	6.7 g
Amino acid mixture W/O uracil (Sigma) Yeast synthetic drop-out medium supplement	1.92 g
Bacto ™ agar (Difco)	20 g
Bacto ™ Dextrose (Difco)	20 g

Table 13. Agar formula for S.C. ura- media (induced system)

Ingredient	1L
Yeast nitrogen base W/O amino acid (Difco)	6.7 g
Amino acid mixture W/O uracil (Sigma) Yeast synthetic drop-out medium supplement	1.92 g
Bacto ™ agar (Difco)	20 g
Galactose	20g

VITA

NAME	San Yoon Nwe
DATE OF BIRTH	26 July 1994
PLACE OF BIRTH	Danaphyu Township, Ayeyarwady Division
INSTITUTIONS ATTENDED	University of Pharmacy (Yangon)
HOME ADDRESS	Room (24), 3rd fl, University of Pharmacy Campus, NorthOakkalapa township, Yangon.
PUBLICATION	-
AWARD RECEIVED	-